Selected Topics in THz and Ultrafast Photonics

Ci-Ling Pan 潘犀靈
Department of Physics
National Tsing Hua University
Hsinchu, Taiwan 30013, ROC

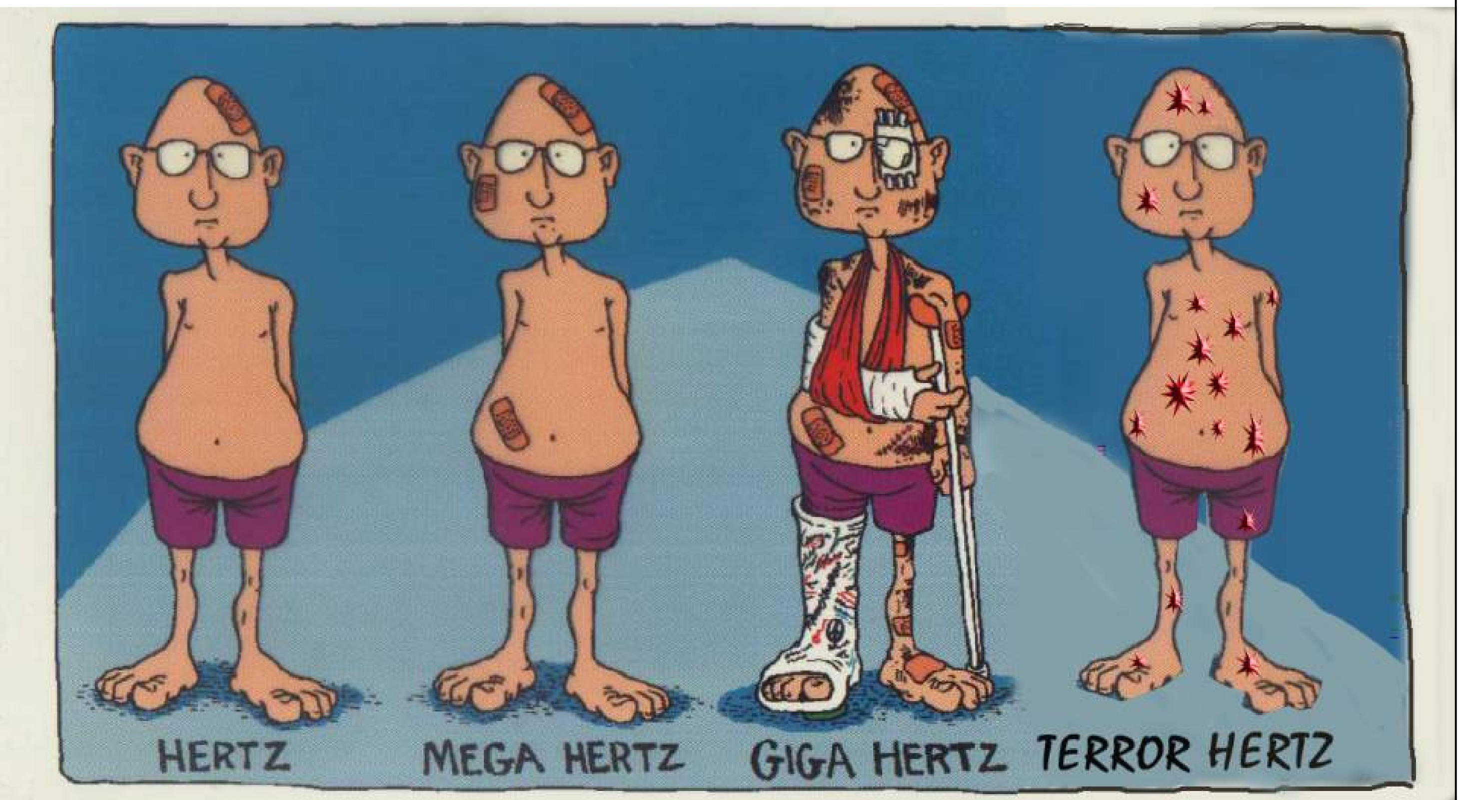

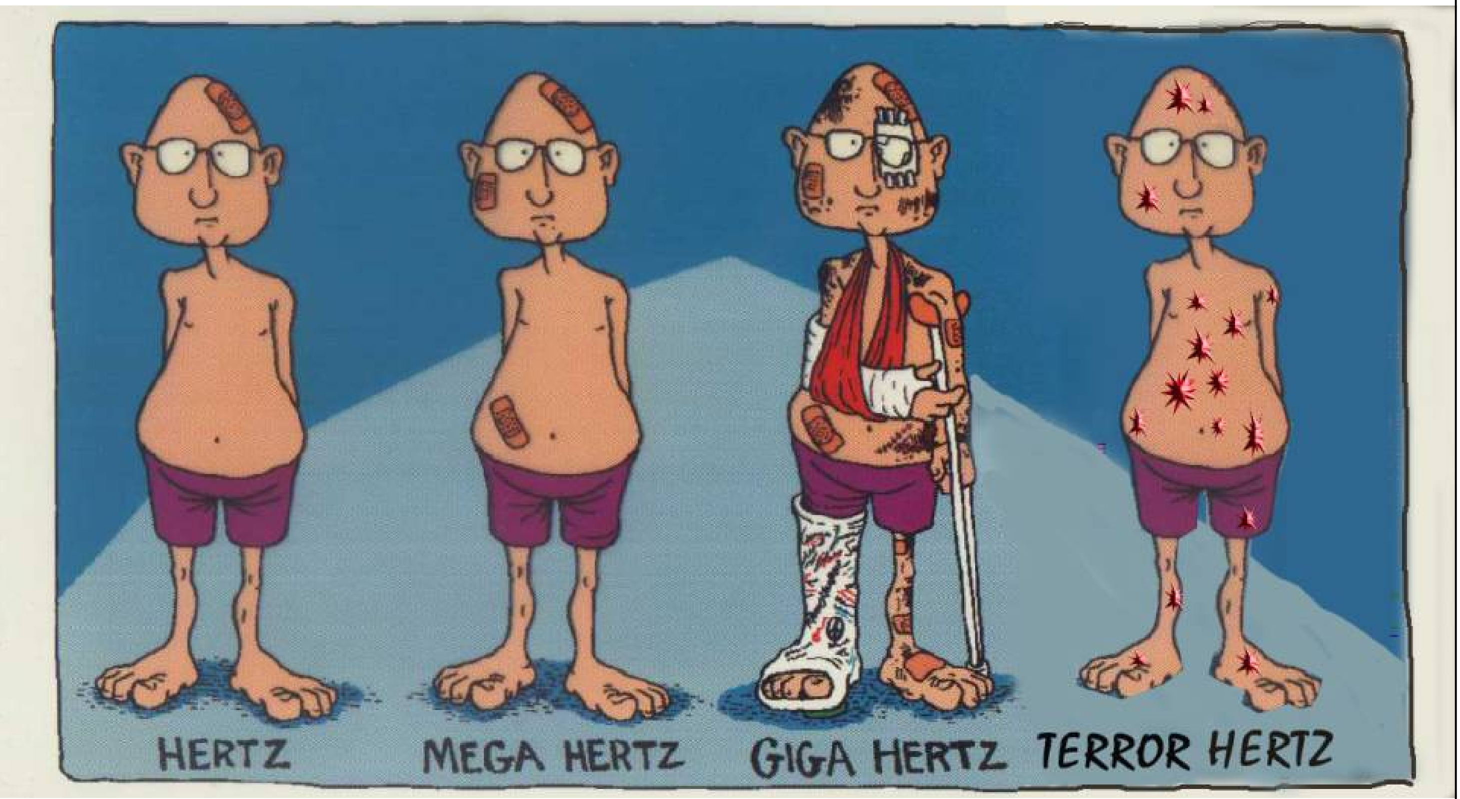

Hertz = Hurts

T-Ray: Next frontier in Science and Technology

Terahertz wave (or T-ray), which is electromagnetic radiation in a frequency interval from 0.1 to 10 THz, lies a frequency range with rich science but limited technology.

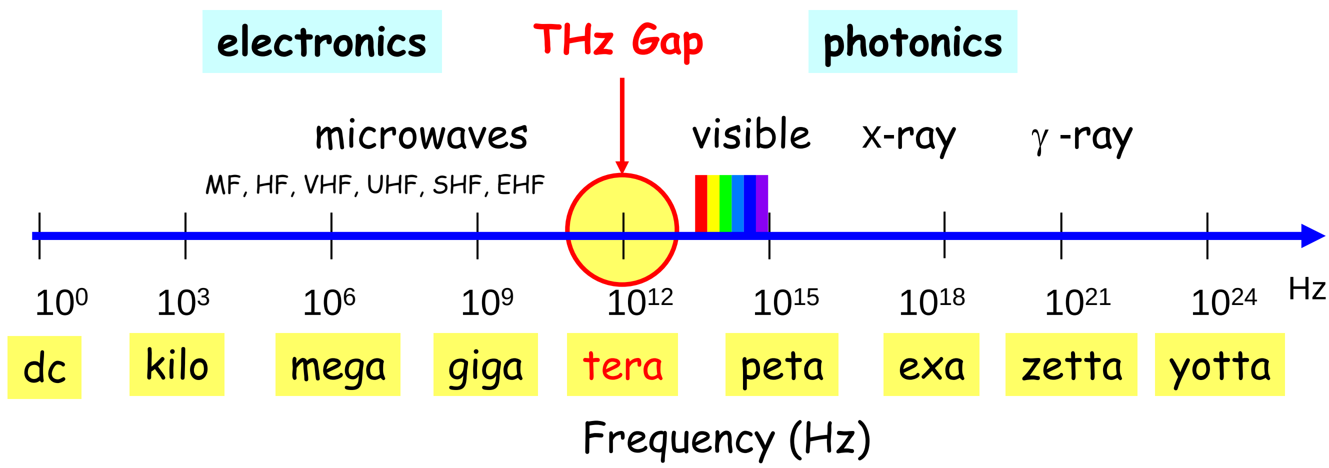

1 THz ~ 1 ps ~ 300 μm ~ 33 cm^{-1} ~ 4.1 meV ~ 47.6 °K

Courtesy: X.-C. Zhang (RPI)

Applications

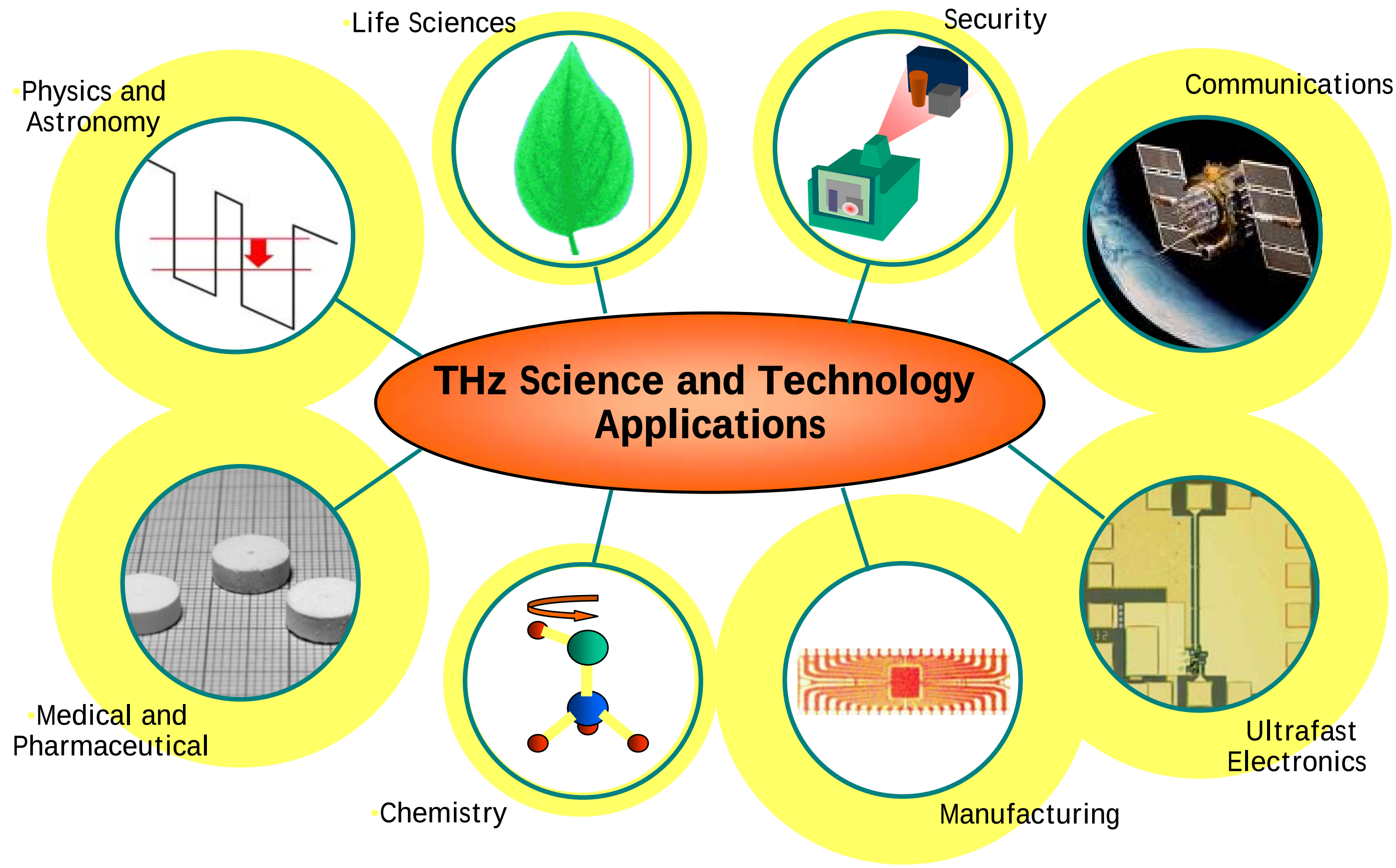

THz Technologies

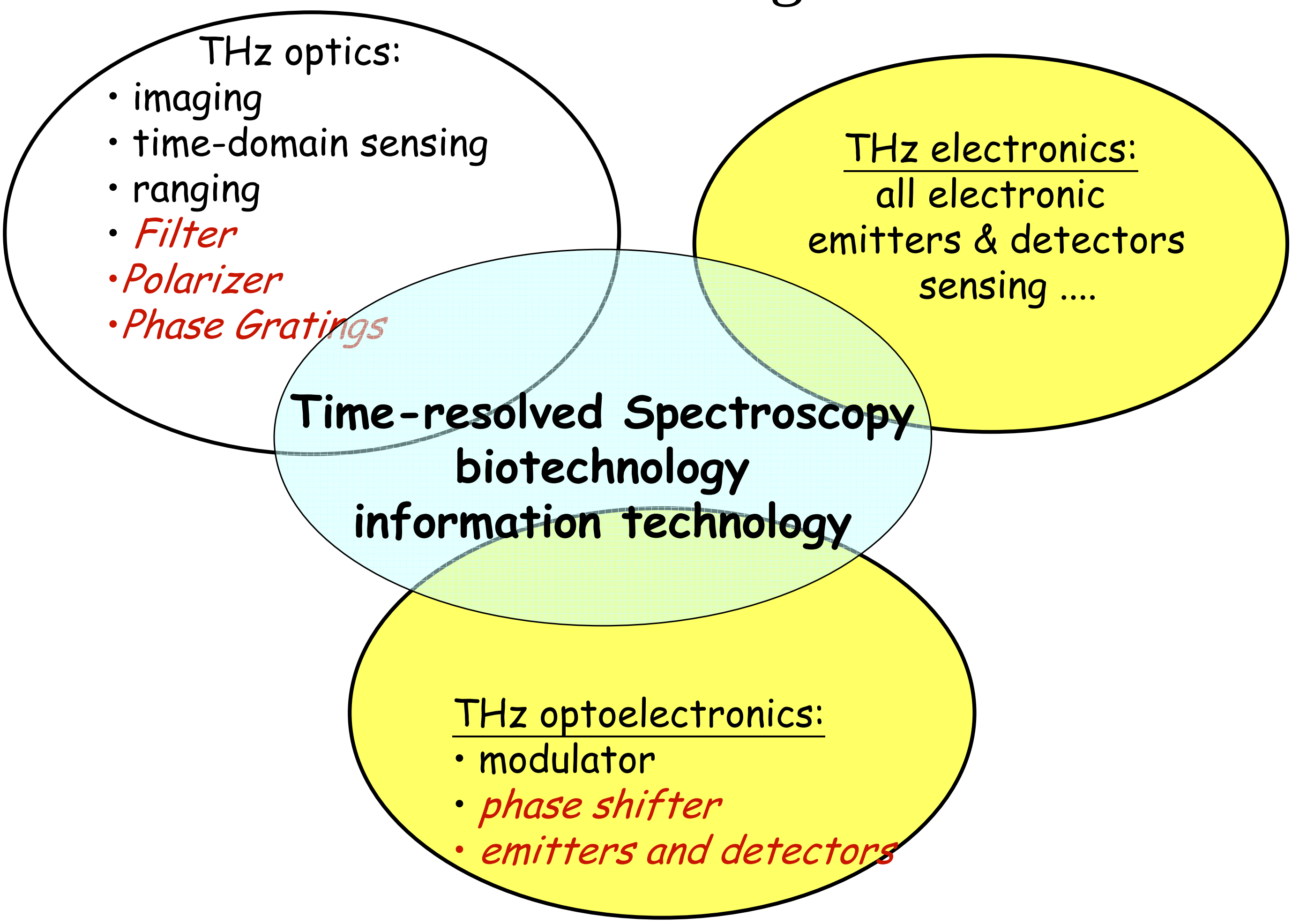

THz Sources and Sensors

- **THz Sources:**
  - Free electron laser, gas lasers, quantum cascade lasers
  - Gunn oscillators, Bloch oscillation, cold plasma, etc
  - Photoconductive antenna (more power)
  - Electro-optic crystal (optical rectification)

- **THz Detectors:**
  - Bolometer
  - Pyroelectric detector
  - Schottky or point-contact diode, novel semiconductor devices
  - Photoconductive dipole antenna (great sensitivity)
  - Electro-optic crystal (electro-optic effect)

Generation of THz Wave: current surge effect

- **Photo-excited Hertzian dipole antenna in free space.**

$$J(t) = n(t) e \mu E_b$$

$$E(r,t) \propto \frac{1}{r} \frac{\partial J(t)}{\partial t}$$

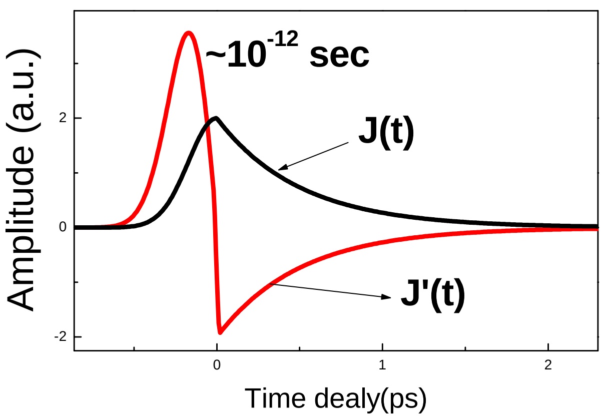

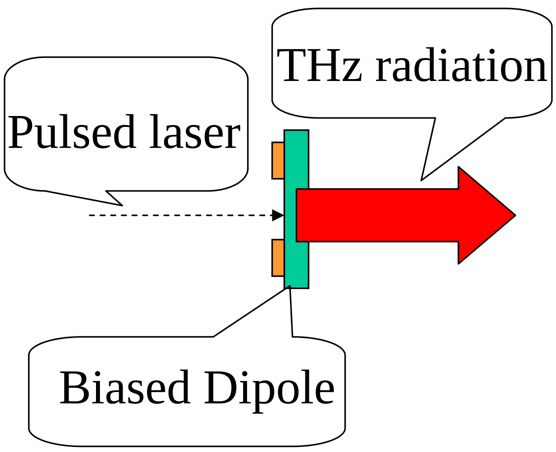

Ultrashort-pulse-induced THz light is typically a single-cycle pulse!

Detection of THz Wave: Photoconductive Antenna

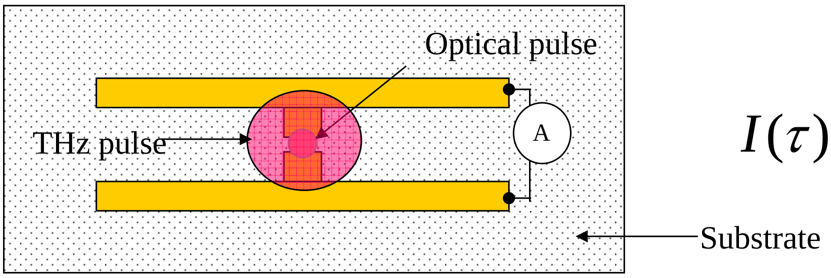

$$I(\tau) \propto e\mu\tau_c \int_{t_1}^{t_2} E(t)n(t-\tau)dt$$

I(τ): detected signal current, e: electron charge, μ: carrier mobility, τ_c: carrier life time, m: repetition rate, τ: relative time delay between THz pulse and gating laser pulse, n(t): photo-induced transient carrier density, E(t): THz field.

Substrate with

- Shorter carrier life time: n(t) ~ delta function =>$E(t) \propto I(t)$
- Long carrier life time: n(t) ~ step function =>$E(t) \propto dI(t)/dt$

SI-GaAs vs GaAs:As THz Emitters: Carrier Lifetimes

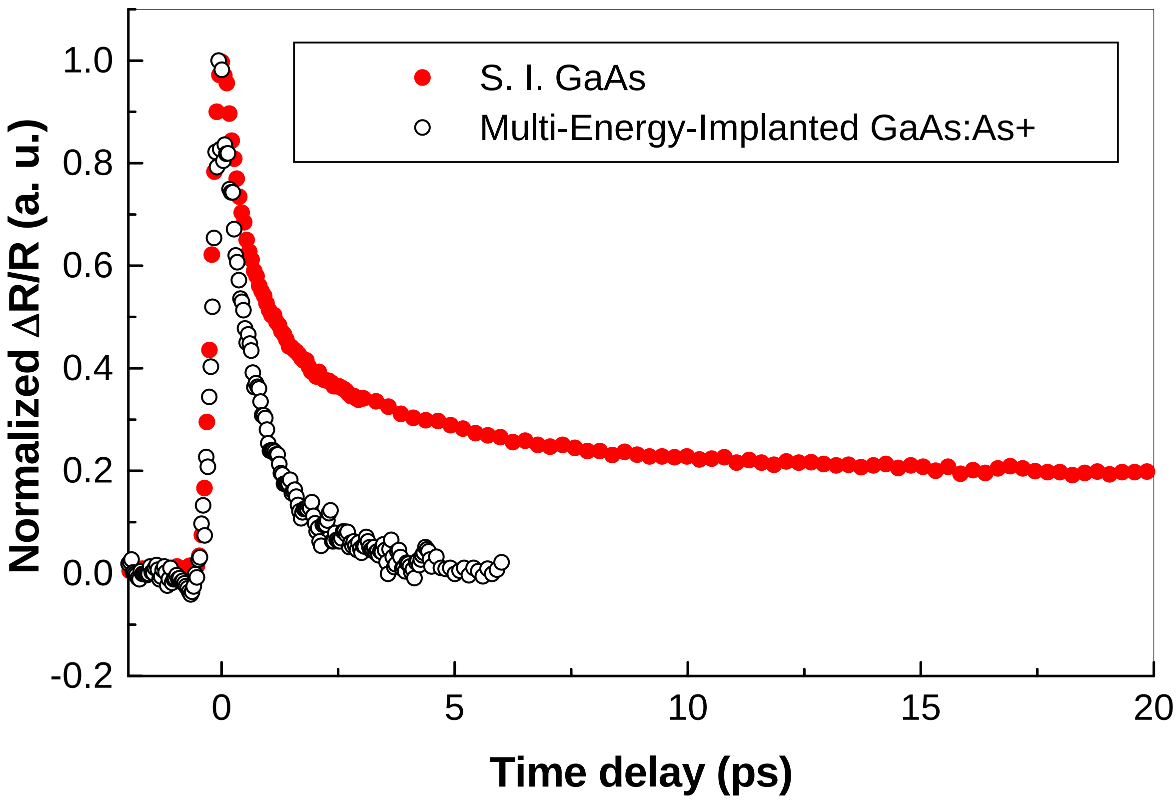

Wideband GaAs:As+ and InP:H+ THz Antenna

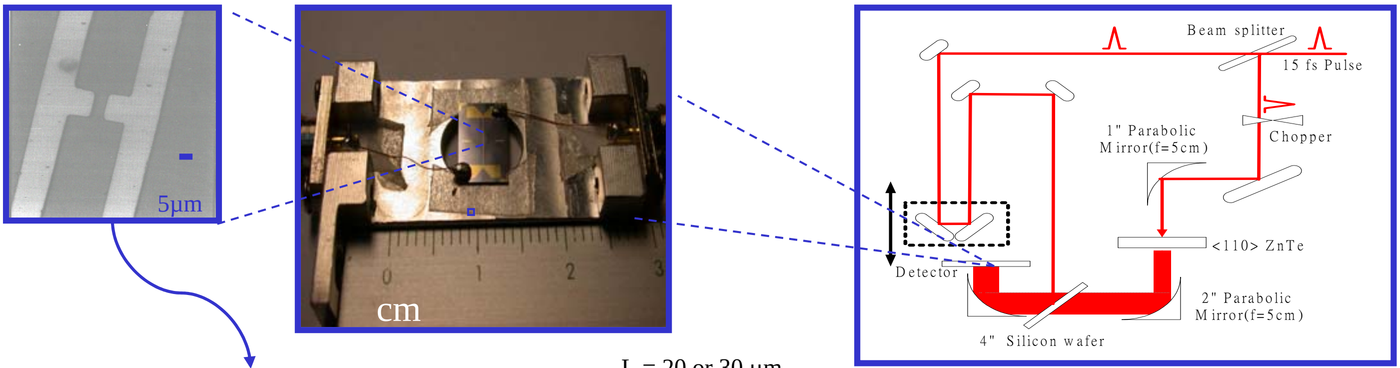

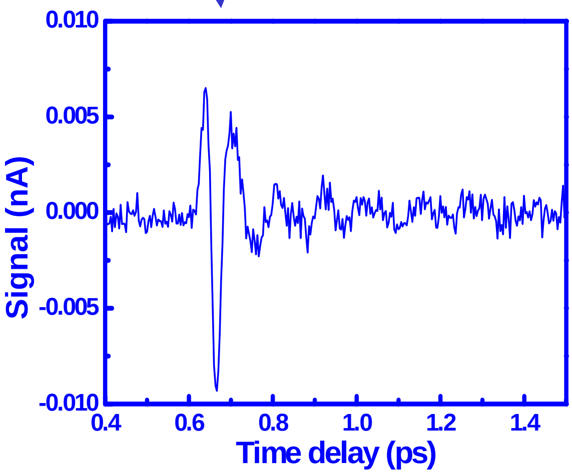

L = 20 or 30 μm

W = 10 μm

G or D = 5 μm

F.F.T.

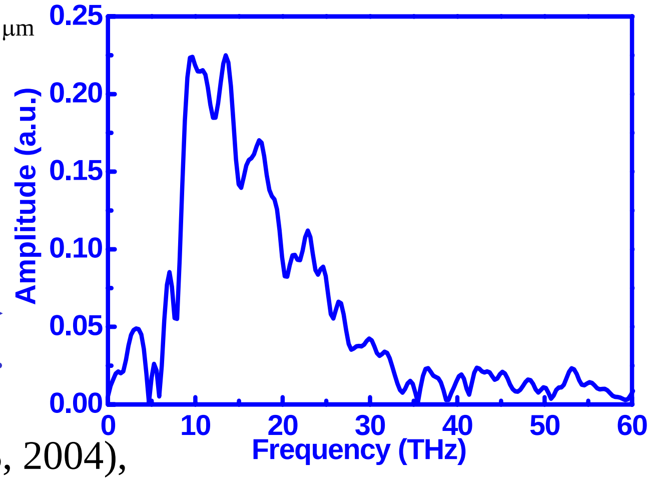

APL(Aug 18, 2003), Opt. Exp (June 28, 2004), both selected by Virtual J of Ultrafast Sci.,

THz radiation emission properties of GaAs:O based Photocondoutive Antenna

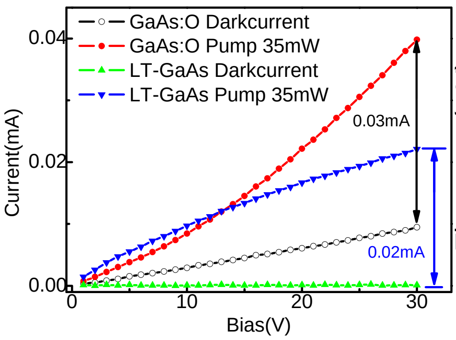

Fig1. Electrical characterization

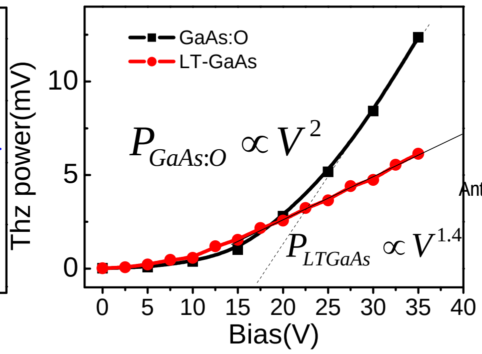

Fig2. Output THz power verse bias

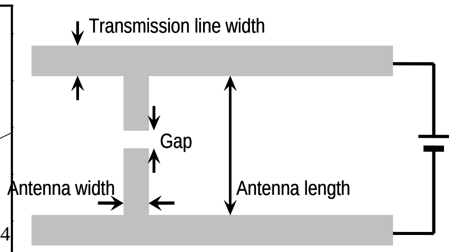

Gap=5um

Antenna length =30 um

Fig3. Antenna Structure

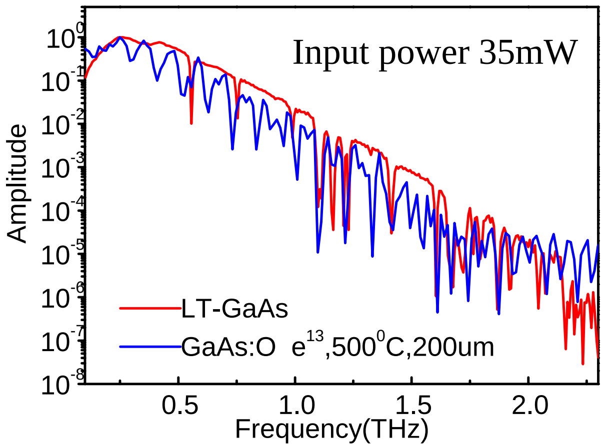

Fig4. THz spectrum measured by TDS

- **GaAs:O antenna exhibits higher output than LT-GaAs based PC antenna (around 2times under bias of 35 volt) .**
- Noise is higher, but S/N comparable

In collaboration with Prof. K. T. Chan's group, CUHK

Photonic Sub-THz Modulator/Transmitter

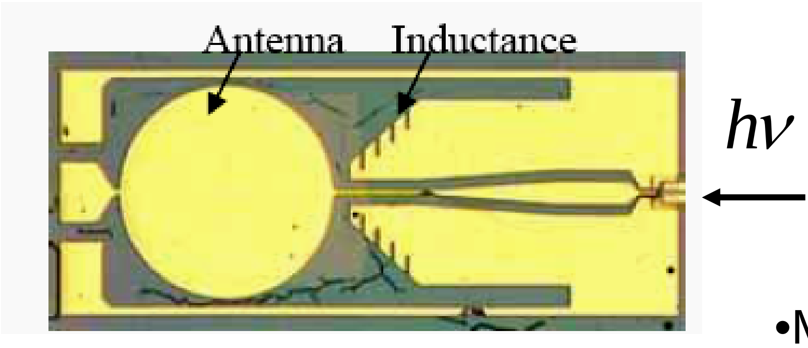

presented at CLEO'08
PTL, Aug. 15, 2008

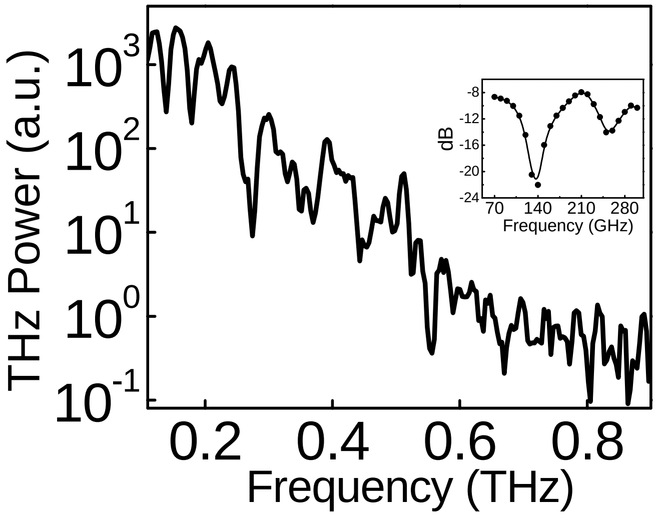

- Monolithic integration of a UTC PD and broadband micomachined antenna.
- P_{peak} = 20 mW
- Pulse width<2 ps
- An order-of-magnitude improvement over current technology

THz Time-Domain Spectroscopy (THz-TDS)

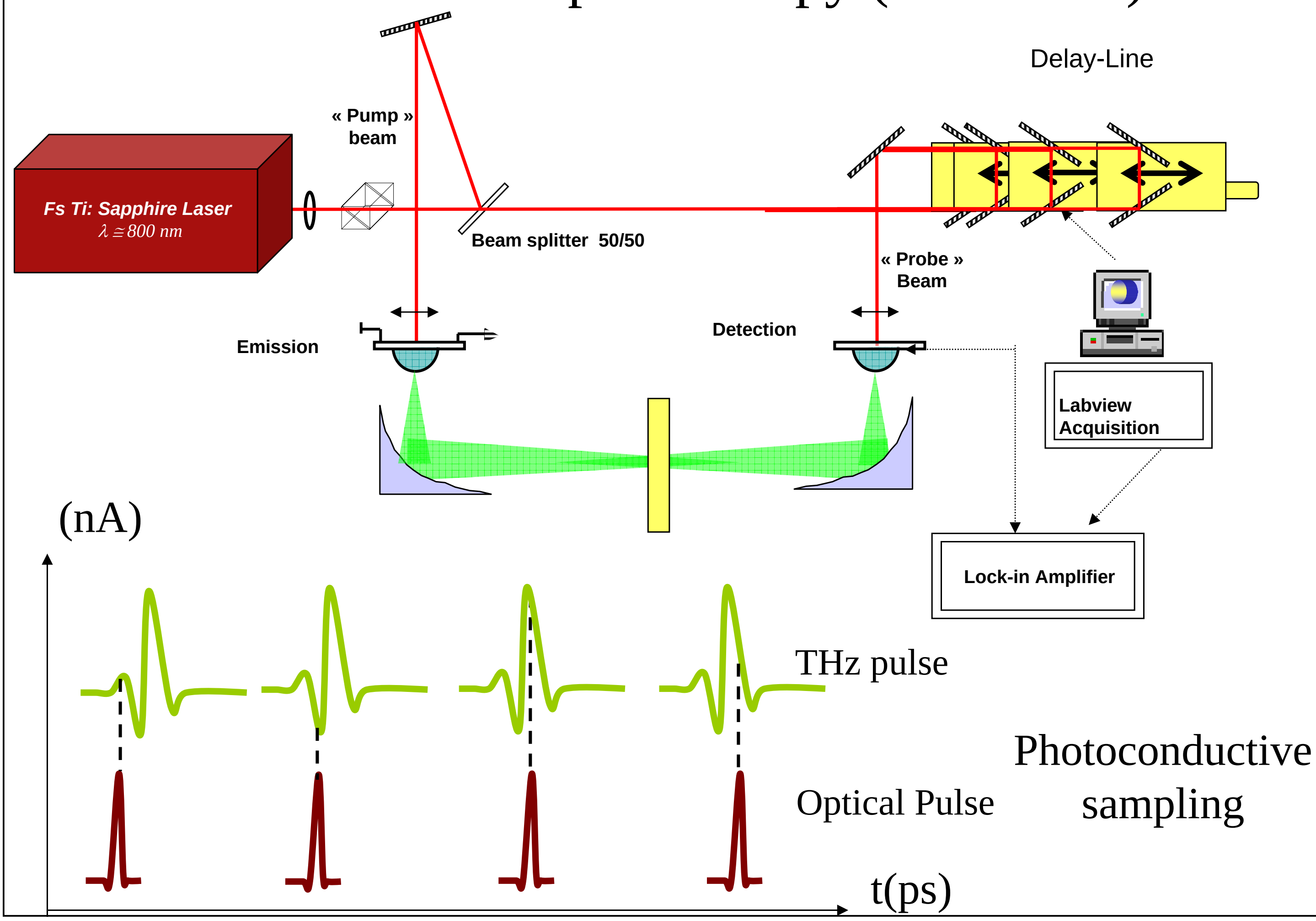

THz time-domain spectroscopy (THZ-TDS)

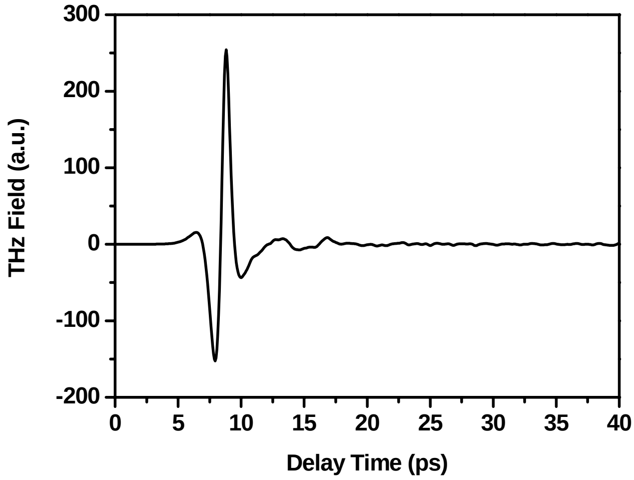

FFT

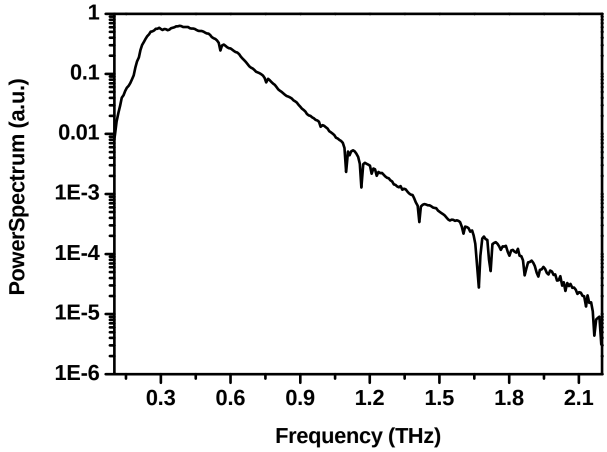

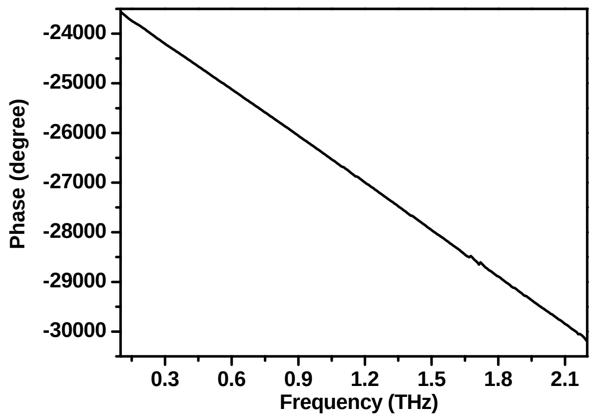

Time-domain signal

THz-TDS: Extraction of Far IR Optical Constants of Materials

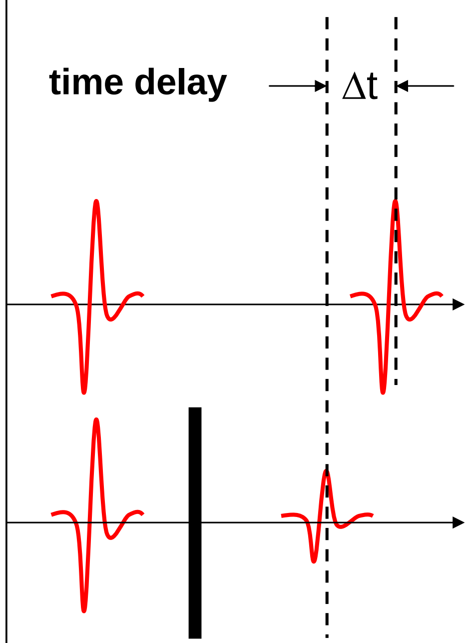

Spectral Absorption

Power Spectrum

Phase

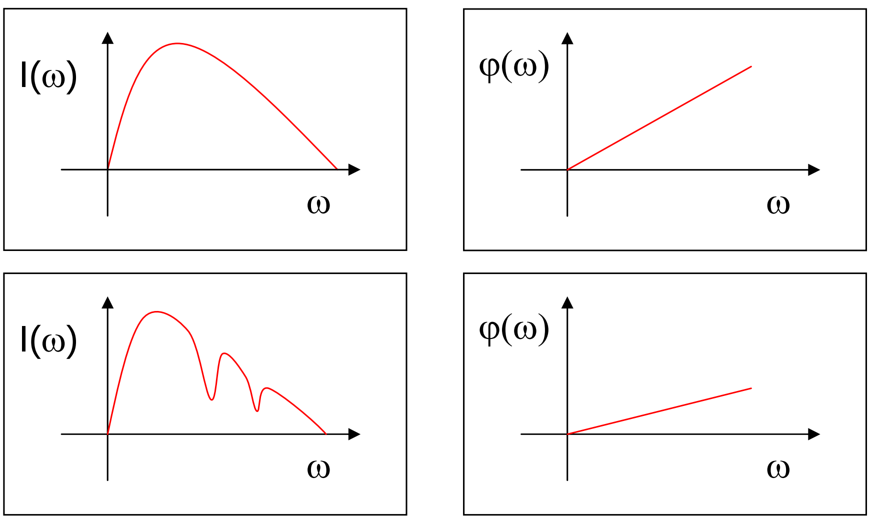

Imaginary index κ + Real index n

Generation of a THz Wave: Optical Rectification

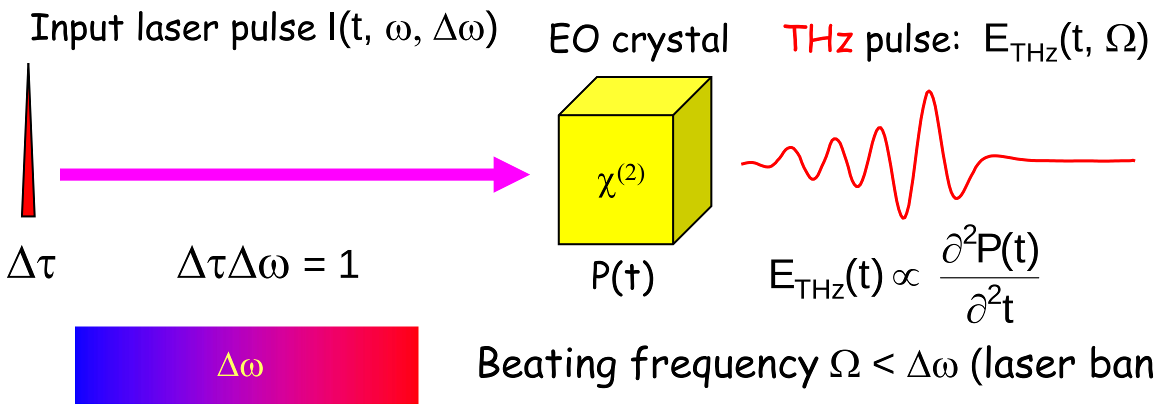

Beating frequency Ω < Δω (laser bandwidth)

polarization: $P(\Omega) = \chi^{(2)}(\Omega, \omega+\Omega, -\omega)\, E(\omega+\Omega)E^*(\omega)$

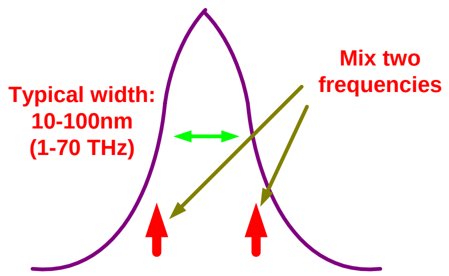

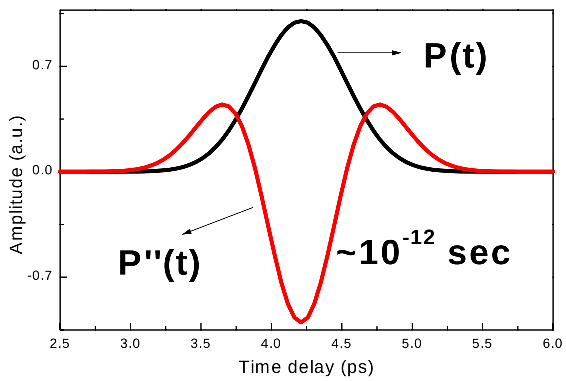

Detection of THz Wave: Electro-Optic Sampling

$\Delta I(t) = I_0 \sin(\Delta\Gamma)$

$$\Delta\Gamma = \frac{\pi d r_{41} n_0^3}{\lambda} E_{THz}(t)$$

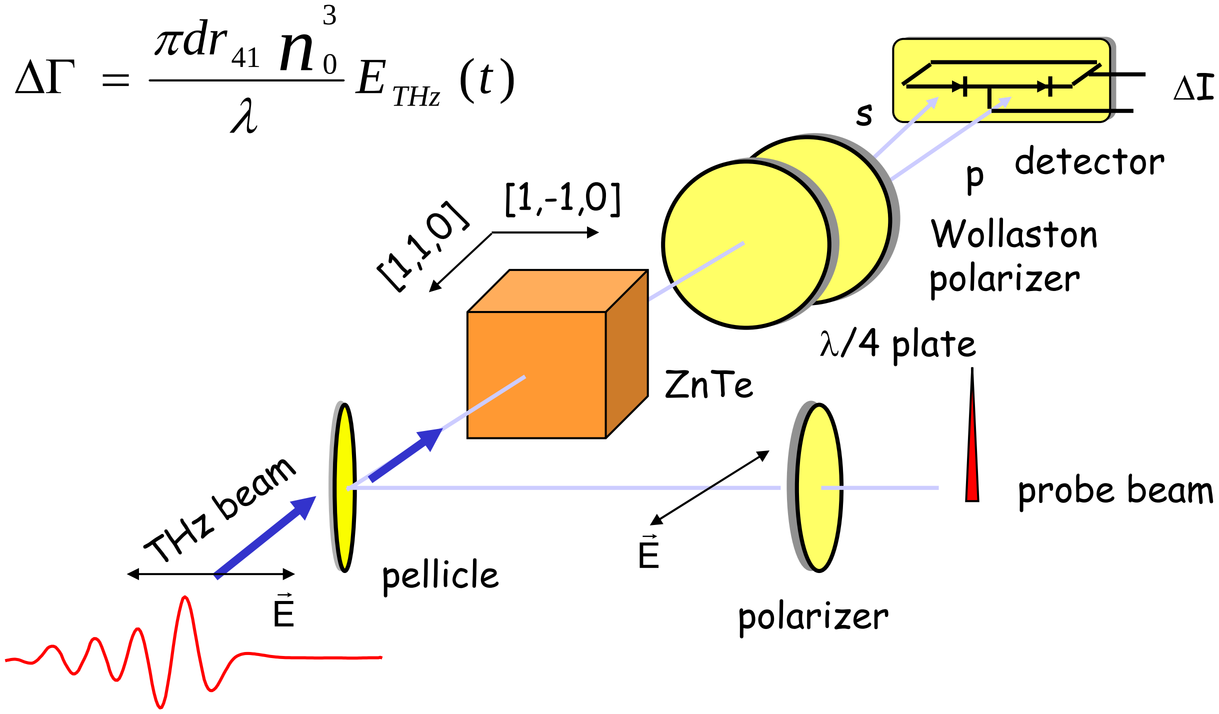

Polarization of the THz field, the probe, and ZnTe [1,-1,0] are parallel
Phase matching condition (Δk=0): optical group velocity = THz phase velocity

Free-Space THz Sensing and Imaging (Reflection Mode)

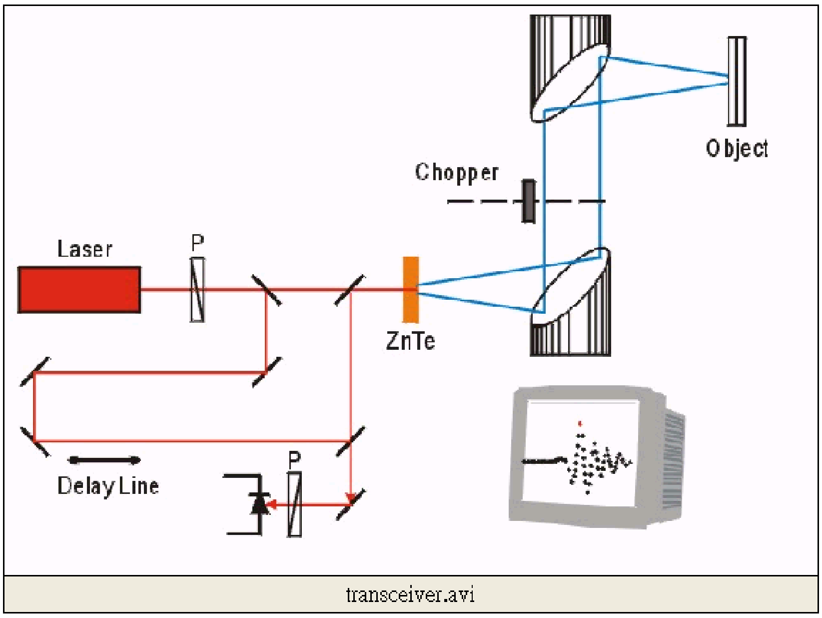

Coherent generation and spectral synthesis of THz radiation with multiple stages of optical rectification

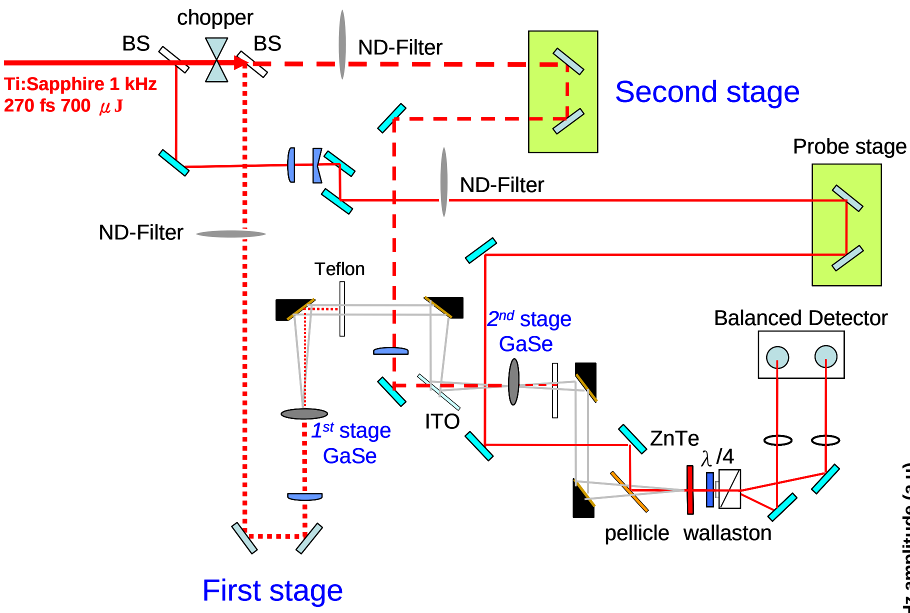

Experimental

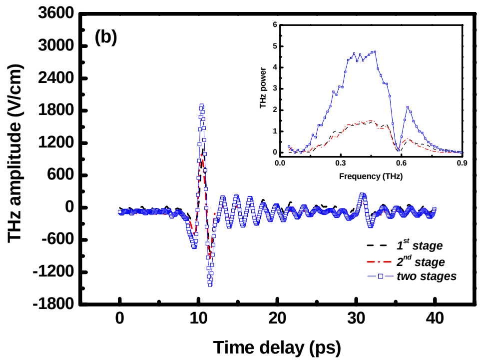

Theoretical

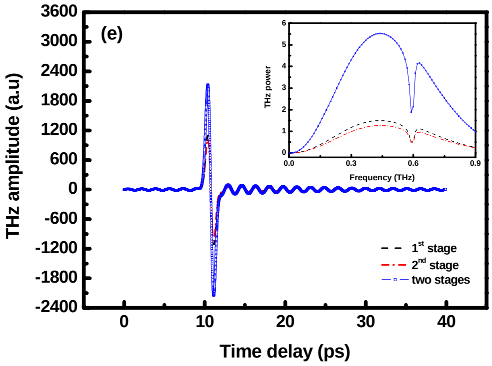

Opt. Exp., September 1, 2008

AIP VJUS, patents filed

CW THz Generation by Photomixing or Heterodying

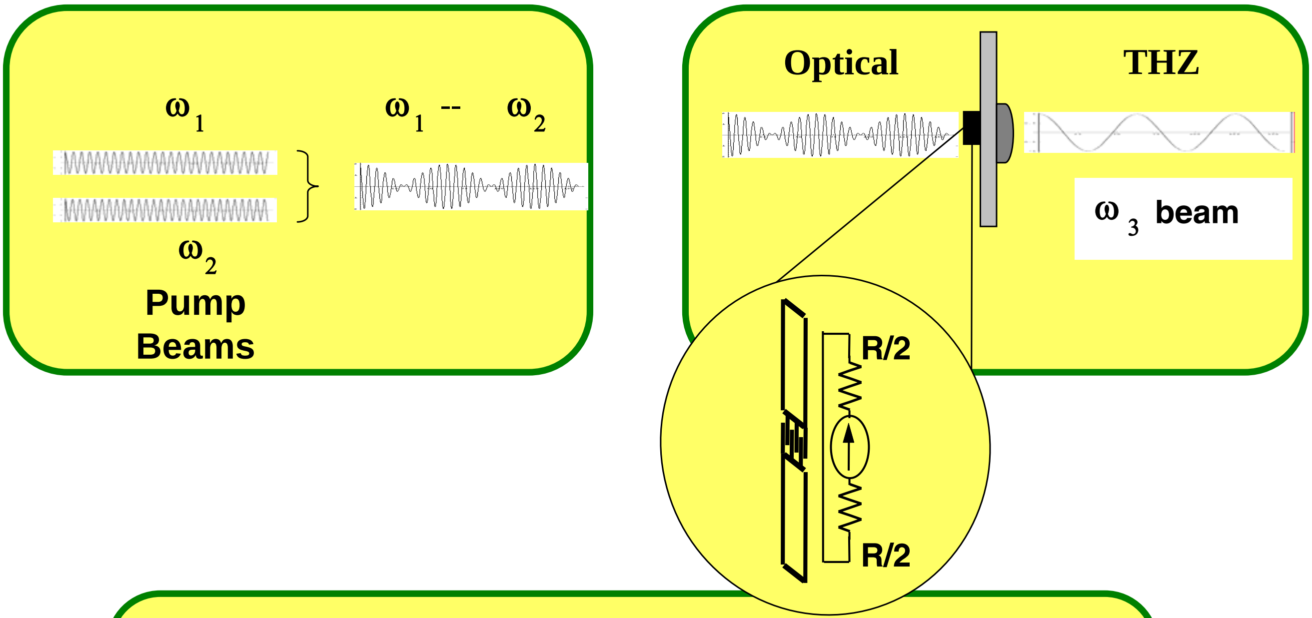

$$P_3 = \frac{R}{2}\eta_1\lambda_1\eta_2\lambda_2\left(\frac{eg}{hc}\right)^2 \frac{P_1P_2}{\left[1+(\omega_3\tau)^2\right]\left[1+(\omega_3RC)^2\right]}$$

CW THz Generation w/ 2 LDs

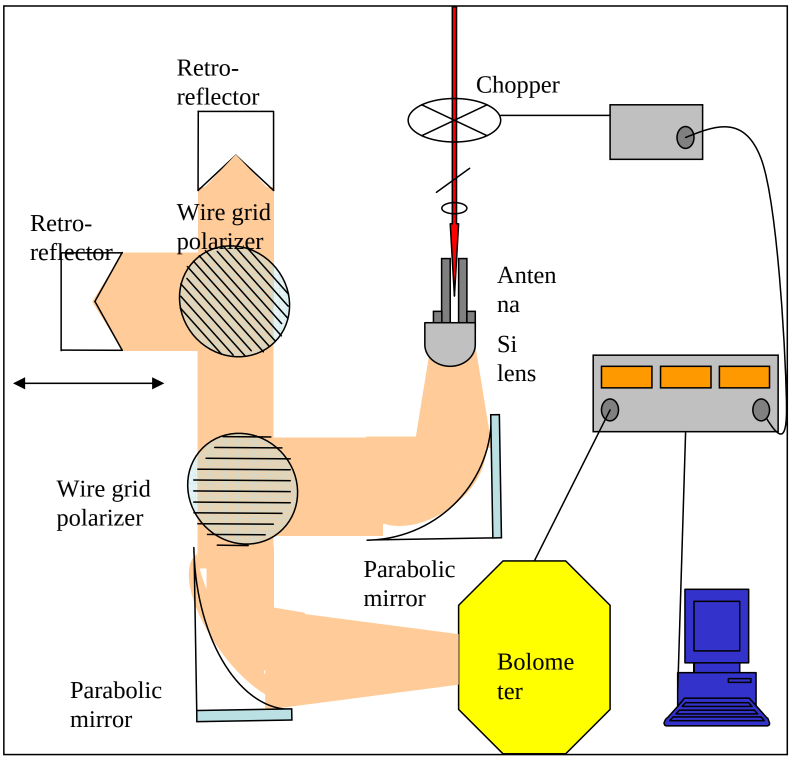

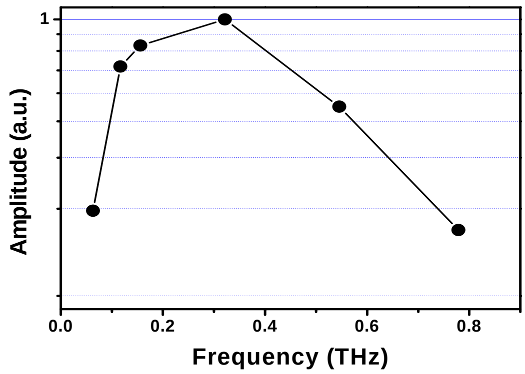

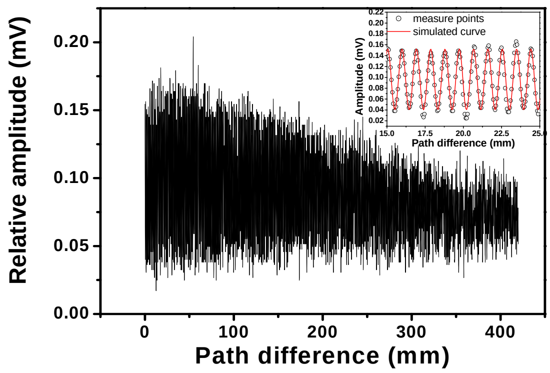

Narrow line width CW THz radiation generation and detection by photoconductive antenna

Dual wavelength frequency stability~250MHz ==> CW THz linewidth

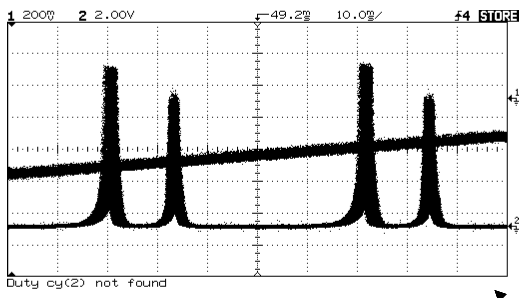

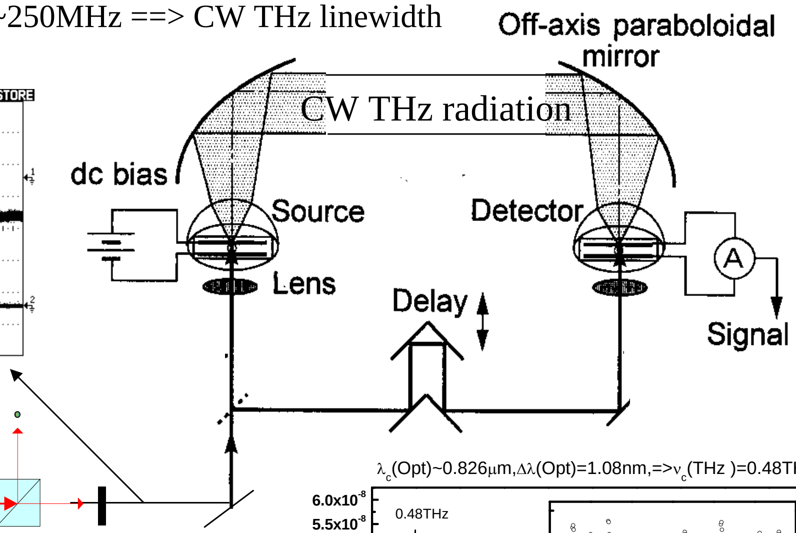

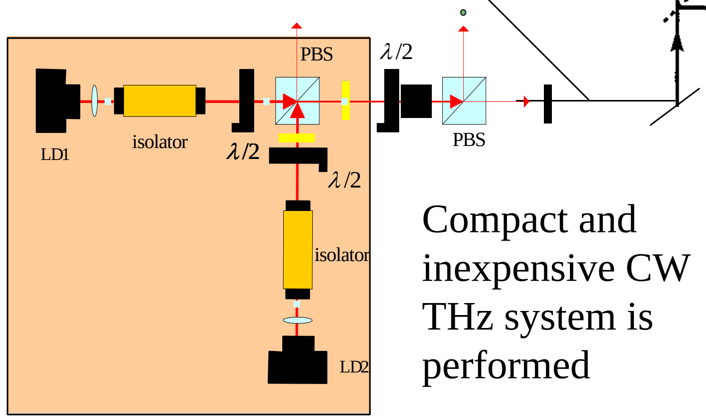

Compact and inexpensive CW THz system is performed

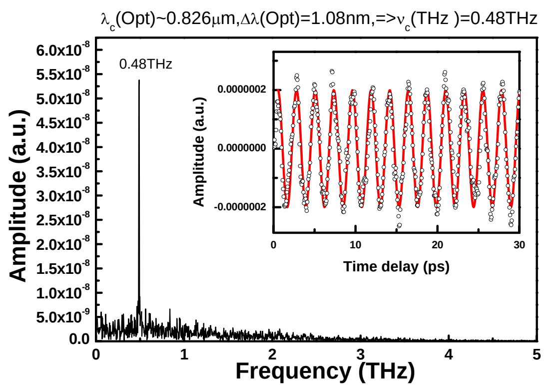

Optical-Pump-Terahertz-Probe studies of femtosecond-laser annealed a-Si

Fitting with Drude model

Grain size : 500 nm

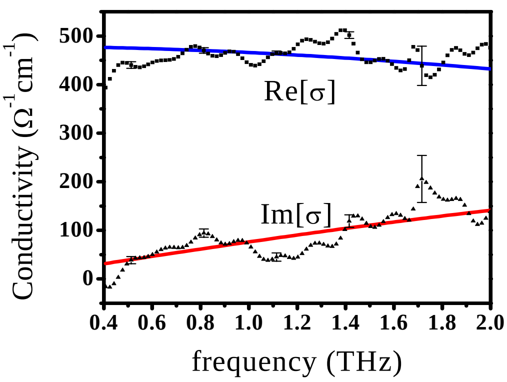

Grain size : 50 nm

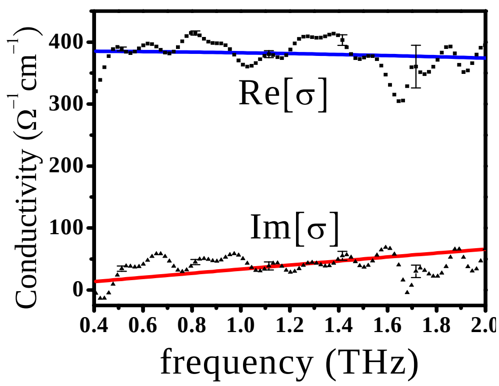

Sample	Average grain size (nm)	mobility (cm^2/Vs)	Plasma frequency (10^{13} Hz)
Bulk-Si (Hall measurement)		158-299	
Bulk-Si (THz-TDS)		162±6.5	8.29±0.21
Poly-Si with large grain size	~ 500	175±19.4	7.26±0.36
Poly-Si with small grain size	~ 50	94.5±20.2	7.20±0.04

- » The mobility measured by THz-TDS is in good agreement with electrical Hall effect measurement result.
- » OPTP and THz-TDS are effective techniques to differentiate annealed quality of polycrystalline silicon.

Motivation

» Thin Film Transistors (**TFTs**) for Flat Panel Displays (**FPDs**).
  - » Mobility of *amorphous silicon (a-Si:H)* : 0.5~1 cm^2/Vs.
  - » Mobility of *polycrystalline silicon (poly-Si)* : 30~300 cm^2/Vs.

» Diagnose of poly-Si.
  - » The Hall Measurement.
  - » SEM picture – *tiny area*.
  - » TFTs fabrication and electrical measurement – *several days and more complicated*.

» OPTP and THz-TDS system → directly identify the average annealing quality of poly-Si in a large area.

Laser Annealing Station

Schematic annealing station

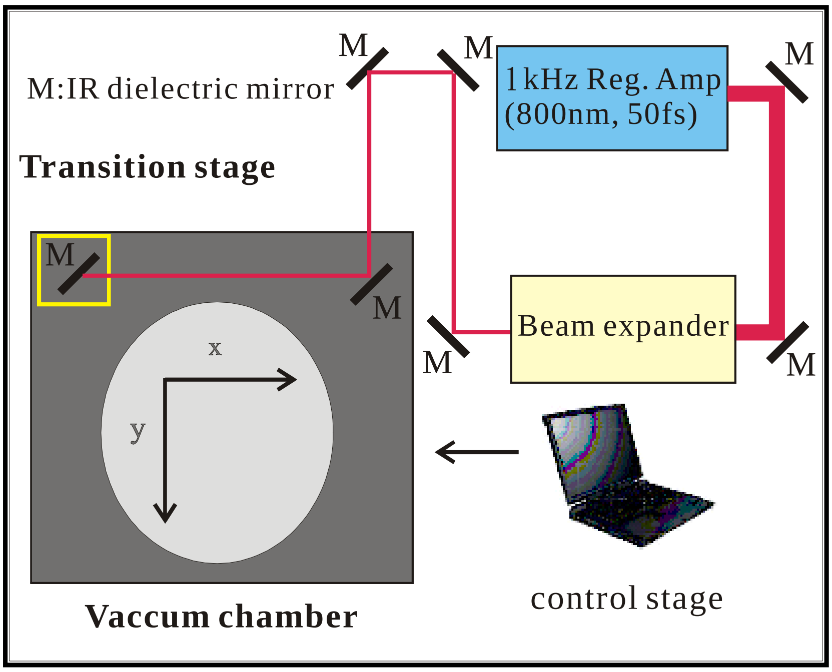

Femtosecond laser annealing chamber and transition stage.

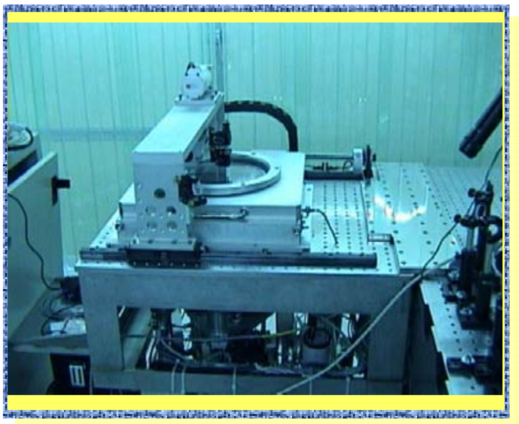

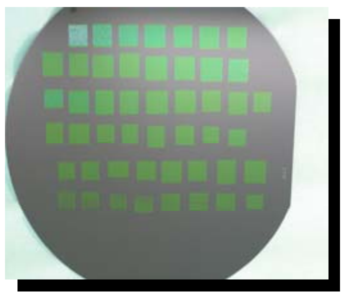

Characterization of Annealed Samples

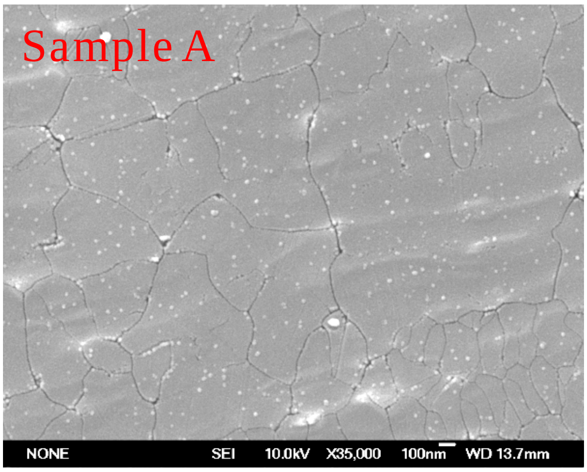

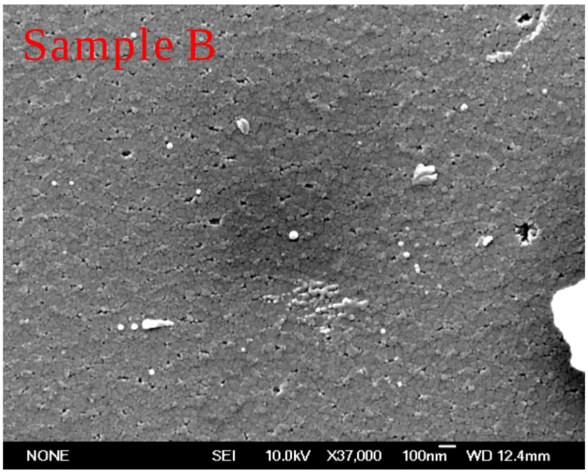

Fluence	40±0.5 mJ/cm^2
Grain size	~500 nm

Fluence	35±0.5 mJ/cm^2
Grain size	~50 nm

Experimental setup for Optical-Pump THz Probe

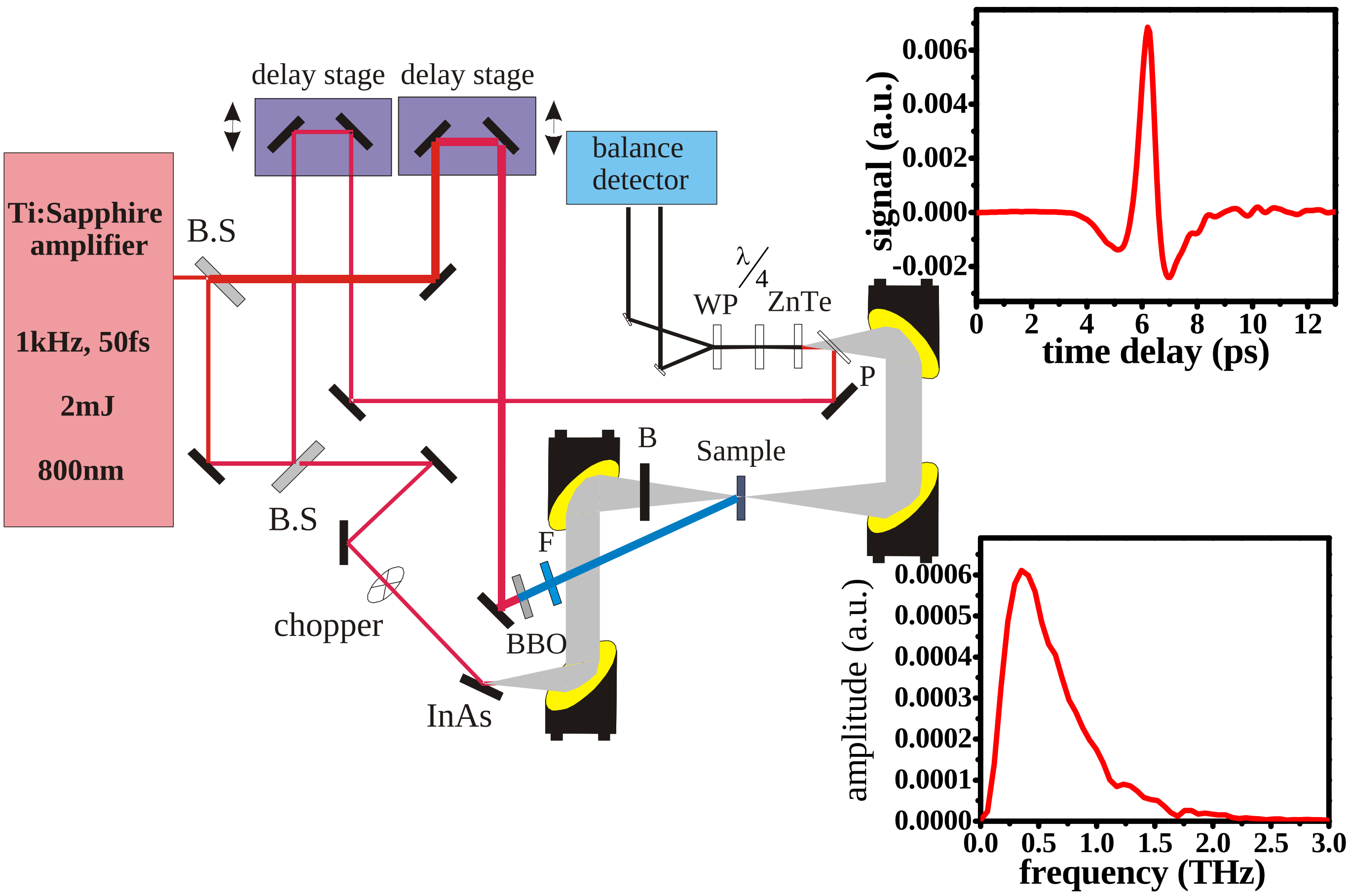

Optical Pump Terahertz Probe

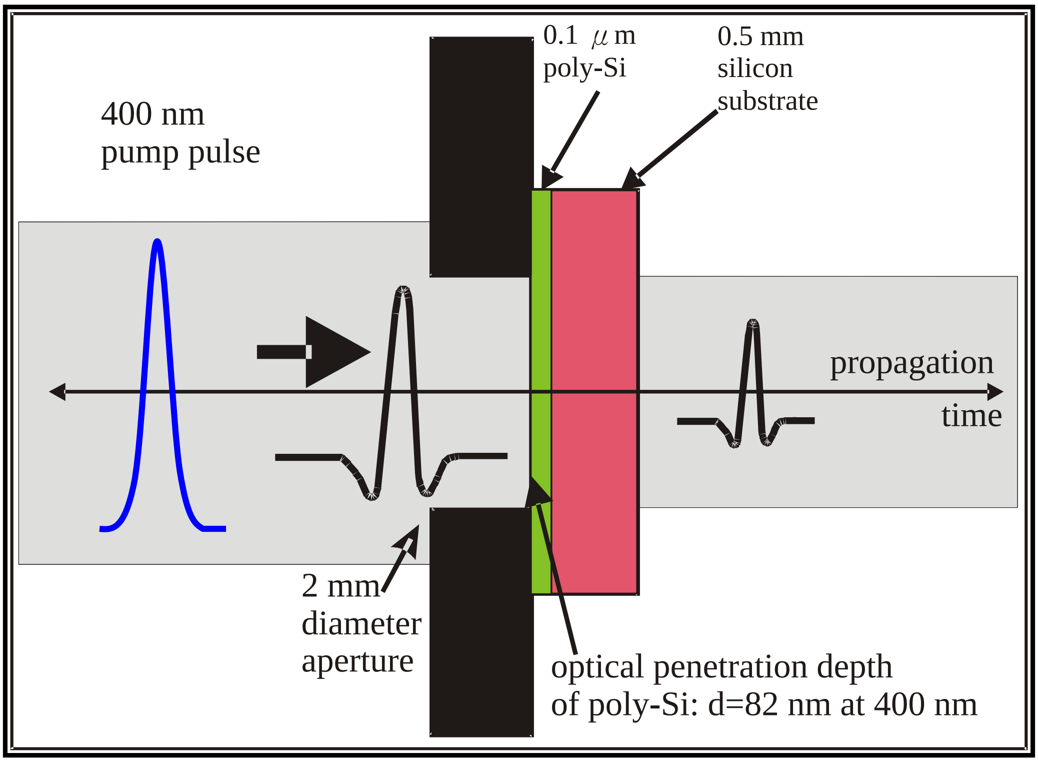

Differential transmission, $\Delta T / T_0 = (T - T_0) / T_0$

InN as efficient THz emitter and its THz spectroscopy

InN

- Eg ~ 0.7 eV
- Wide absorption spectra
- High mobility

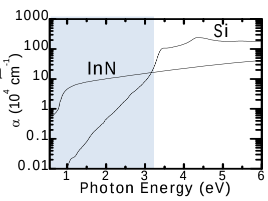

Challenges for semiconductor-based THz emitter

- Power loss due to total internal reflection at the interface
- Improvement of light extraction from emitter

Solution

- Nanostructured emitter
- Rotation of surface electric field

Prof. H. Ahn
Prof. C.-L. Pan

THz emission from nanostructures

H. Ahn, et al., APL ***91****, 132108 (2007)*

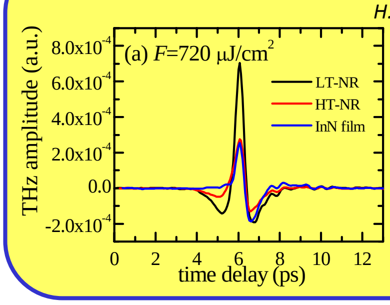

Increase of absorption/emission surface in nanostructure

10 times of power enhancement from nanostructured InN

THz emission from nonpolar InN

H. Ahn, et al., APL ***92****, 102103 (2008)*

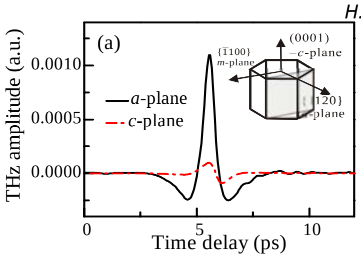

Rotation of dipole oscillation for efficient light extraction

100 times of power enhancement from a-plane InN compared to c-plane InN

THz spectroscopy of InN

H. Ahn, et al., APL ***91****, 163105 (2007)*

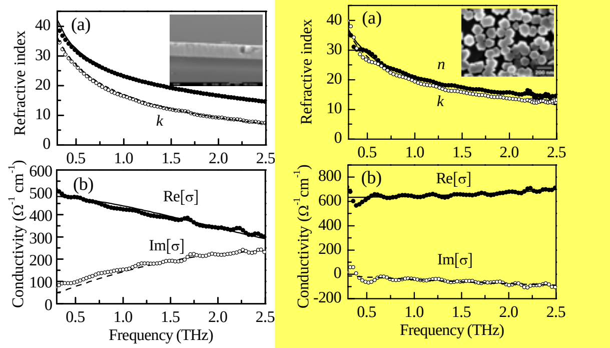

Conductivity of nanostructured material cannot be described by the Drude model..

InN epilayer	InN nanorod
Drude model	Non-Drude (Drude-Smith) model
$\sigma(\omega) = \frac{\varepsilon_0 \omega_p^2 \tau_0}{1 - i\omega\tau_0}$	$\sigma(\omega) = \frac{\varepsilon_0 \omega_p^2 \tau_0}{1 - i\omega\tau_0}\left[1 + \frac{c}{1 - i\omega\tau_0}\right]$

c<0 for nanorods due to backscattering of electrons

THz Imaging: Examples

1. Water marks on bills

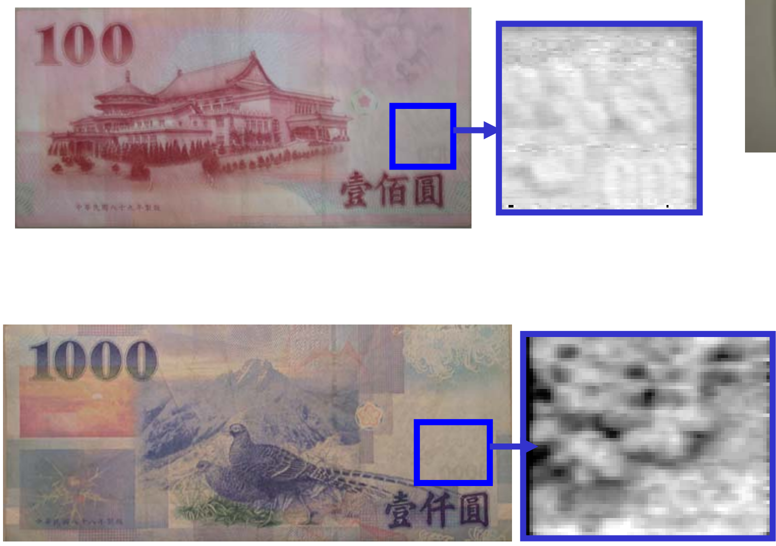

2. Non-contact content-specific detection of powers

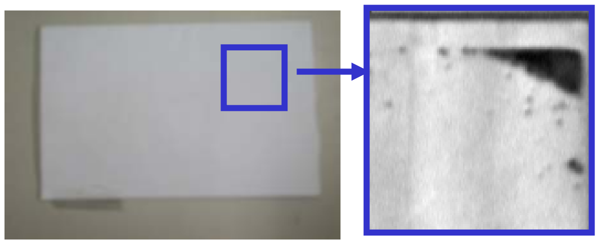

Advantages and Applications

- Safe to humans
- Non-contact
- Excellent S/N
- Applications limited by your imagination

THz Movie of a Match Box

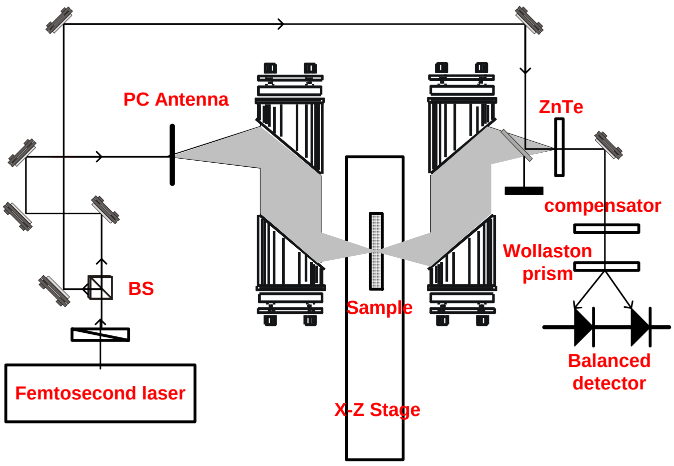

time domain (amplitude)

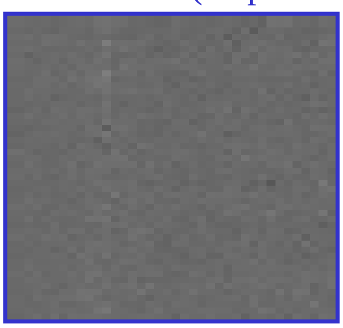

frequency domain (amplitude)

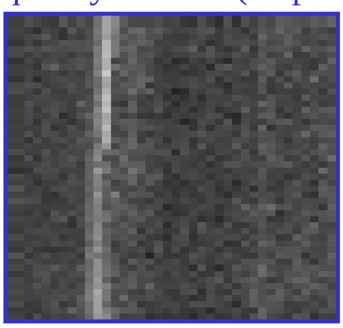

phase

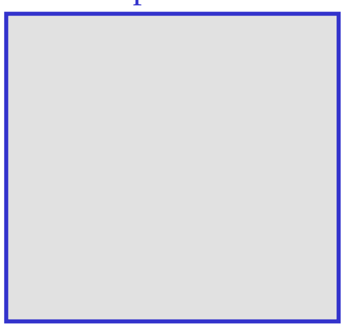

Burn-depth detection with T-ray technology

In collaboration w/ITRI

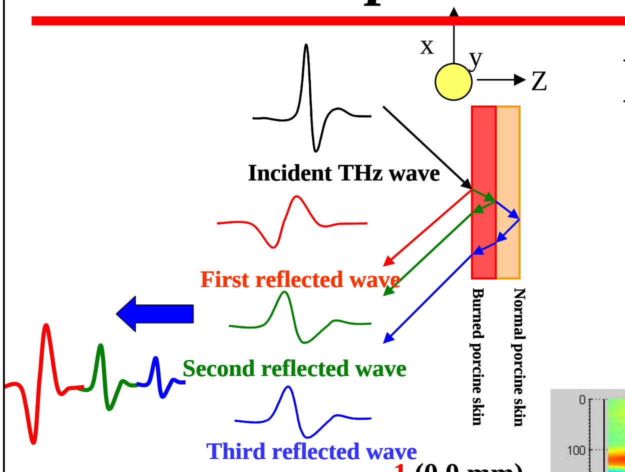

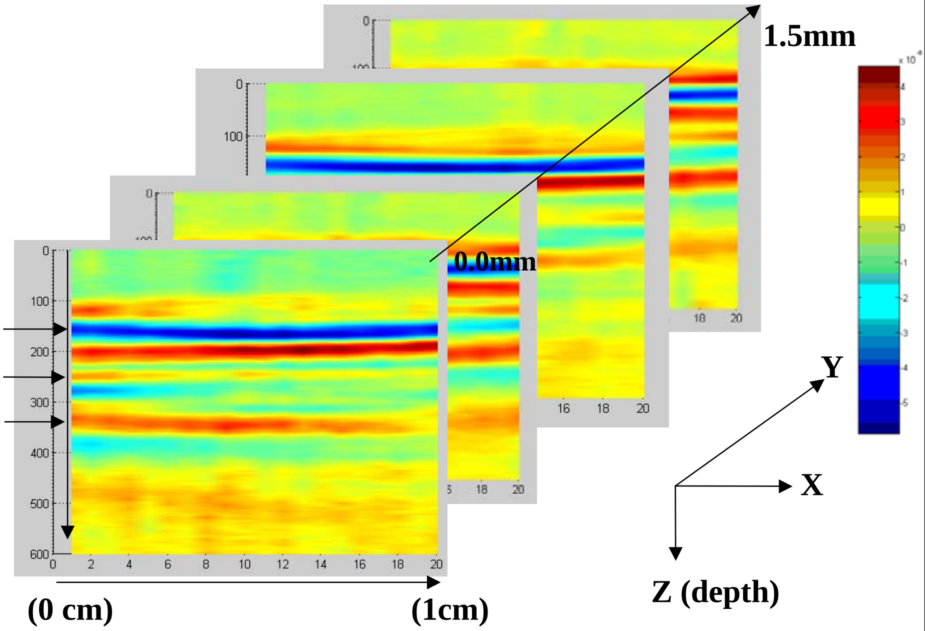

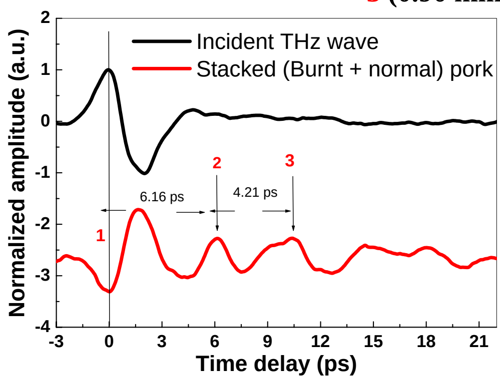

Burnt depth of 0.53mm is resolved via THz imaging , Taiwan patent I276425, U.S. Patent allowed on Aug. 3, 2007

Terahertz air-core microstructure fiber

RESEARCH HIGHLIGHTS

QUANTUM OPTICS

One at a time

Science **319**, 1062–1065 (2008)

Nonlinear optics usually involves the interaction of a large number of photons with a large number of atoms. To reduce this down to the single-atom and single-photon level, the strength of the interaction between light and matter must be enhanced. Barak Dayan and colleagues at the California Institute of Technology have now used microresonators to achieve this enhancement, enabling them to dynamically control the flow of individual photons using just one atom.

High-quality cavities or resonators are now frequently used as a means for investigating the quantum interaction of individual atoms and photons. Dayan *et al.* created silica, toroid-shaped cavities with a major diameter of 25 μm and a minor diameter of 6 μm. A caesium atom, laser-trapped and cooled to approximately 10 μK, is then dropped into the resonator. Weak laser light is coupled into and out of the cavity through a tapered waveguide that passes near the resonator. The interaction between the incoming light and the atom creates a 'photon turnstile', where the detection of an initial photon in the forward-propagating direction results in subsequent photons from the incident flux being re-routed. As a result, whereas the number of photons entering the photon turnstile is governed by statistics, the photons exiting in the forward-propagating direction do so one at a time. Such single-photon sources could one day play a key role in quantum information processing, and the small size of the resonators means that they are compatible with atom-chip technology.

OPTICAL CLOCKS

Beating the standard

Science doi: 10.1126/science.1153341 (2008)

The timing accuracy offered by optical atomic clocks makes the mind boggle, far surpassing many other timekeeping techniques. Now, Andrew Ludlow and co-workers at the National Institute of Standards and Technology (NIST) and the University of Colorado have overcome the limitations in measuring the accuracy of these devices.

The only way to get an idea of the accuracy of one clock is by comparing it to another. But when just a single device requires a large amount of expensive, complicated and stable optics, the chance of having two in the same laboratory is very slim. The alternative is to compare two remote set-ups. However, conventional ways of doing this, for example the use of global-positioning satellites or microwave-frequency networks, are simply not stable enough to transfer the phenomenal accuracy of optical clocks.

Ludlow *et al.* have now shown how an optical link can be used to compare two optical atomic clocks. Their aim was to assess the accuracy of a clock at the University of Colorado, which uses an ensemble of neutral strontium atoms, using a calcium-atom-based clock at NIST, 4 km away. Optical frequency combs are the key: each optical clock can be phase-locked to a frequency comb. The comb at the University of Colorado can in turn be locked to a 1,064-nm laser beam, which is sent to NIST along an optical-fibre link, enabling a comparison. In this way, the team show that the uncertainty of their strontium-based clock now surpasses that of the caesium clocks used as the primary standard.

TERAHERTZ WAVEGUIDES

Low-loss guides

Appl. Phys. Lett. **92**, 064105 (2008)

High dielectric loss and conduction in metals have been troublesome for the design of optical-fibre and metal-waveguide systems at terahertz frequencies. To overcome these problems, a collaboration of scientists in Taiwan has proposed the use of terahertz air-core microstructure fibres.

The researchers fabricated fibres comprising a hollow core surrounded by a cladding layer formed from periodic arrangements of flexible, commercially available polytetrafluoroethylene tubes. They made four different fibres with inner and outer diameters varying between 0.81 mm and 1.68 mm, and between 1.11 mm and 2.08 mm, respectively. They also varied the centre-to-centre distance between the cladding tubes.

The combined coupling and propagation losses of the fibres were measured to be much less than 0.01 cm^{-1}, and the band of frequencies across which each fibre operated could be adjusted by linear scaling of the fibre size. At 770 GHz, an attenuation as low as 0.002 cm^{-1} was achieved.

Simulations of the terahertz transmission spectra, calculated using the finite-difference time-domain method, were in quite good agreement with the experimental results. However, the photonic-bandgap spectra did not match so well, suggesting that the bandgap does not dominate the guiding mechanism. The same frequency-dependent behaviour was shown for both one ring and three rings of cladding tubes. According to the researchers, these trends suggest that the guiding mechanism is similar to a phenomenon known as antiresonant reflecting optical guiding (ARROW).

METAMATERIALS

Tunable transmission

Opt. Lett. **33**, 545–547 (2008)

Metamaterials have captured the imagination recently owing to the unique optical properties gained from their artificial structure and the fascinating phenomena they make possible, such as superlensing and cloaking. With the aim of extending their usefulness still further, researchers from Pennsylvania State University in the USA have proposed a near-infrared, metamaterial film that has reconfigurable transmission and reflection properties.

To achieve this, Do-Hoon Kwon and co-workers exploit the characteristics of nematic liquid crystals. Their metamaterial design consists of a planar, periodic array of subwavelength resonators embedded in silica: each resonator is made up of two silver nanoplates sandwiching a spacer layer of anisotropic nematic liquid crystals. By rotating the orientation of the liquid crystals, their optical behaviour can be controlled. This, in turn, enables tuning of the material parameters of the metamaterials. Numerical calculations were used to optimize the dimensions of the resonators and to maximize the difference between the achievable transmittance and reflectance: the thickness of the silver nanoplates should be 149 nm, and that of the liquid-crystal spacer 200 nm, the minimum practical value. Both should have a width of 391 nm. Further simulations predicted that the transmittance of 1.1-μm light through this structure could be continuously tuned from 0.1% to 98.7%.

© 2008 Nature Publishing Group

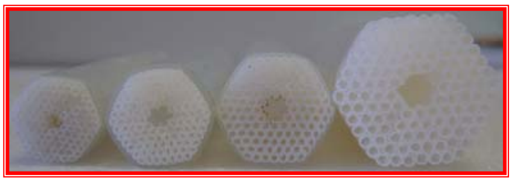

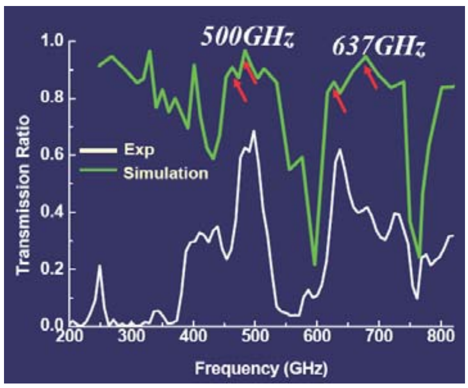

APL, 14 February 2008 highlighted by **Nature Photonics**, April, 2008

http://www.nature.com/nphoton/journal/v2/n4/full/nphoton.2008.39.html

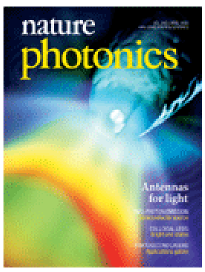

THz Endoscope (Prof. C. K. Sun, NTU)

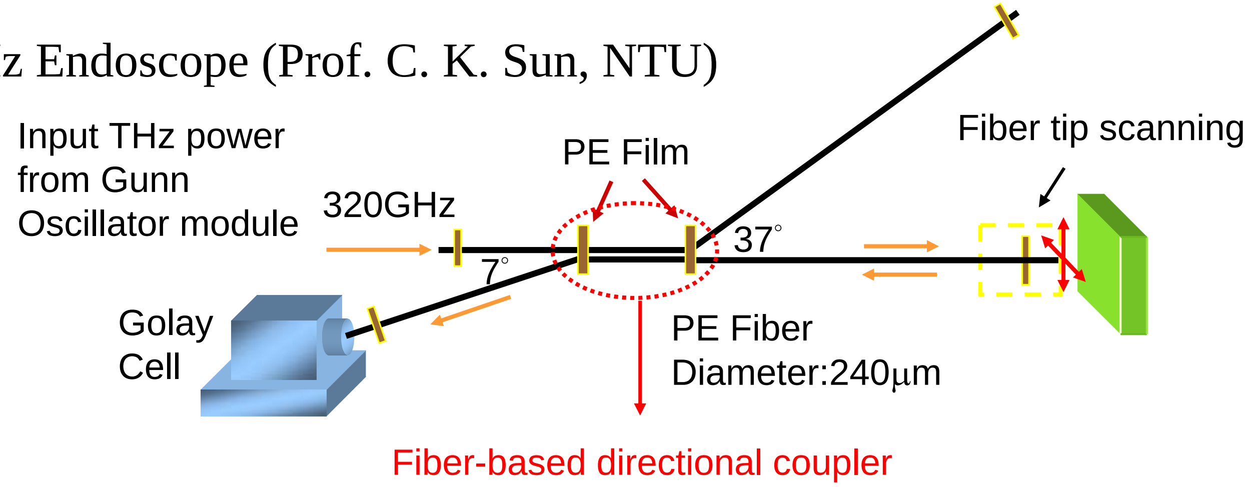

Application: 3D Reconstructed Image of Burned Porcine Skin

Burned area

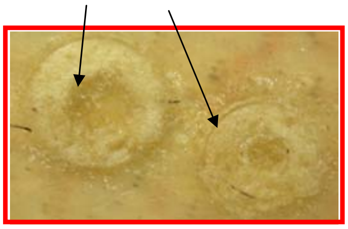

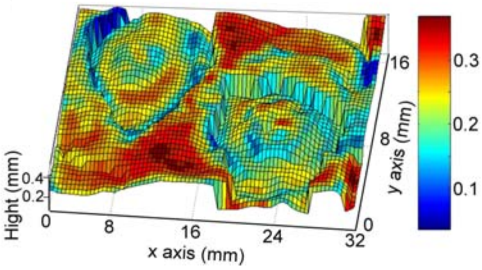

Advantages

- *Suitable for imaging of highly absorbed material*
- *Directive scanning fiber tip for 2D imaging*

APL and Opt. Exp, 2008

Terahertz air-core microstructure fiber

RESEARCH HIGHLIGHTS

QUANTUM OPTICS

One at a time

Science **319**, 1062–1065 (2008)

Nonlinear optics usually involves the interaction of a large number of photons with a large number of atoms. To reduce this down to the single-atom and single-photon level, the strength of the interaction between light and matter must be enhanced. Barak Dayan and colleagues at the California Institute of Technology have now used microresonators to achieve this enhancement, enabling them to dynamically control the flow of individual photons using just one atom.

High-quality cavities or resonators are now frequently used as a means for investigating the quantum interaction of individual atoms and photons. Dayan *et al.* created silica, toroid-shaped cavities with a major diameter of 25 μm and a minor diameter of 6 μm. A caesium atom, laser-trapped and cooled to approximately 10 μK, is then dropped into the resonator. Weak laser light is coupled into and out of the cavity through a tapered waveguide that passes near the resonator. The interaction between the incoming light and the atom creates a 'photon turnstile', where the detection of an initial photon in the forward-propagating direction results in subsequent photons from the incident flux being re-routed. As a result, whereas the number of photons entering the photon turnstile is governed by statistics, the photons exiting in the forward-propagating direction do so one at a time. Such single-photon sources could one day play a key role in quantum information processing, and the small size of the resonators means that they are compatible with atom-chip technology.

OPTICAL CLOCKS

Beating the standard

Science doi: 10.1126/science.1153341 (2008)

The timing accuracy offered by optical atomic clocks makes the mind boggle, far surpassing many other timekeeping techniques. Now, Andrew Ludlow and co-workers at the National Institute of Standards and Technology (NIST) and the University of Colorado have overcome the limitations in measuring the accuracy of these devices.

The only way to get an idea of the accuracy of one clock is by comparing it to another. But when just a single device requires a large amount of expensive, complicated and stable optics, the chance of having two in the same laboratory is very slim. The alternative is to compare two remote set-ups. However, conventional ways of doing this, for example the use of global-positioning satellites or microwave-frequency networks, are simply not stable enough to transfer the phenomenal accuracy of optical clocks.

Ludlow *et al.* have now shown how an optical link can be used to compare two optical atomic clocks. Their aim was to assess the accuracy of a clock at the University of Colorado, which uses an ensemble of neutral strontium atoms, using a calcium-atom-based clock at NIST, 4 km away. Optical frequency combs are the key: each optical clock can be phase-locked to a frequency comb. The comb at the University of Colorado can in turn be locked to a 1,064-nm laser beam, which is sent to NIST along an optical-fibre link, enabling a comparison. In this way, the team show that the uncertainty of their strontium-based clock now surpasses that of the caesium clocks used as the primary standard.

TERAHERTZ WAVEGUIDES

Low-loss guides

Appl. Phys. Lett. **92**, 064105 (2008)

High dielectric loss and conduction in metals have been troublesome for the design of optical-fibre and metal-waveguide systems at terahertz frequencies. To overcome these problems, a collaboration of scientists in Taiwan has proposed the use of terahertz air-core microstructure fibres.

The researchers fabricated fibres comprising a hollow core surrounded by a cladding layer formed from periodic arrangements of flexible, commercially available polytetrafluoroethylene tubes. They made four different fibres with inner and outer diameters varying between 0.81 mm and 1.68 mm, and between 1.11 mm and 2.08 mm, respectively. They also varied the centre-to-centre distance between the cladding tubes.

The combined coupling and propagation losses of the fibres were measured to be much less than 0.01 cm^{-1}, and the band of frequencies across which each fibre operated could be adjusted by linear scaling of the fibre size. At 770 GHz, an attenuation as low as 0.002 cm^{-1} was achieved.

Simulations of the terahertz transmission spectra, calculated using the finite-difference time-domain method, were in quite good agreement with the experimental results. However, the photonic-bandgap spectra did not match so well, suggesting that the bandgap does not dominate the guiding mechanism. The same frequency-dependent behaviour was shown for both one ring and three rings of cladding tubes. According to the researchers, these trends suggest that the guiding mechanism is similar to a phenomenon known as antiresonant reflecting optical guiding (ARROW).

METAMATERIALS

Tunable transmission

Opt. Lett. **33**, 545–547 (2008)

Metamaterials have captured the imagination recently owing to the unique optical properties gained from their artificial structure and the fascinating phenomena they make possible, such as superlensing and cloaking. With the aim of extending their usefulness still further, researchers from Pennsylvania State University in the USA have proposed a near-infrared, metamaterial film that has reconfigurable transmission and reflection properties.

To achieve this, Do-Hoon Kwon and co-workers exploit the characteristics of nematic liquid crystals. Their metamaterial design consists of a planar, periodic array of subwavelength resonators embedded in silica: each resonator is made up of two silver nanoplates sandwiching a spacer layer of anisotropic nematic liquid crystals. By rotating the orientation of the liquid crystals, their optical behaviour can be controlled. This, in turn, enables tuning of the material parameters of the metamaterials. Numerical calculations were used to optimize the dimensions of the resonators and to maximize the difference between the achievable transmittance and reflectance: the thickness of the silver nanoplates should be 149 nm, and that of the liquid-crystal spacer 200 nm, the minimum practical value. Both should have a width of 391 nm. Further simulations predicted that the transmittance of 1.1-μm light through this structure could be continuously tuned from 0.1% to 98.7%.

206

nature photonics | VOL 2 | APRIL 2008 | www.nature.com/naturephotonics

© 2008 Nature Publishing Group

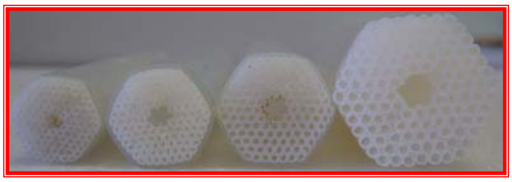

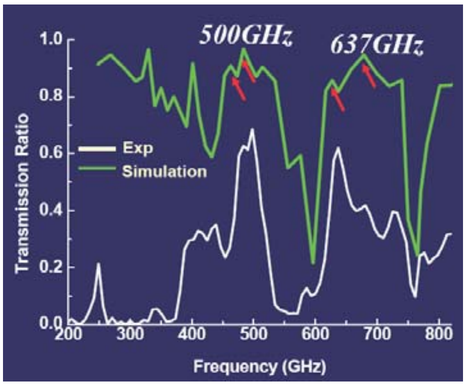

APL, 14 February 2008 highlighted by **Nature Photonics**, April, 2008

http://www.nature.com/nphoton/journal/v2/n4/full/nphoton.2008.39.html

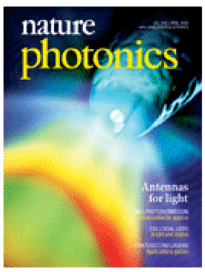

Towards multi-service THz radio-over-fiber

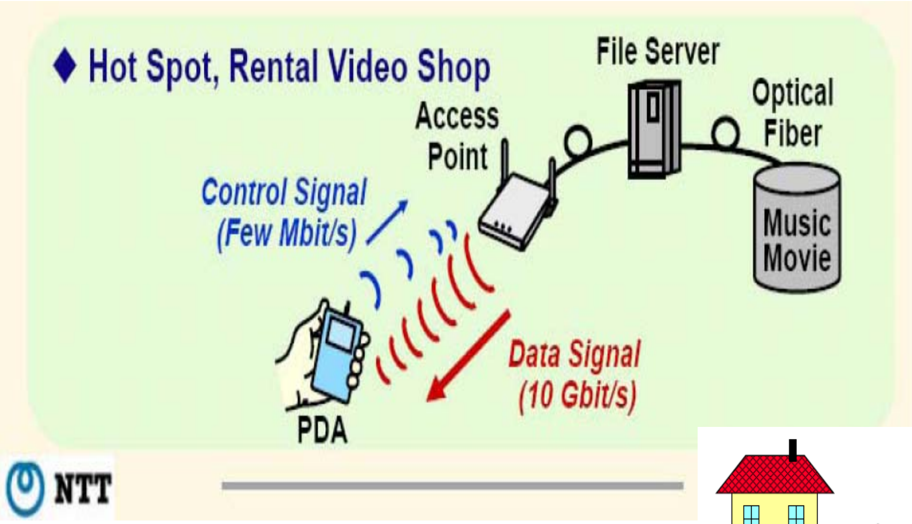

Download your video:
Vision from NTT

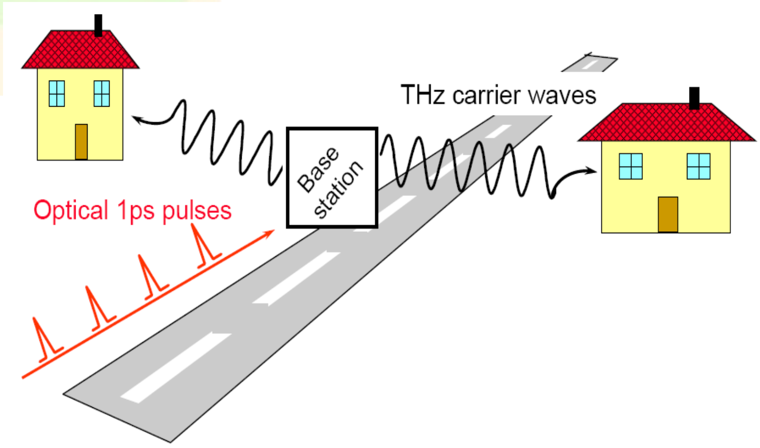

Inexpensive hybrid
fiber-to-home concept

Transmission of burst and audio signal through a Directly-modulated THz communication link

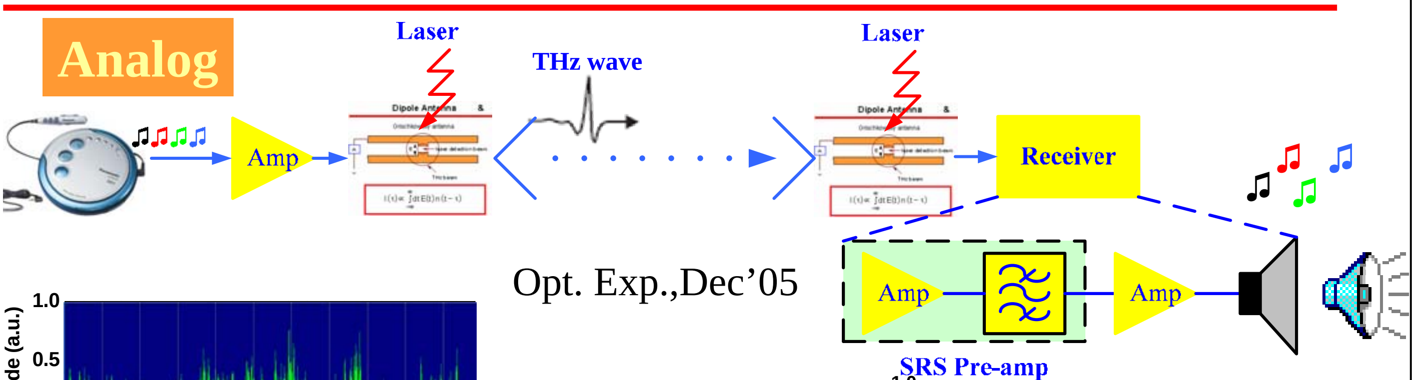

Opt. Exp.,Dec'05

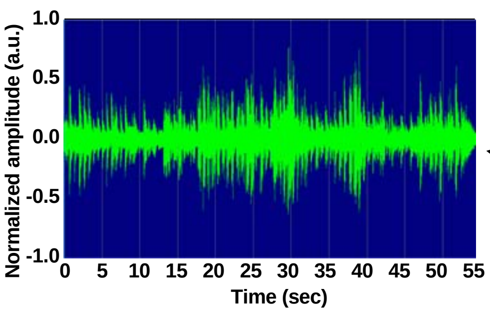

Original music time sequence and a portion of spectrum

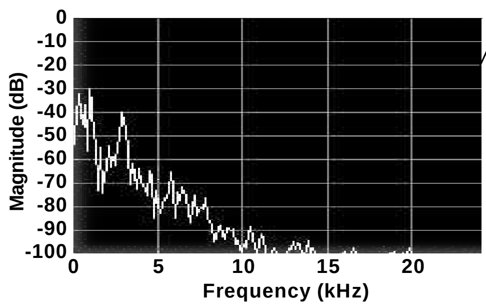

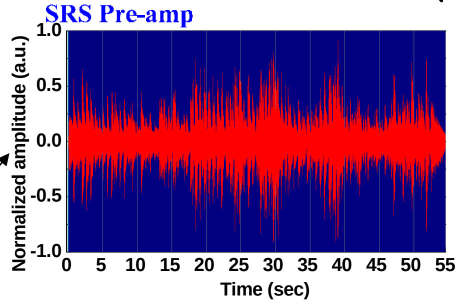

Received music time sequence and a portion of spectrum

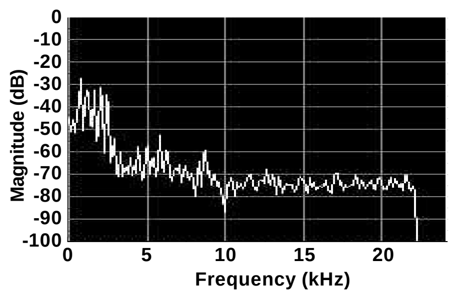

CL Pan Group

Frequency response of our system

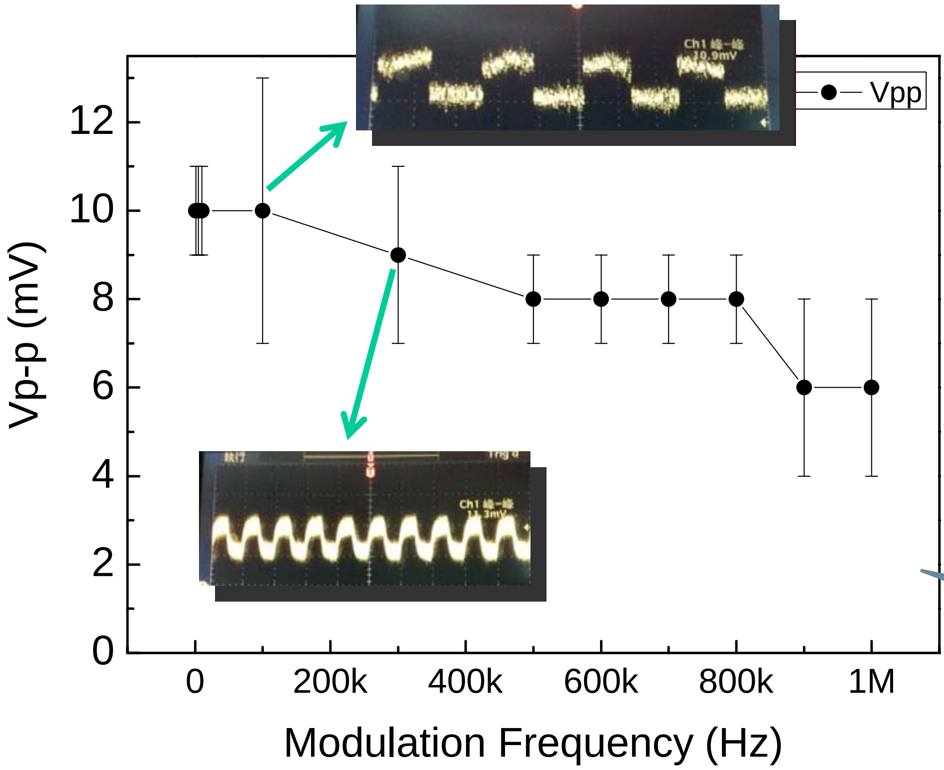

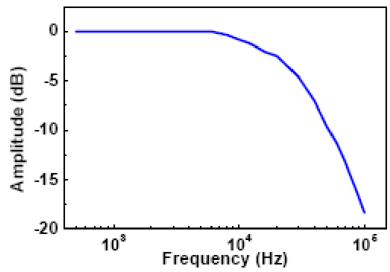

The bandwidth of THz audio link is 20 kHz

The bandwidth of Our system is higher 1MHz

THz Photonics
with
Liquid Crystal Enabled Functionalities

Motivation and Objectives

- Motivations:
  - Increasing demands for THz quasi-optic components.
  - LC has played an important role in the visible optics as well as electro-optics and could be as eminent in THz optics.

- Objectives:
  - Characterization of LCs in the THz regime
  - To develop THz photonic devices with LC-enabled functionality

Liquid Crystal: A Unique State of Matter

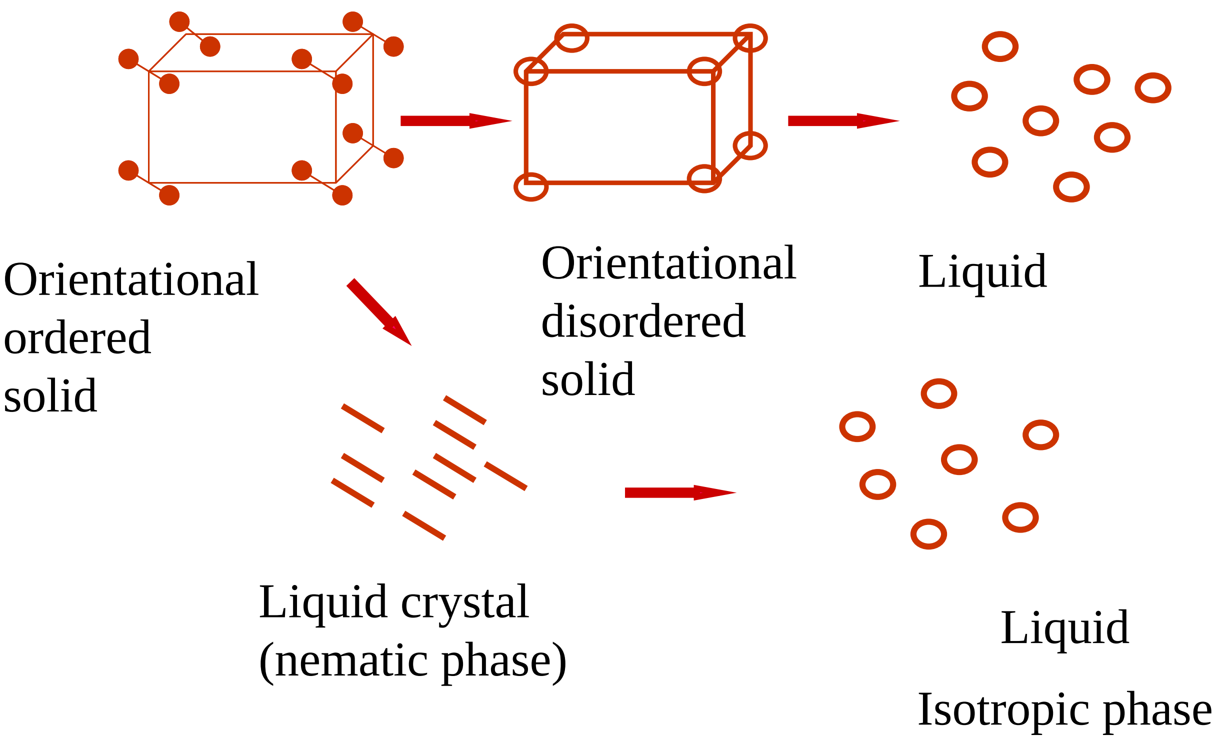

Nemetic Liquid Crystal (N)

Director: $\hat{n}$

$\Rightarrow$Anisotropical

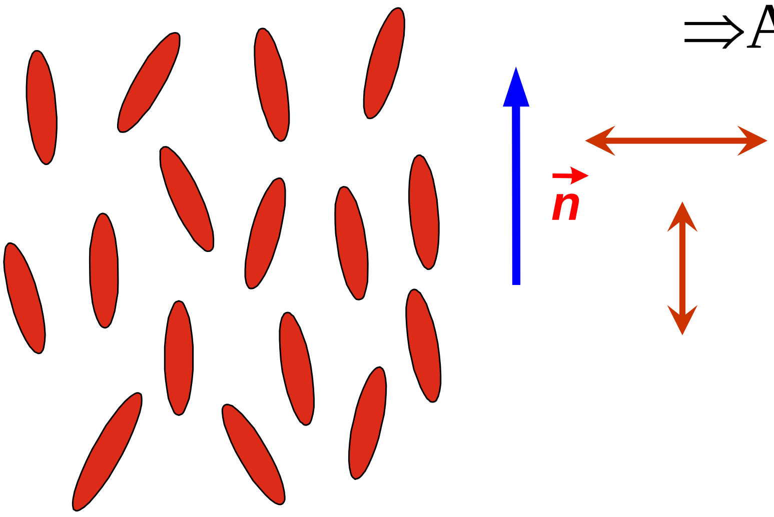

$E_{\perp}$, $\varepsilon_{\perp}$

$E_{\parallel}$, $\varepsilon_{\parallel}$

$\Delta\varepsilon = \varepsilon_{\parallel} - \varepsilon_{\perp}$

$\Delta\chi = \chi_{\parallel} - \chi_{\perp}$

Liquid Crystal Optics

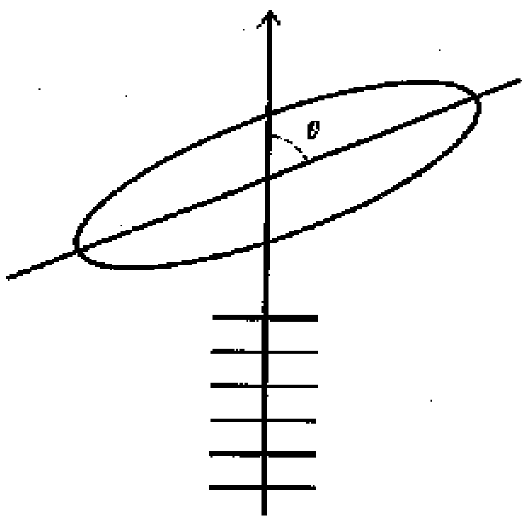

ordinary ray: $n_o = n_{\perp}$

extraordinary ray: $$n_{eff} = \left(\frac{\sin^2\theta}{n_{//}^2} + \frac{\cos^2\theta}{n_{\perp}^2} \right)^{-1/2}$$

Index of refraction and dielectric constant

Typical values:

dielectric constants

$\varepsilon_{//} = 18$

$\varepsilon_{\perp} = 6$

indeces of refraction

$n_{//} = 1.8$

$n_{\perp} = 1.6$

$$n = \sqrt{\varepsilon}$$

5CB: a typical NLC

•5CB (K15): 4’-*n*-pentyl-4-cyanobiphenyl

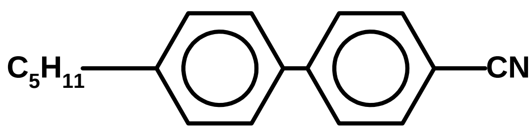

Nematic phase

***T* = 22.4 °C ---- 34.5 °C**

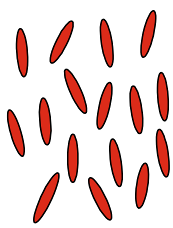

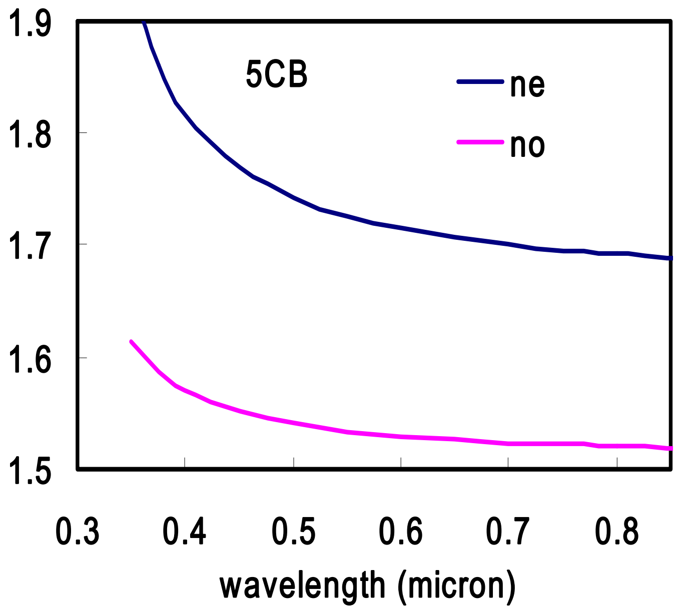

In the visible,

$\Delta n\ (\lambda, T) = n_e - n_o = 0.14 \sim 0.19$

Optical Anisotropy: Phase Shift

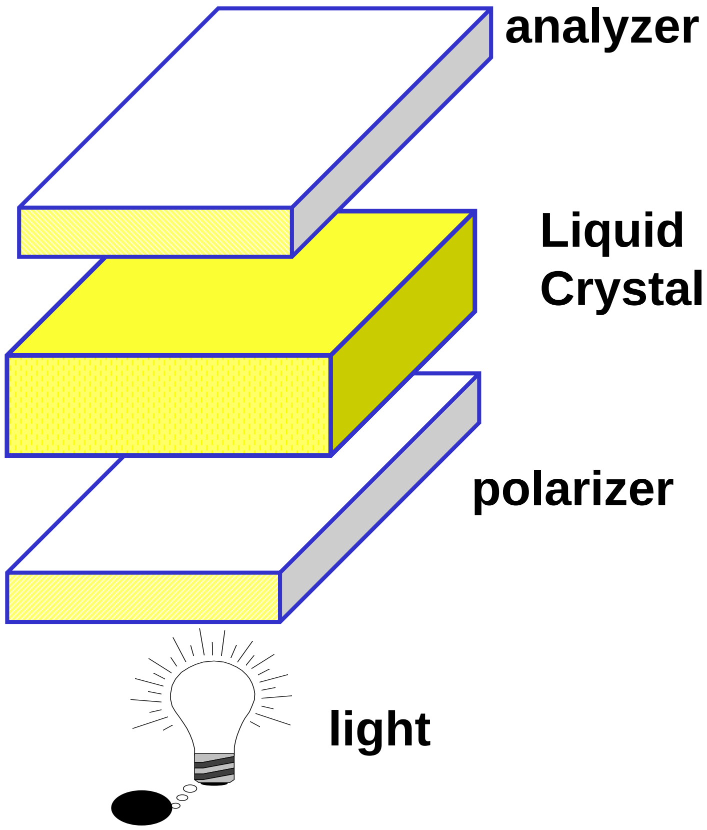

$$\phi = 2\pi d n_{o,e}/\lambda$$

$$\Delta\phi = \phi_e - \phi_o = 2\pi d \Delta n/\lambda$$

$$\Delta n = n_e - n_o$$

$$0 < \Delta n < 0.2$$

depending on deformation

$$380 \text{ nm} < \lambda < 780 \text{ nm}$$

visible light

Twisted Nematic LC Cell: Normally Black

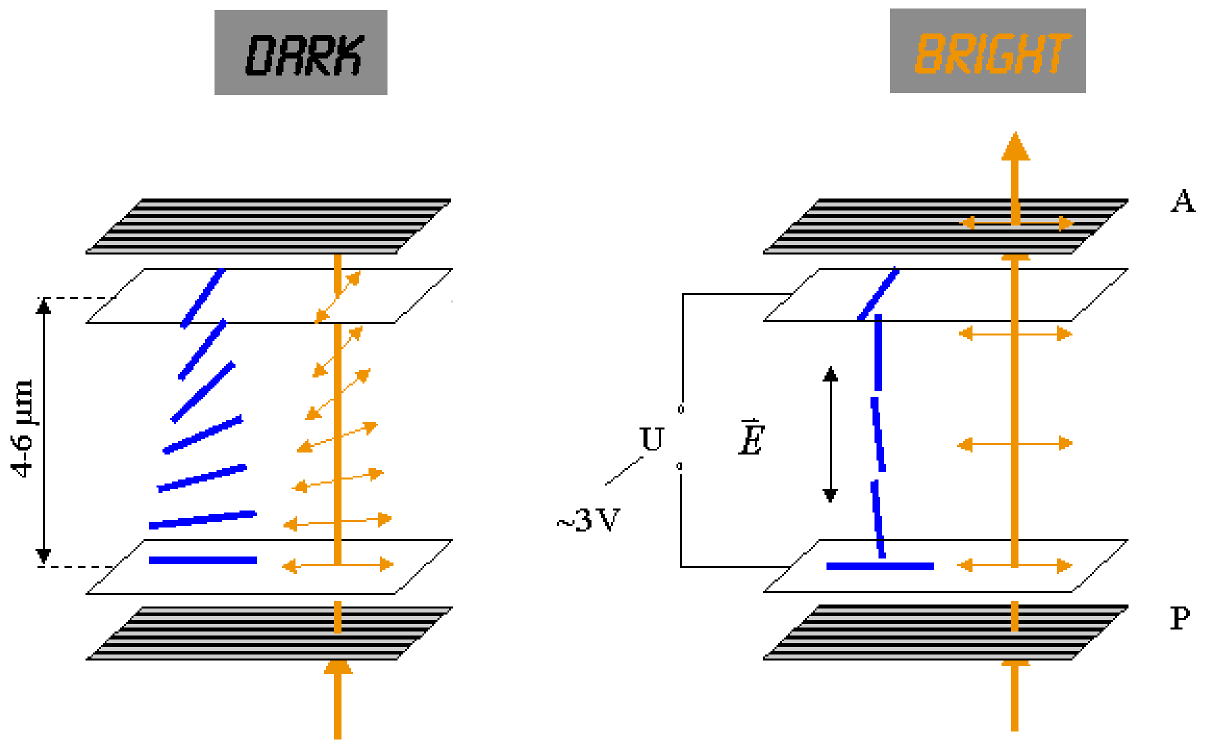

LC optical constants in THz range

$$\tilde{n} = (n, \kappa)$$

Temperature Dependence for 5CB

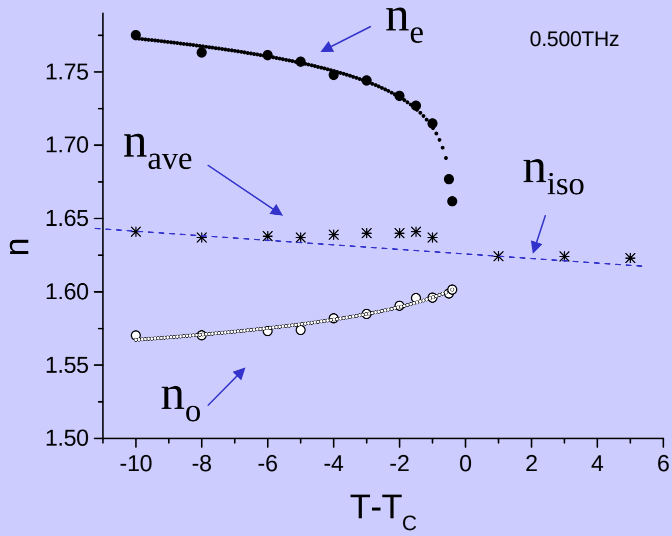

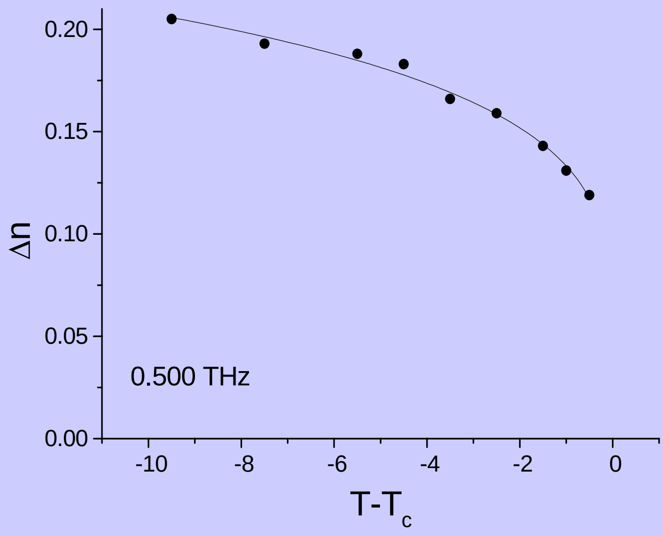

$$n_{ave} = \frac{2n_o + n_e}{3}$$

Measured T_c: 34.5℃

Δn of 5CB: 0.15 ~0.2

Optical Constants of E7 in the THz range

Nematic range: -20°C~60°C

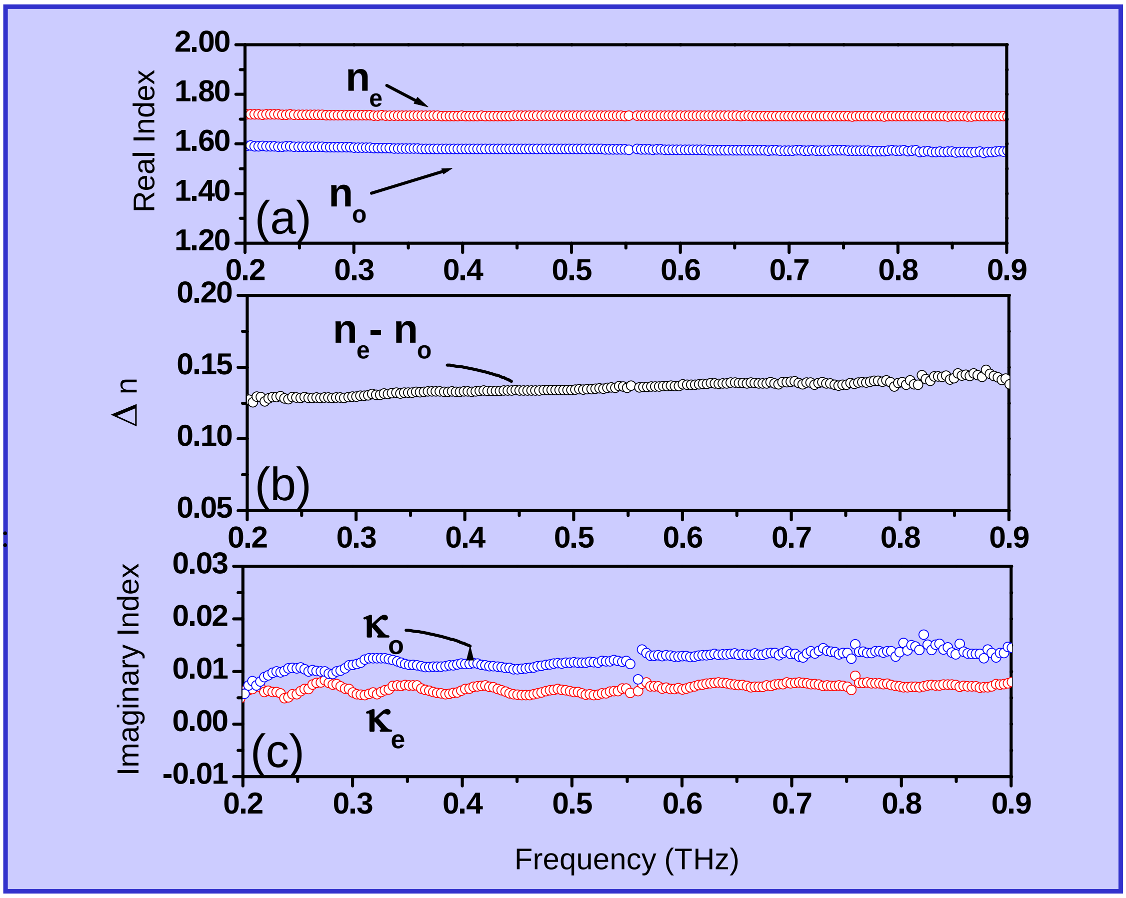

Optical Constants of PCH5 in the THz range

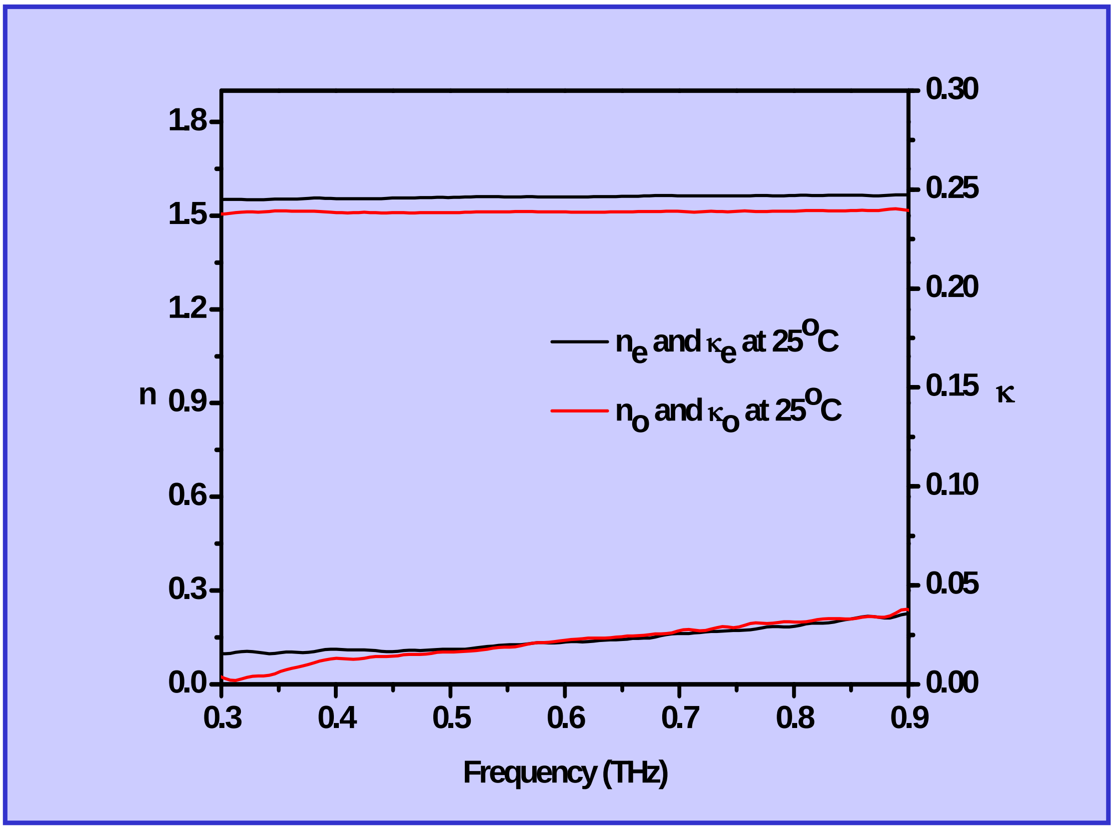

Summary about birefringence

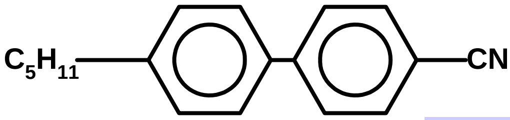

5CB: 0.18 → about 0.18

Similar as in visible and near IR

E7: 0.22 →0.17

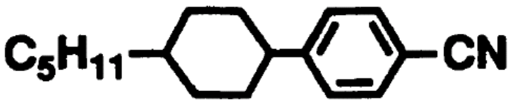

PCH5: 0.08 →0.04

Smaller than in visible and near IR

LC devices for THz

Magnetically controlled tunable THz phase shifter using LC

APL, Dec'03, Opt. Exp., June'04, selected by the Virtual Journal on Ultrafast Sciences, Taiwan Patent, US patents filed

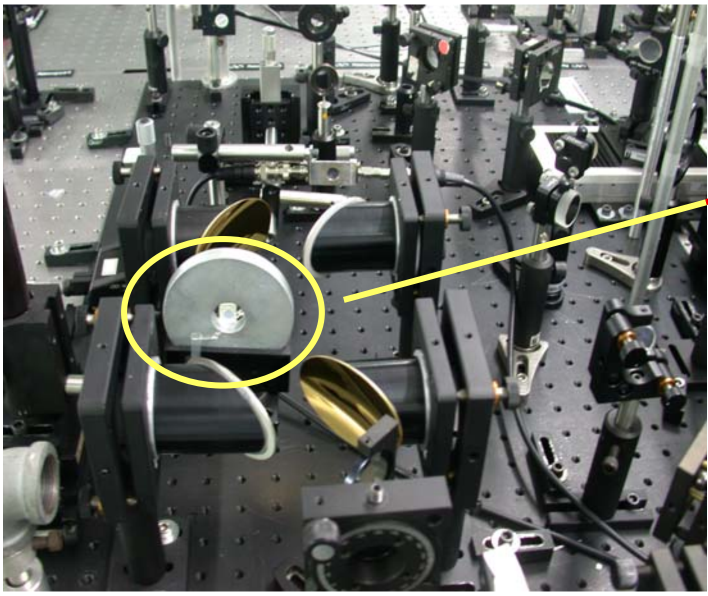

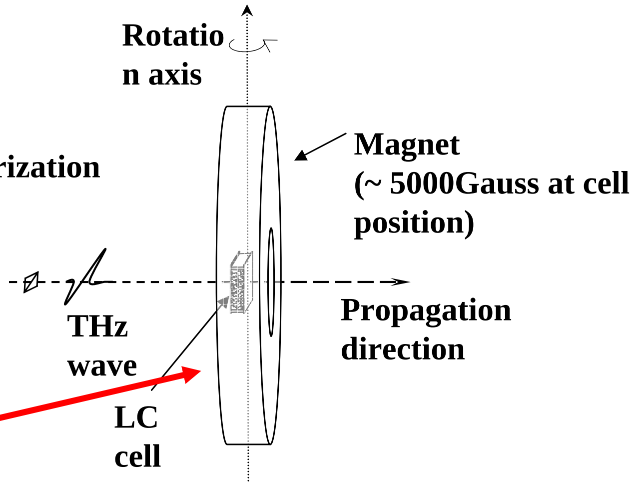

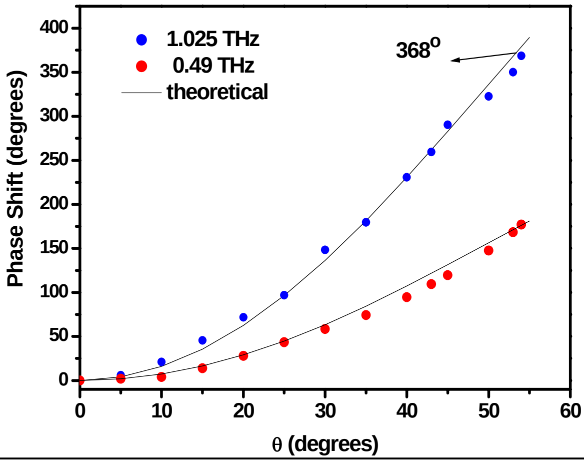

How does the Phase Shifter work?

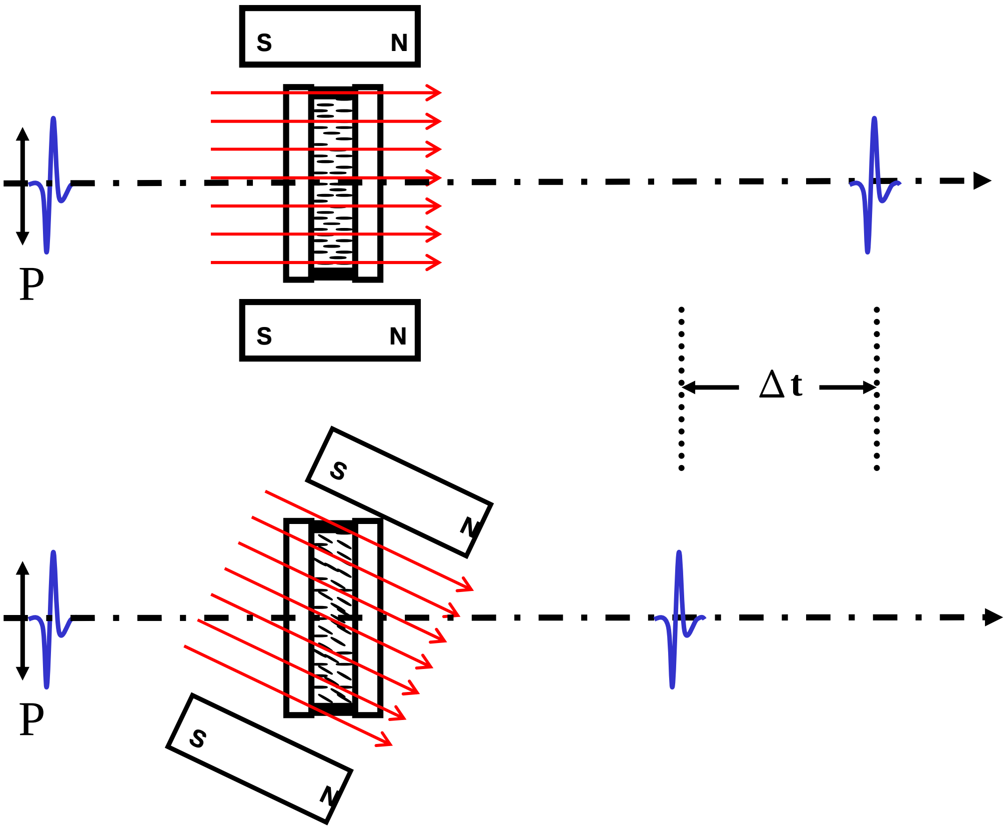

Theoretical Analysis

Phase shift, $\delta(\theta)$, can be written as

$$\delta(\theta) = \int_0^L \frac{2\pi f}{c} \Delta n_{eff}(\theta, z) dz$$

where L is the thickness of LC layer

Δn_{eff} is the change of effective birefringence

f is the frequency of the THz waves

c is the speed of light in vacuum

- **Threshold magnetic field ≈ 100 Gauss**
- **Magnetic field of magnet ≈ 5000Gauss**

We can assume that the LC molecules are reoriented parallel to the magnetic field direction, the phase shift can then be rewritten as:

$$\delta(\theta) = 2\pi L \frac{f}{c} \left\{ \left[\frac{\cos^2(\theta)}{n_o^2} + \frac{\sin^2(\theta)}{n_e^2} \right]^{-\frac{1}{2}} - n_o \right\}$$

where L is the thickness of LC layer

n_o is ordinary refractive index of LC

n_e is the extra-ordinary refractive index of LC

f is the frequency of the THz waves

c is the speed of light in vacuum

Sandwiched LC Cell Structure

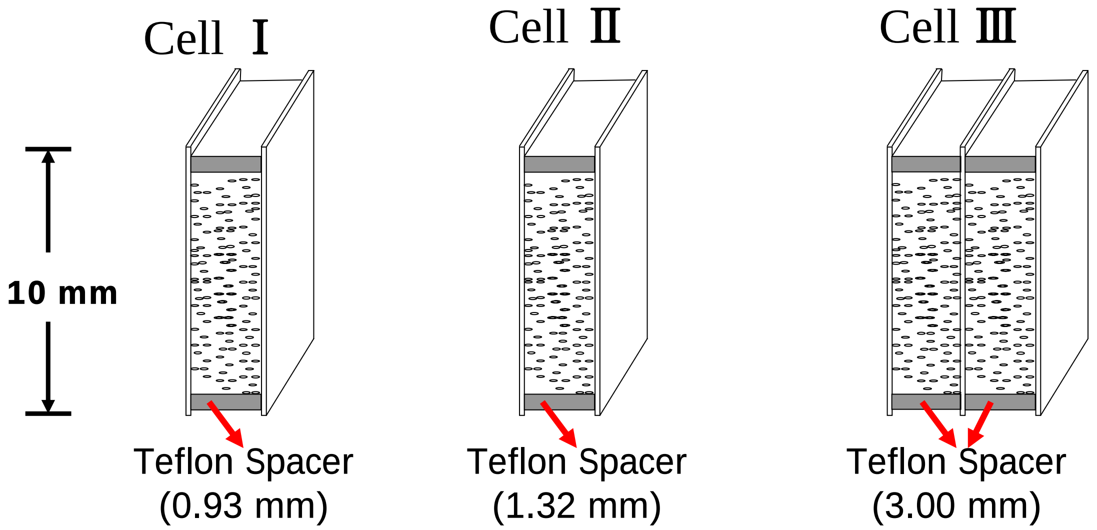

- The fuse silica substrates have been coated w/DMOAP to obtain the homeotropic alignment.
- The thickness of substrates are about 1.57 mm.

Electrically tunable LC THz phase shifter

Sandwiched Cell

E7 layer thickness: 1012 μm×2

electrode separation: 10.2 mm

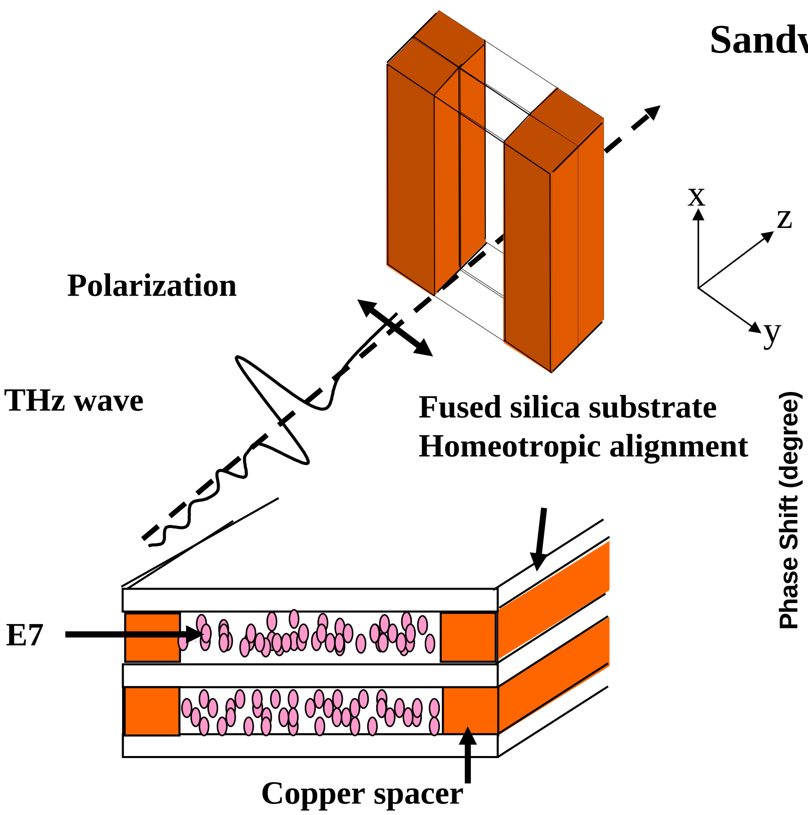

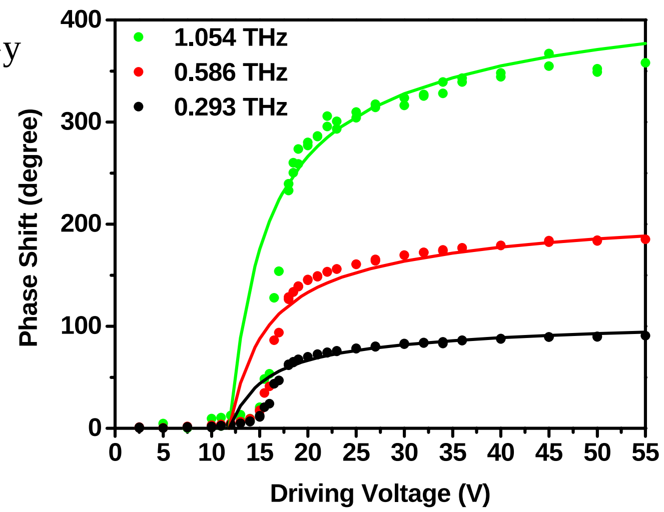

THz wave propagation and polarization directions are z and y, respectively

Lyot-type Birefringent LC Tunable THz filter

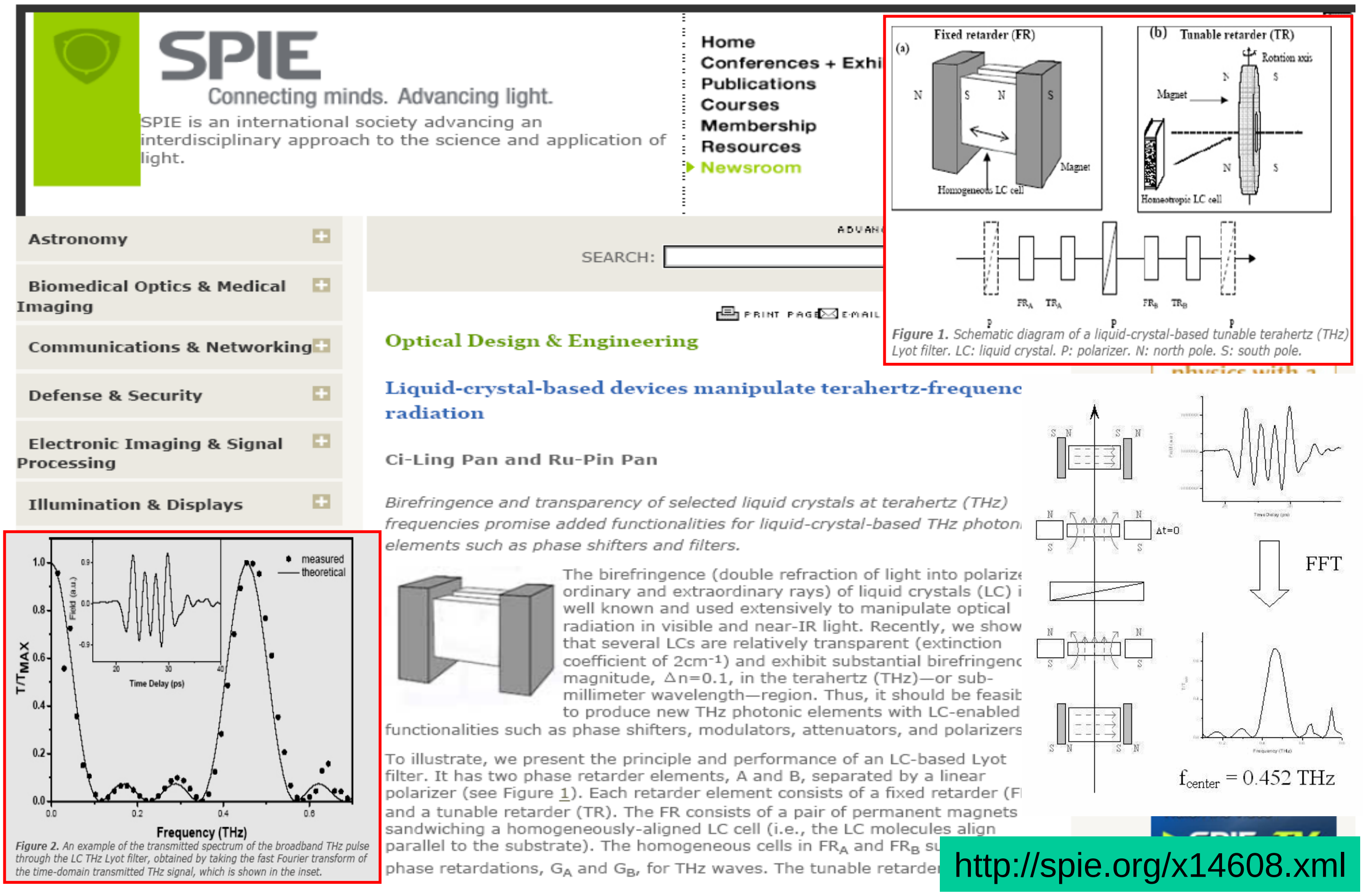

Principle of the Lyot Filter

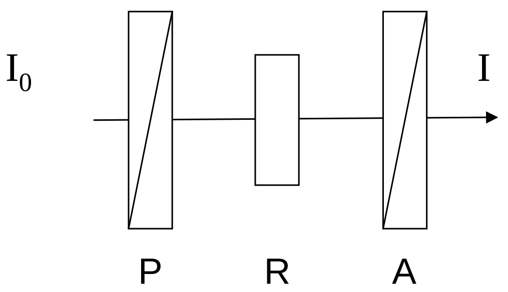

Polarizer || Analyzer

R: Retarder with retardation of Γ

$$T \equiv \frac{I}{I_0} = \cos(\frac{\Gamma}{2})^2 = \cos(\pi \cdot f \cdot \Delta\tau)^2$$

$$\left(\Gamma = \frac{2\pi\cdot\Delta n\cdot d}{\lambda} = \frac{2\pi\cdot\Delta n\cdot d\cdot f}{c} = 2\pi\cdot\Delta\tau\cdot f\right)$$

T is function of frequency (f) → *Filter*

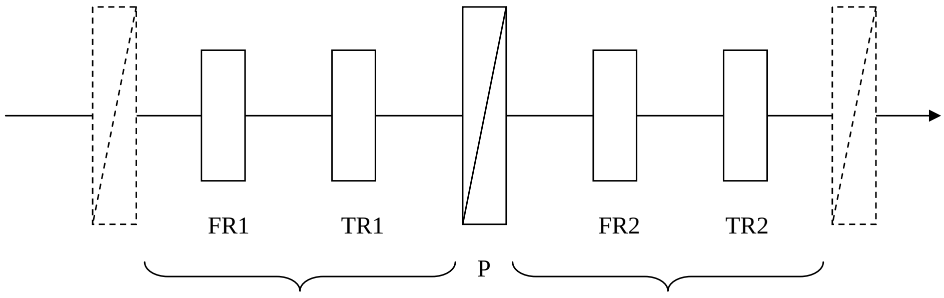

Unit A : *Unit B* = *1 : 2 (retardation)*

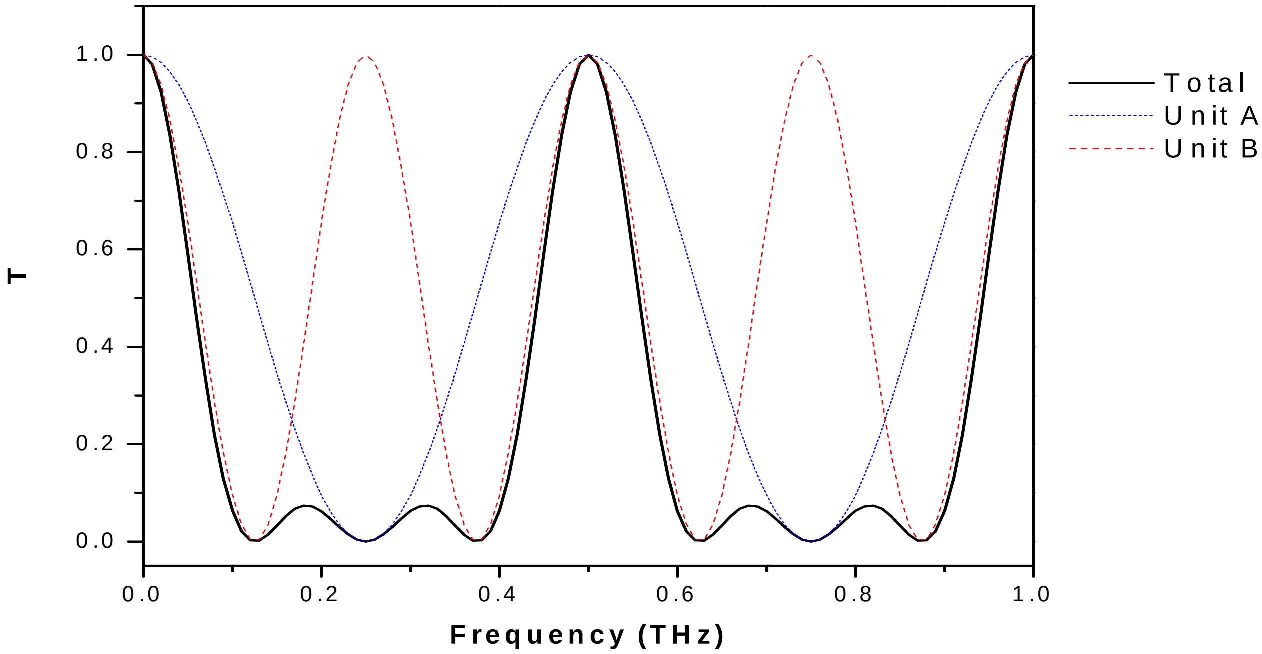

Solc-type Birefringent LC THz filter

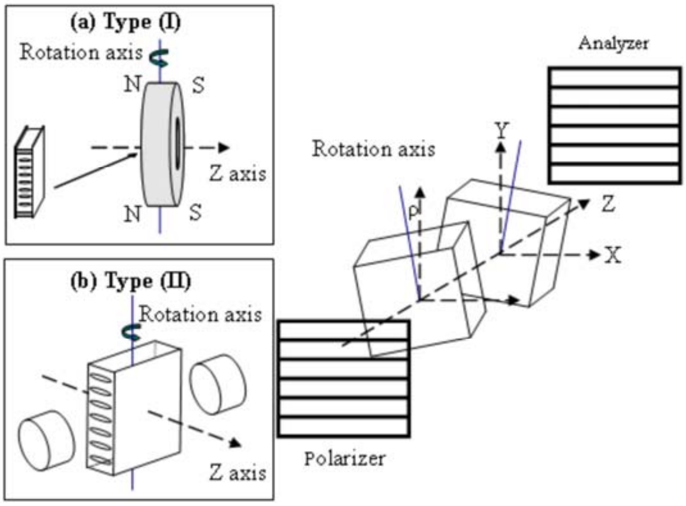

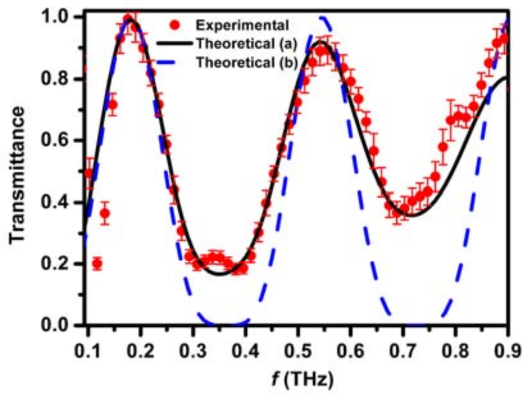

- Magnetically controlled LC-based THz Tunable SolcFilter has been demonstrated successfully.
- A two-stage Solc filter shows a tunable range of from 0.176 THz to 0.793 THz (a fractional tuning range of 350%) is larger than that from other published designs.
- Linewidth depends on frequency, ≥ 0.2 THz
- Insertion loss ~ 5dB, attributed to scattering in the thick LC cell.
- The LC-THz filter can be operated at room temperature.
- The theoretical predictions show good agreement with measured results.

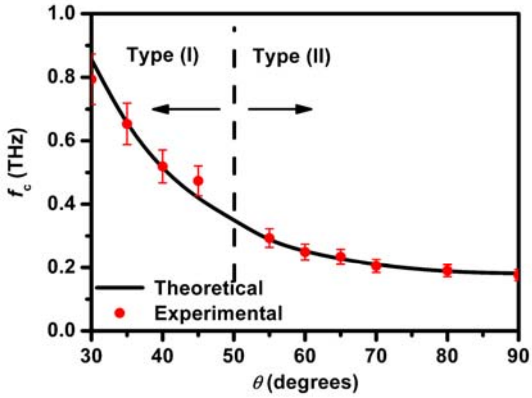

$$f_c = \frac{(2m+1)c}{2(n_e - n_o)d}, m = 0,1,2,3...,$$

Opt. Lett., July 1 2008

Tunable THz phase grating

Lin et al., Opt. Exp, 3 March 2008

Taiwan and U.S. Patents filed

Diffraction profile of 0.3-THz-beam

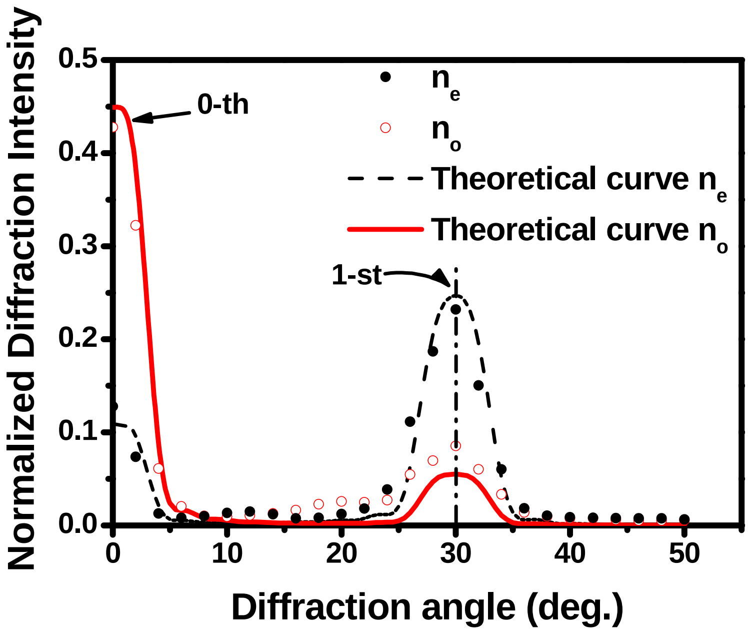

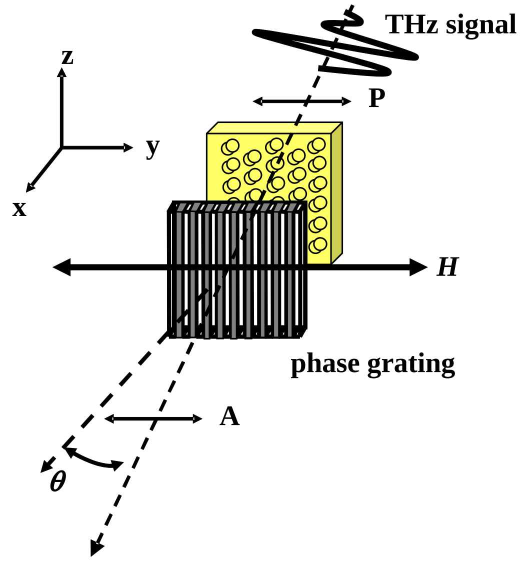

• The first order diffraction position is located at θ = 30°, which corresponds to the grating theory $\Lambda \sin\theta = m\lambda$.

• The phase grating could be used as a tunable beam splitter, the beam splitting ratio could be tuned from 4:1 to 1:2.

Feussner-type LC THz polarizer

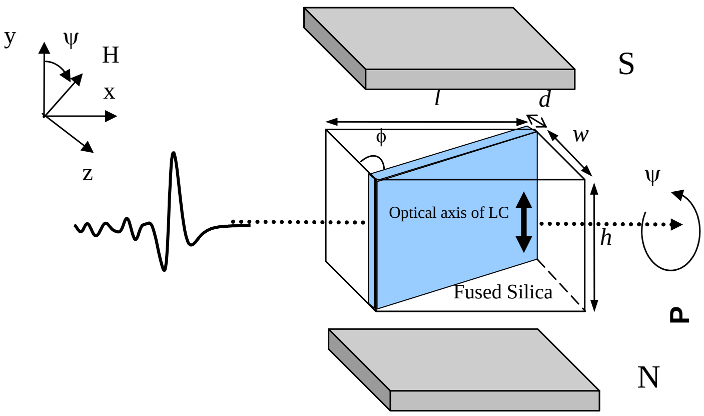

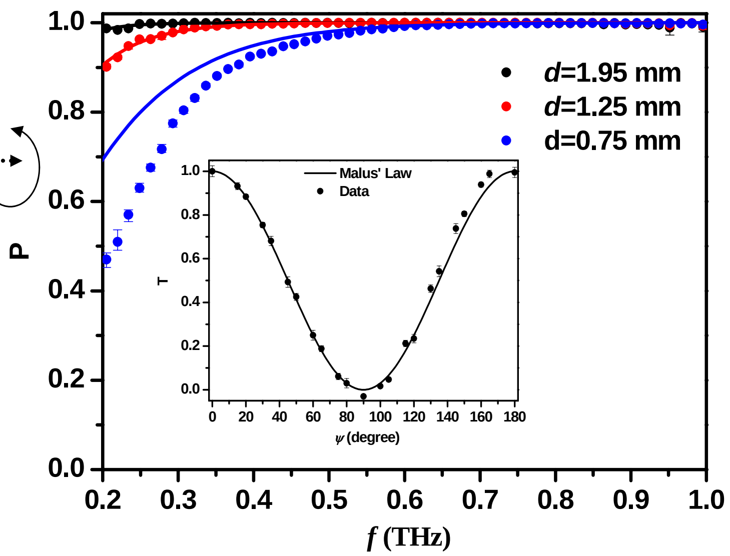

• n_q =1.95, n_o =1.58 and n_e =1.71

• θ_{co} = 54.12° and θ_{ce} = 61.27°,

• ϕ = 56 ± 0.5°

• ψ = 90°, TIR is satisfied for o-ray, T = 0.

• ψ = 0° , T = 100%.

$$P = \frac{T_e(f) - T_o(f)}{T_e(f) + T_o(f)}$$

Opt. Lett., June 1 2008

Taiwan and U. S. patents being filed.

Tunable THz Photonic Crystal Filter Using Nematic Liquid Crystal

- The 2D-MPC sample was made from 0.5 mm-thick Al plate
- The triangular lattice constant: s = 0.99 mm,
- The diameter of each hole: d = 0.56 mm.

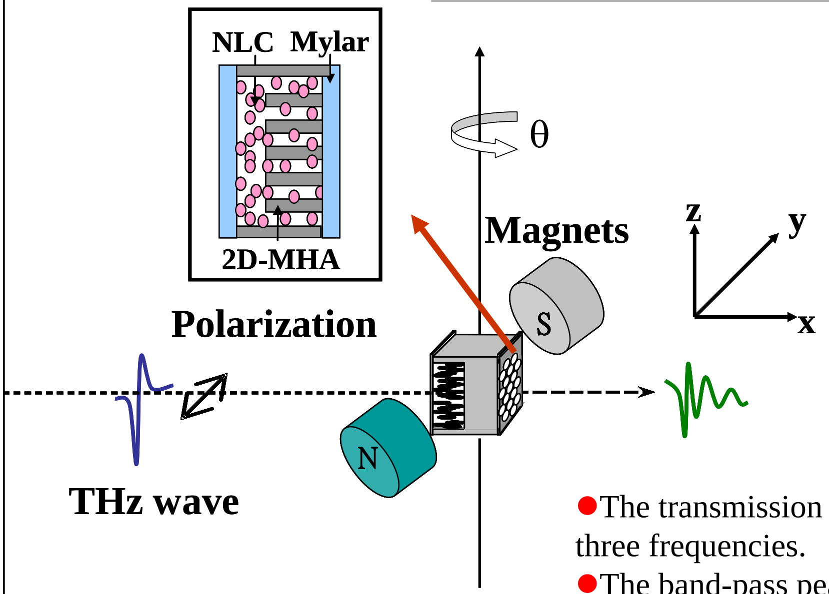

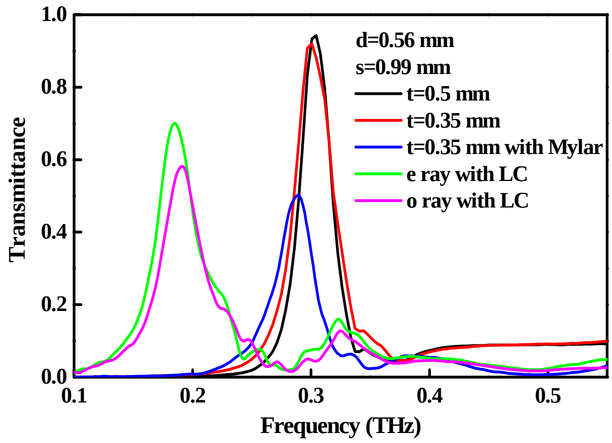

- The transmission spectrum of the 2D-MHA is characterized by three frequencies.
- The band-pass peak frequency is above the cutoff frequency.
- The transmittance is several times larger than the porosity of the holes.

Summary

- Optical constants of several LCs measured in the THz range. Birefringence of 5CB and E7 comparable to those in the visible. Attenuation negligible.
- Several LC-based THz devices demonstrated.

1. Room-temperature 2π magnetically tunable THz phase shifter
2. LC-based THz quarter-wave plate w/fine electrical tuning and 2π magnetically tunable THz phase shifter
3. LC-type tunable Lyot-type THz filter.
4. LC-type tunable photonic crystal THz filter.
5. Other novel devices: Solc filter, polarizer, phase grating

References (LC THz Devices)

1. Chau-Yuan Chen, Tsong-Ru Tsai, Ci-Ling Pan, and Ru-Pin Pan“Terahertz Phase Shifter with Nematic Liquid Crystal in a Magnetic Field”, Appl. Phy. Letts, Vol.83, no.22, pp. 4497-4499, December 1, 2003.
2. Tsong-Ru Tsai, Chao-Yuan Chen, Ci-Ling Pan, Ru-Pin Pan, and X.-C. Zhang, “Room Temperature Electrically Controlled Terahertz Phase Shifter,” IEEE Microwave and Wireless Components Lett., Vol. 14, No. 2, pp. 77-79, 2004.
3. Chao-Yuan Chen, Cho-Fan Hsieh, Yea-Feng Lin, Ru-Pin Pan, and Ci-Ling Pan, “Magnetically Tunable Room-Temperature 2π Liquid Crystal Terahertz Phase Shifter,” Opt. Express, Vol. 12, No. 12, pp. 2625-2630 June 14, 2004.
4. Ci-Ling Pan, Cho-Fan Hsieh, and Ru-Pin Pan, Masaki Tanaka, Fumiaki Miyamaru, Masahiko Tani, and Masanori Hangyo, “Control of enhanced THz transmission through metallic hole arrays using nematic liquid crystal,” Optics Express, Vol. 13, No. 11, pp. 3921 - 3930, May 30, 2005.
5. Chao-Yuan Chen, Cho-Fan Hsieh, Yea-Feng Lin, Ci-Ling Pan and Ru-Pin Pan, “A Liquid-Crystal-Based Terahertz Tunable Lyot Filter,” Appl. Phys. Lett., Vol. 88, 101107, March 6, 2006.
6. Cho-Fan Hsieh and Ru-Pin Pan, Tsung-Ta Tang, Hung-Lung Chen, and Ci-Ling Pan, “Voltage-controlled liquid crystal terahertz phase shifter and quarter wave plate,” Optics Letters, Vol. 31, No. 8, pp. 1112-1114, April 15, 2006.
7. Hsin-Ying Wu, Cho-Fan Hsieh, Tsung-Ta Tang, Ru-Pin Pan, and Ci-Ling Pan, “Electrically Tunable Room-Temperature 2π Liquid Crystal Terahertz Phase Shifter,” IEEE Photon. Technol. Lett., Vol. 18, No. 14, pp. 1488-1490, July 15, 2006.

Utrafast Photonics: Single-Cycle Optical Pulse Generation

Andy H. Kung (Academia Sinica)

Chuck C. K. Lee (NSYSU)

Ru-Pin Pan (NCTU)

In a blink of your eye…

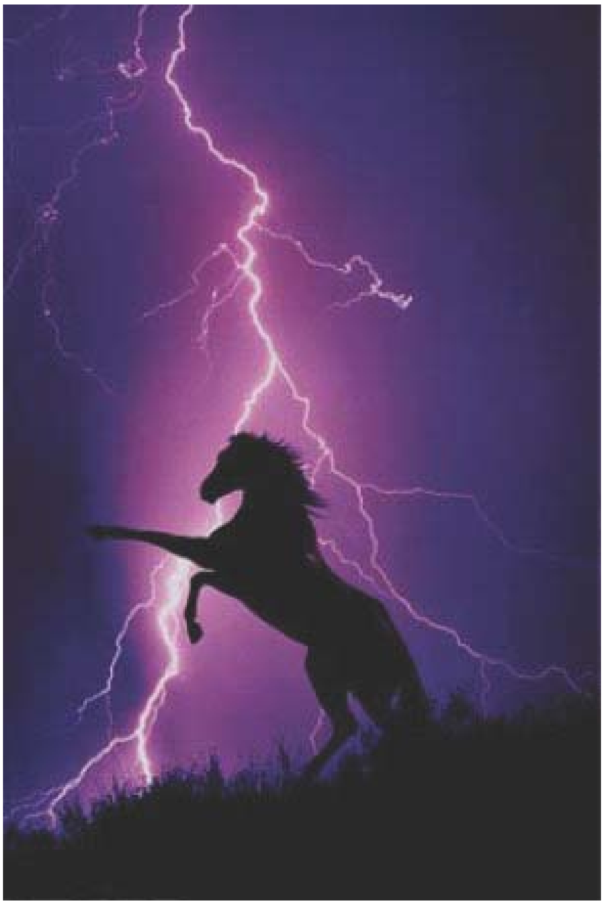

Response time of human vision: ~ 10 ms.

The birth of Modern ultrafast technology

Bar bet: Do all four hooves of a galloping horse ever simultaneously leave the ground?

The "Galloping Horse" Controversy
Palo Alto, CA 1872

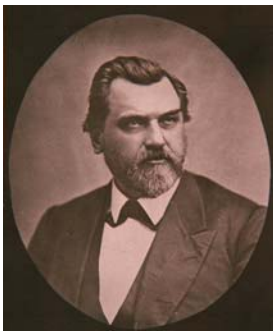

Leland Stanford

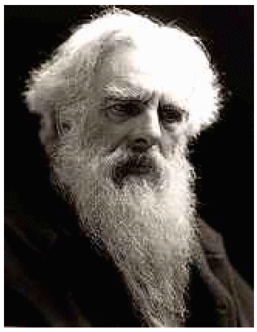

Eadweard Muybridge

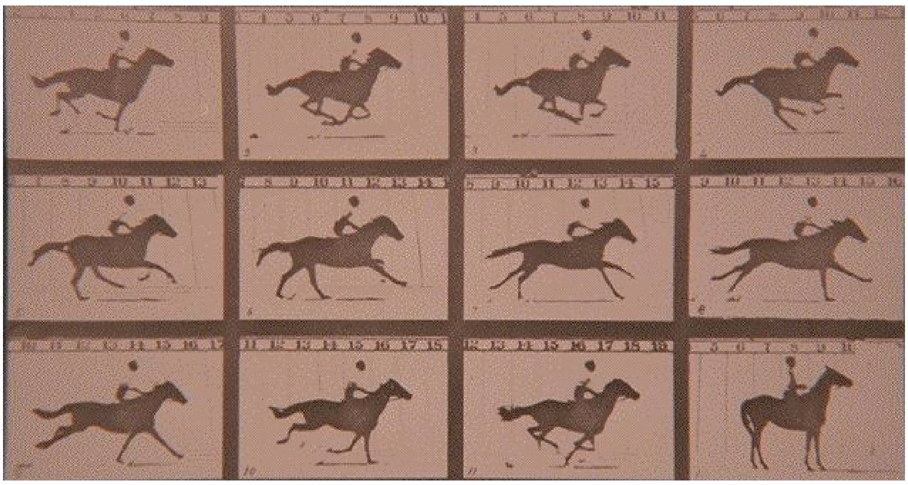

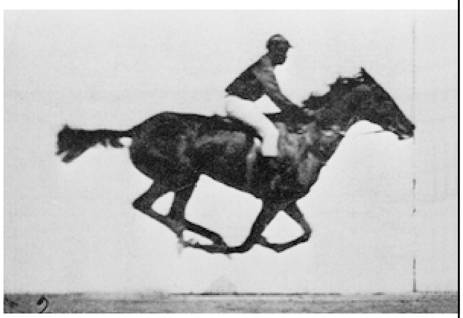

Time resolution:
1/60th of a second

High-speed Photography

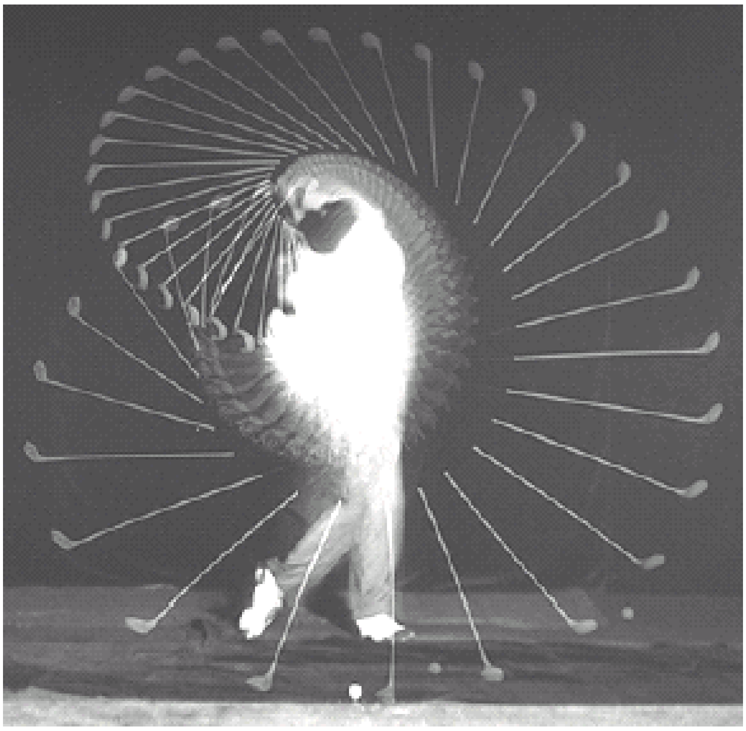

Harold Edgerton (MIT) captured a golf swing by repetitive microsecond flashes in 1938

Breaking the picosecond barrier: Optical Kerr Gate

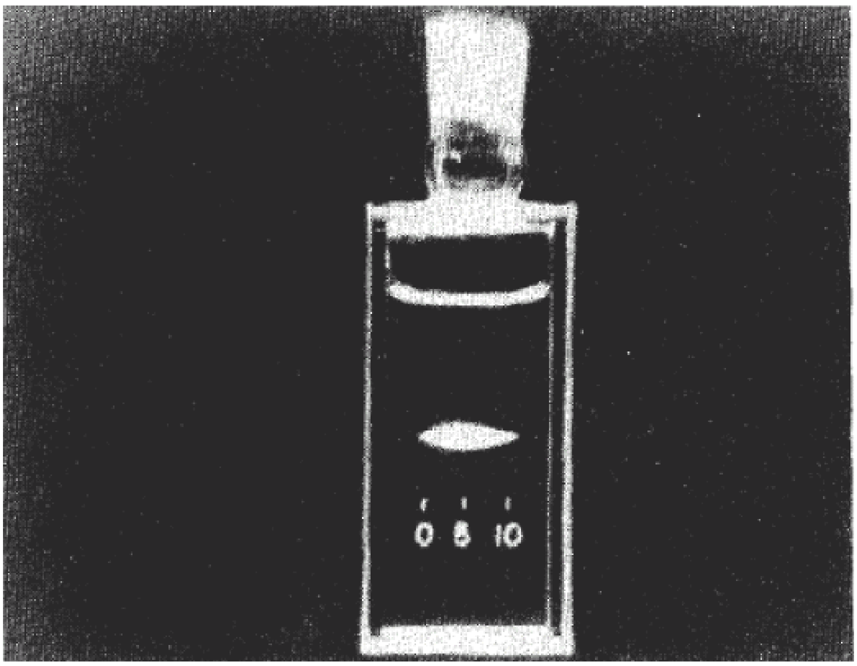

Duguay and Hansen (1971)

Laser pulses got shorter over the years

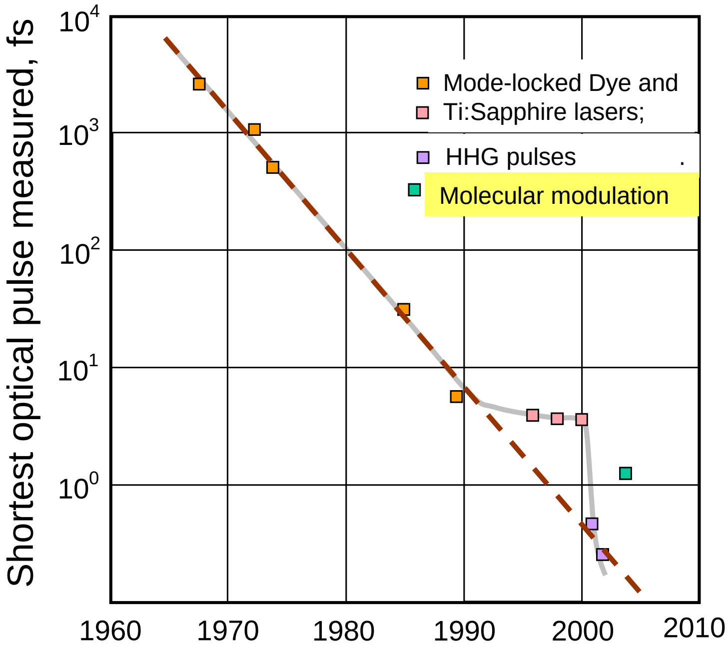

Ultrafast science

Peak intensity increased

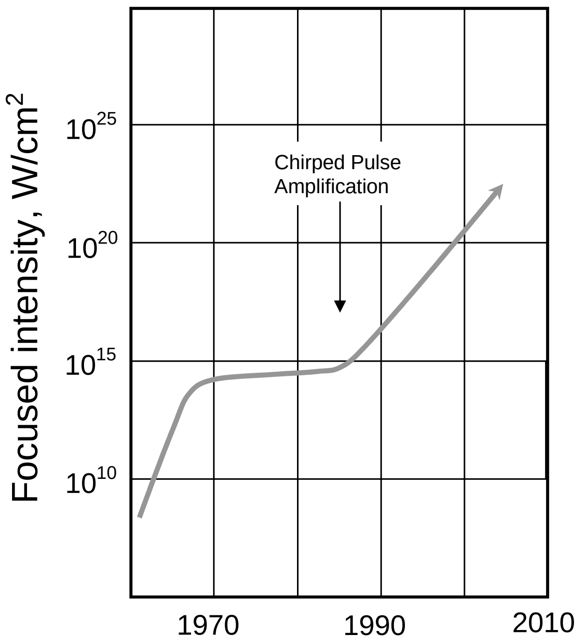

High field physics

The metric system

Prefix for small and large numbers:

micro	10^{-6}	mega	10^{6}
nano	10^{-9}	giga	10^{9}
pico	10^{-12}	tera	10^{12}
femto	10^{-15}	peta	10^{15}
atto	10^{-18}	exa	10^{18}
zepto	10^{-21}	zetta	10^{21}
yotta	10^{-24}	yocto	10^{24}

Man made today:

shortest time -- about 100 as

most intense light -- 10^{23} W/cm^2

Attoworld

Attosecond: 10^{-18} second

C x 10^{-18} sec = 0.3 nm

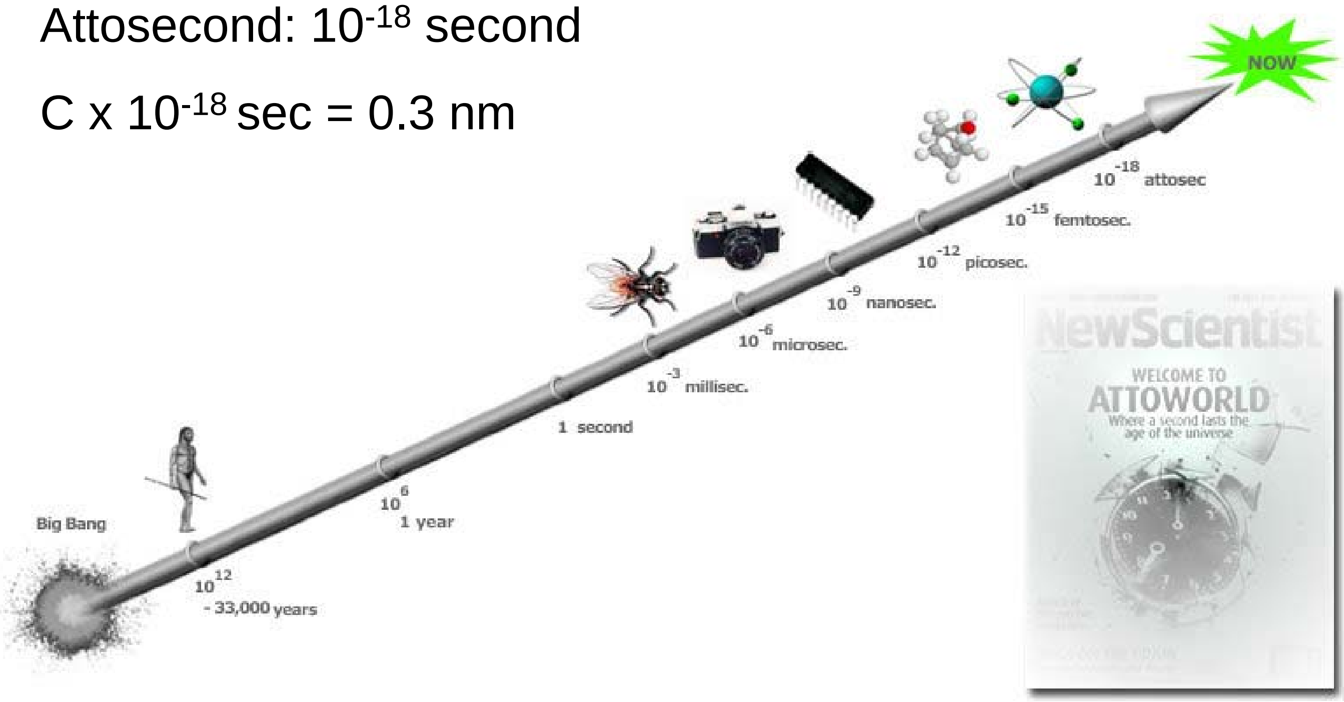

www.attoworld.de/attoworld.html

Time scales

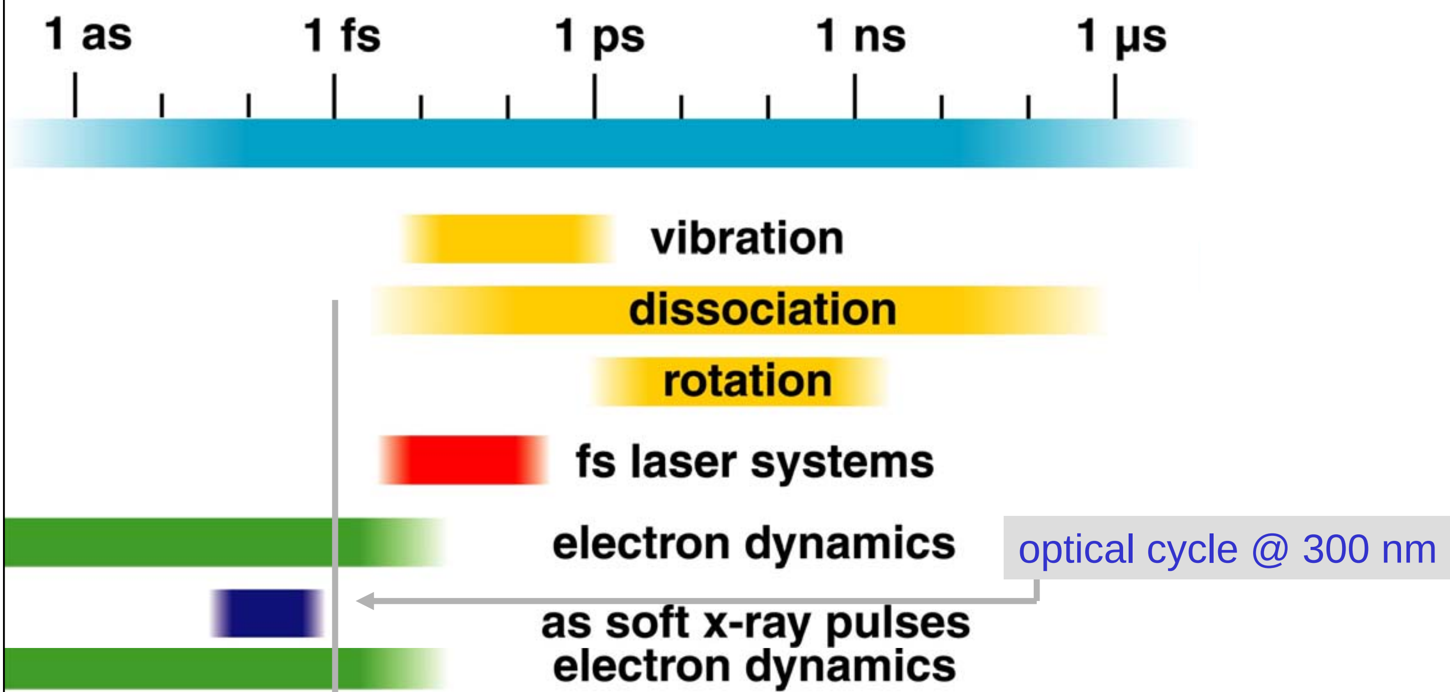

Short pulses can be used to monitor and control molecular and electronic motion

Motivation

- **form sub-femtosecond pulses**
- **produce multi-THz rep rate pulse train**
- **generate tunable high power vacuum uv pulses**
- **Synthesis of arbitrary optical waveforms**

Use molecular modulation in gas phase hydrogen at room temperature

Pros:

- ***large Raman transition of 4155 cm^{-1} for Q(1)***
- ***2/3 population in single quantum state (v=0, j=1) at room temperature***
- ***many parameters are known***
- ***nondestructible***
- ***room temperature is easy to operate***

Cons:

- ***large Doppler width***
- ***requires two tunable high-power high- resolution lasers spaced 4155 cm^{-1} apart***
- ***smaller pulse train pulse-to-pulse spacing***

anti-Stokes sidebands in H_2

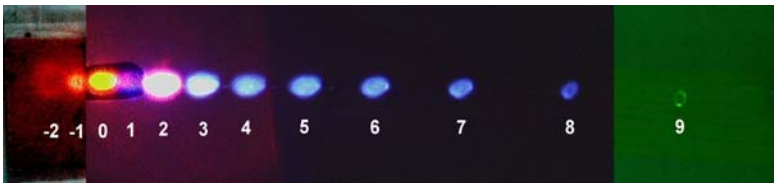

Total spectral span >70,000 cm^{-1}

Single-cycle optical pulse train

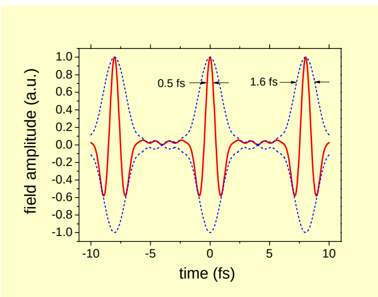

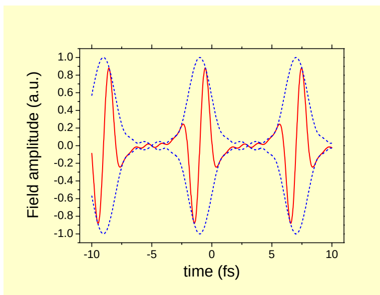

Envelope width ~ 1.4 fs
single cycle width ~ 0.5 fs
constant envelope phase: less than 0.38 cycle slip over 10^6 pulses

Generating short pulses = mode-locking Fourier Synthesis!

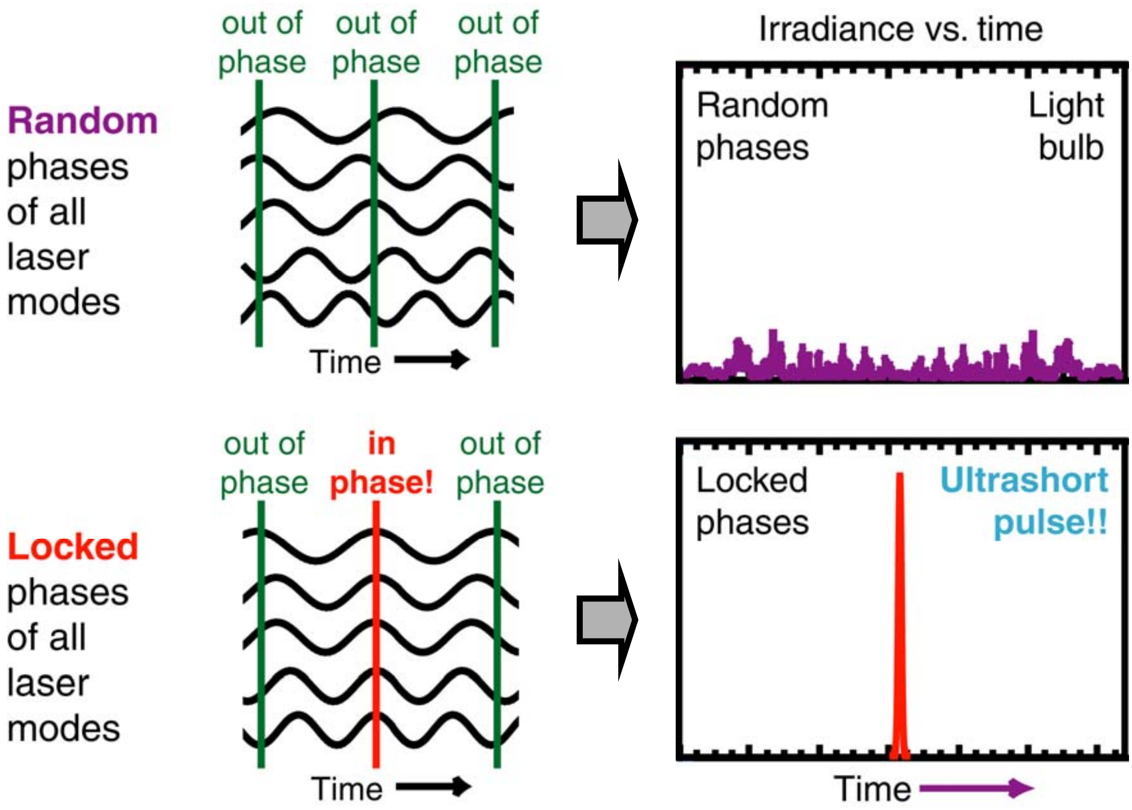

Commensurate pulse train

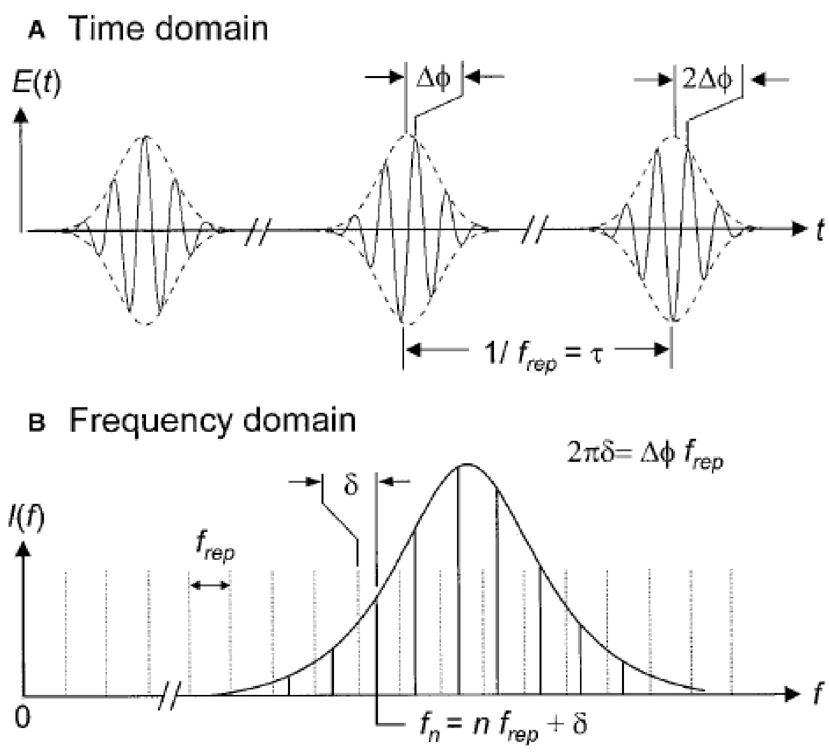

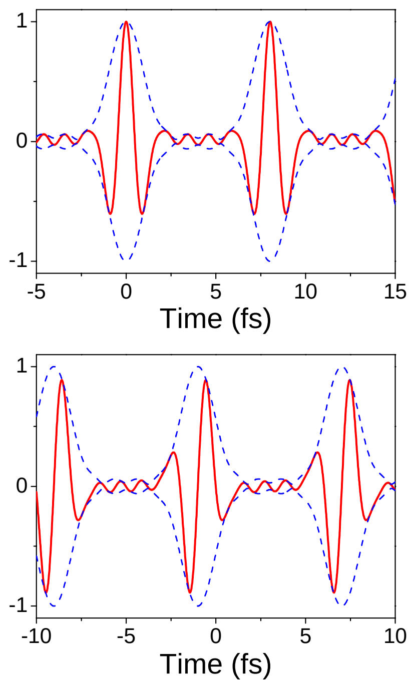

D. J. Jones et al., Science 288, 635 (2000)

Generating Single-cycle Attosecond pulse

The uncertainty principle requires that $\Delta\tau \, \Delta\nu > 1$

So for a sub-fs pulse, $\Delta\nu > 10^{15}$ Hz

Single pulse

Pulse train:

HHG

HSRS

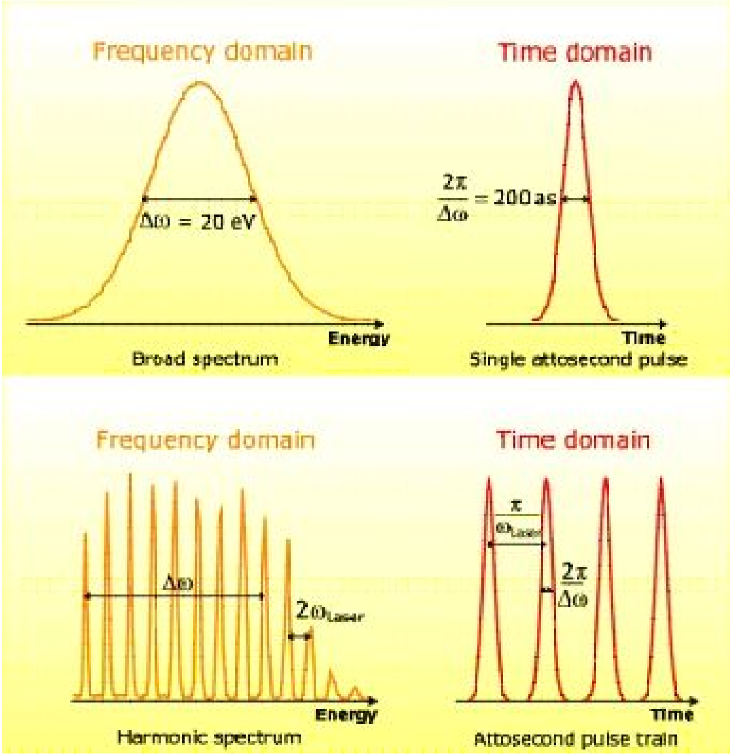

A single-cycle 800-nm pulse has a period of 2.7 fs. To achieve a period of 1 fs requires a wave-length of 300 nm.

Methods of generating attosecond pulses

A

VOLUME 78, NUMBER 7 PHYSICAL REVIEW LETTERS 17 FEBRUARY 1997

High-Harmonic Generation of Attosecond Pulses in the "Single-Cycle" Regime

Ivan P. Christov,* Margaret M. Murnane, and Henry C. Kapteyn†

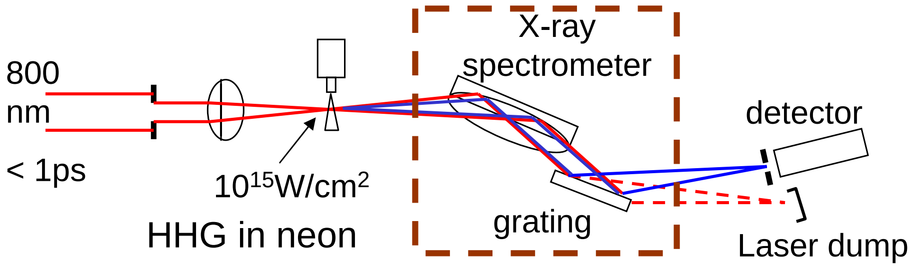

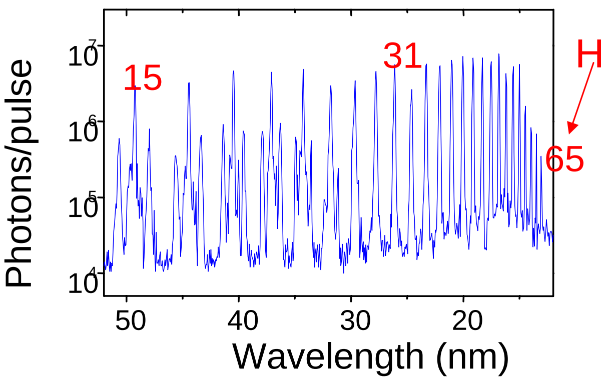

HHG produces equally spaced harmonics out to as much as the 300th harmonic, potentially as short as 10 attoseconds!

Advantages: single pulse
simple
Disadvantages:
80-100 eV photons
very low power
not single cycle
slow convergence

Methods of generating attosecond pulses

A High-order harmonic generation of phase-stabilized femtosecond pulse

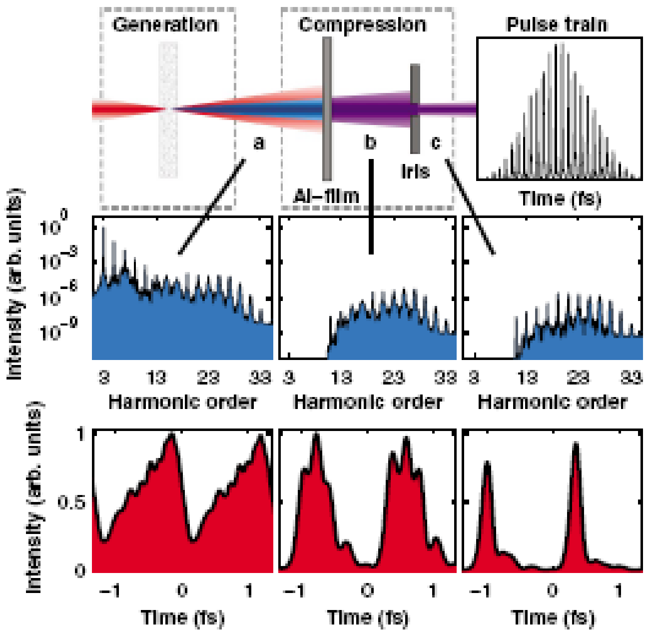

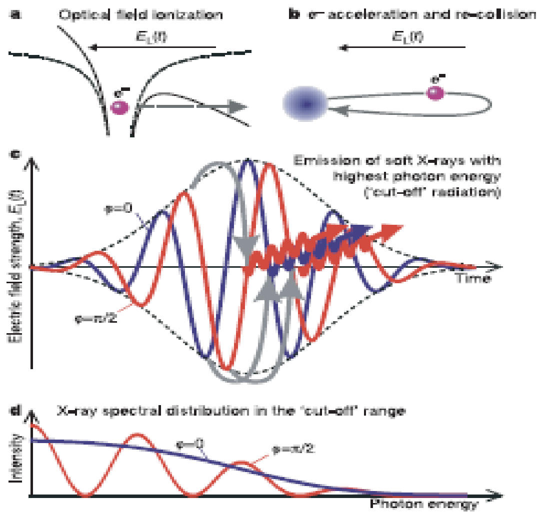

Advantages: single pulse
100 attosecond
Disadvantages: 30-100 eV photons
very low power
still a few cycles

Krauze et.al., Nature 421, 611 (2003)
R. Lopez-Martens et. al., PRL 94, 033001 (2005)

semi-classical description

I *The electron tunnels through the distorted Coulomb barrier*

II *The free electron is accelerated by the field, and may return to the atomic core*

III *The electron recombines with the atom, emitting its energy as a photon*

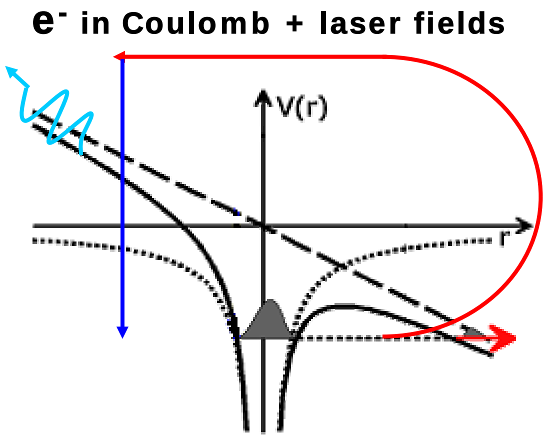

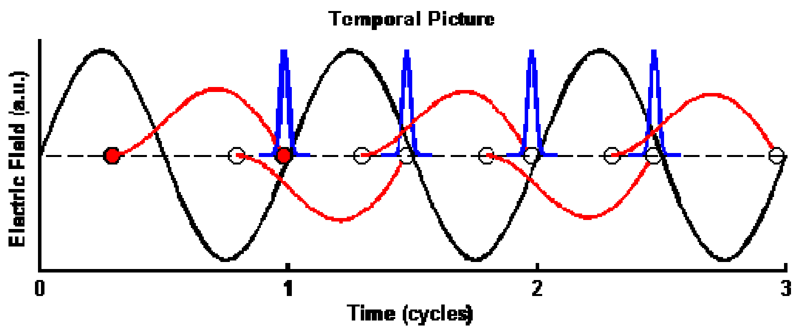

Methods of generating attosecond pulses

B High order anti-Stokes generation using molecular modulation

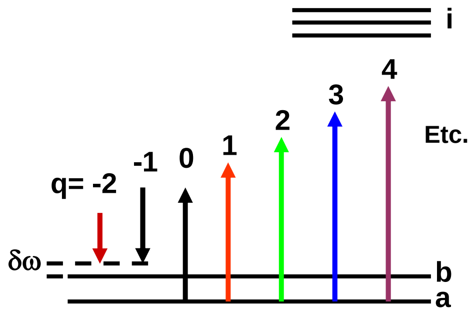

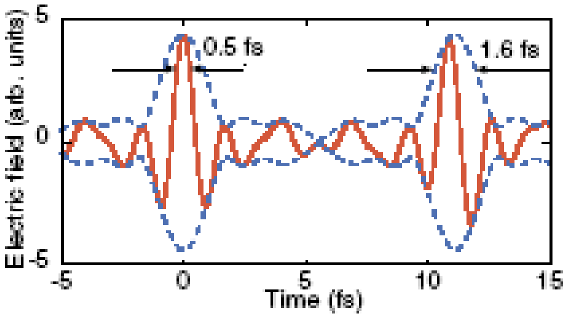

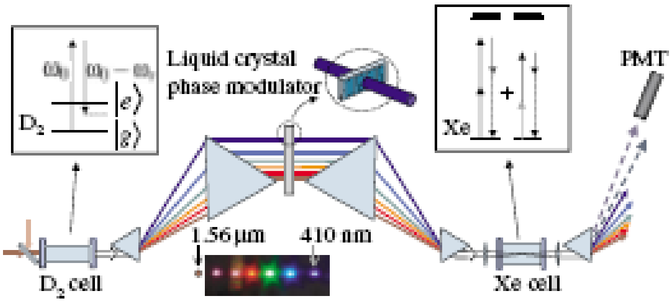

Advantages: uv region
good power
single-cycle
Disadvantages: complex setup
8-50 fs pulse spacing
limited to ~ 300-500 as

M.Y. Shverdin et.al., PRL 94, 033904 (Jan. 2005)

Bandwidth expansion by sideband generation

Frequency modulation by electro-optic modulation

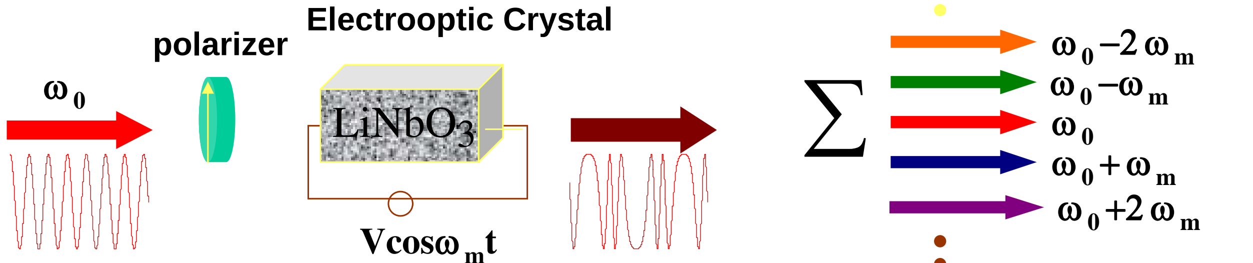

Refractive Index $n = n_0 + \delta \cos \omega_m t$

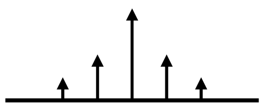

$\omega_q = \omega_0 + q\omega_m$

q^{th} sideband — modulation frequency

incommensurate $\frac{\omega_q}{\omega_m} \neq n$

commensurate $\omega_q = n\omega_m$

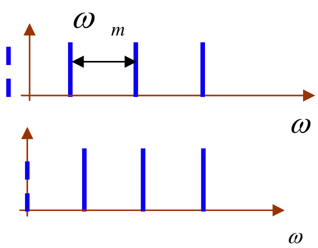

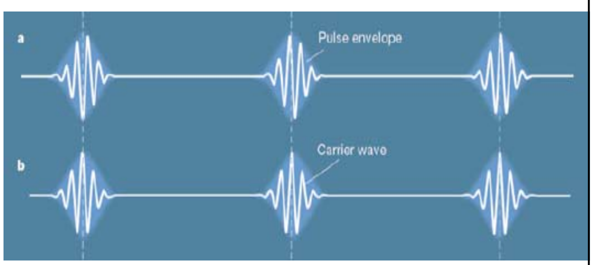

Raman scattering and attosecond pulses

Input two frequencies nearly resonant with a Raman resonance.

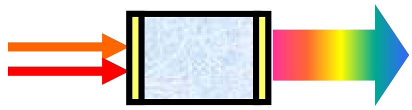

At high intensity, the process cascades many times. Higher-order sidebands are generated.

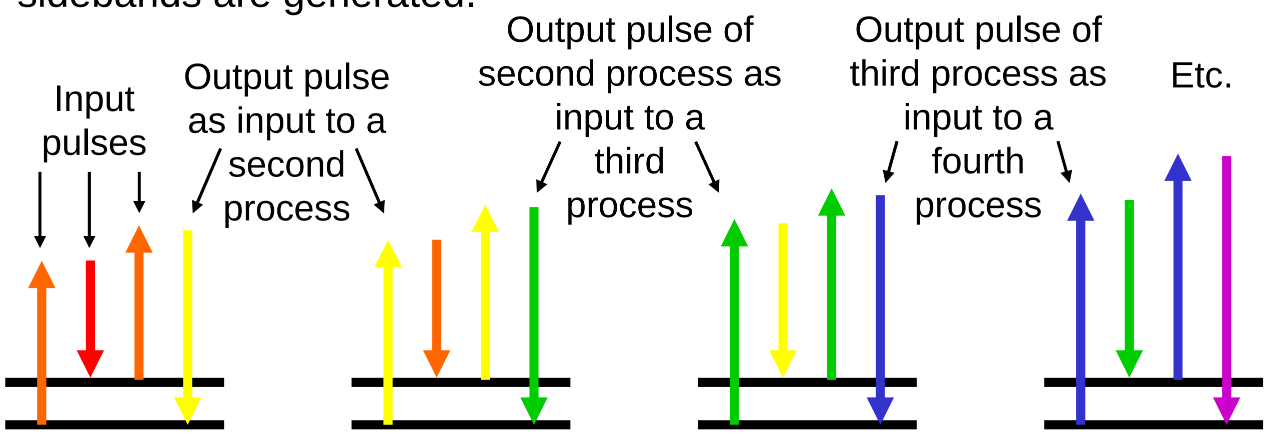

Raman processes can cascade many times, yielding a series of equally spaced modes!

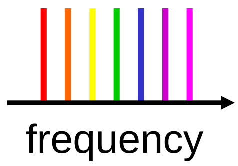

S. E. Harris and A. V. Sokolov PRL 81, 2894 (1998)

Molecular Modulation

Molecular modulation is analogous to electro-optic modulation

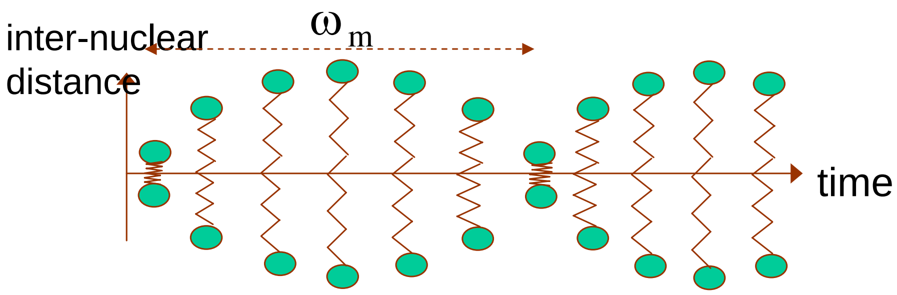

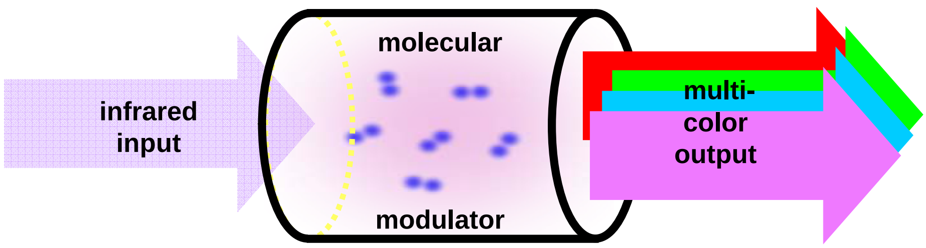

Refractive Index $n = n_0 + \delta \cos \omega_m t$

$\omega_q = \omega_0 + q\omega_m$ q= -2,-1,0,1,2,3….

Experiment Setup

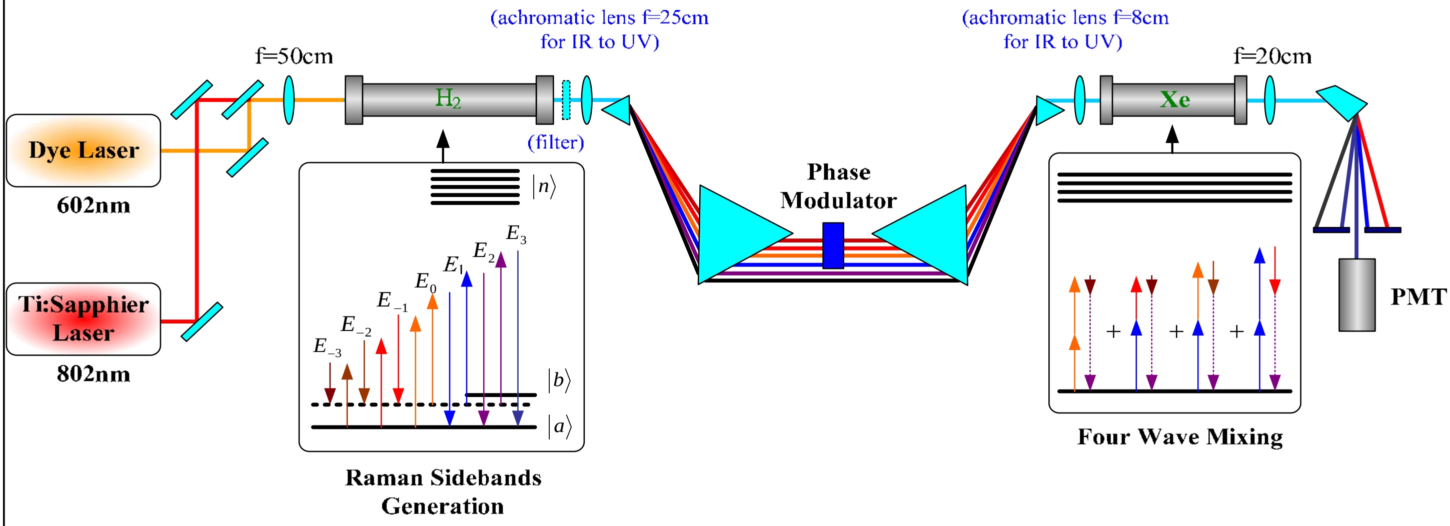

S. W. Huang, W. –J. Chen, and A. H. Kung, Phys. Rev. A 74, 063825 (2006)

W.-J. Chen et al., Phys. Rev. Lett. **100**: 163906, 2008

Raman sidebands generation

Raman Order	nm	cm^{-1}	Four wave mixing order
	∞	0	
-3	2407	4155	
-2	1203	8310	1
-1	802	12465	2
0	602	16620	3
1	481	20775	4
2	401	24930	5
3	344	29085	6
4	301	33240	7
5	267	37395	8
6	241	41550	9
7	219	45705	10
8	201	49860	11
9	185	54015	

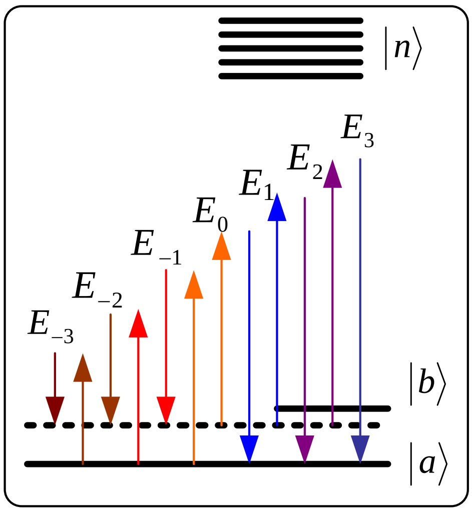

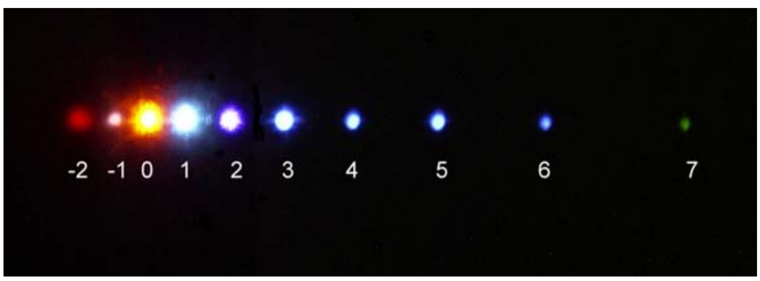

S. W. Huang, W. –J. Chen, and A. H. Kung, Phys. Rev. A 74, 063825 (2006)

Phase control with a LC-SLM

- LC: E7 (Merck), Cell thickness: 0.022 mm
- 5 pixels: 14 mm × 4 mm each, spaced to match the sideband beams
- The five pixels are used to make 7 sidebands (q = -2 to 4, 1203, 802, 602, 481, 401, 344, 301 nm) commensurate in phase.

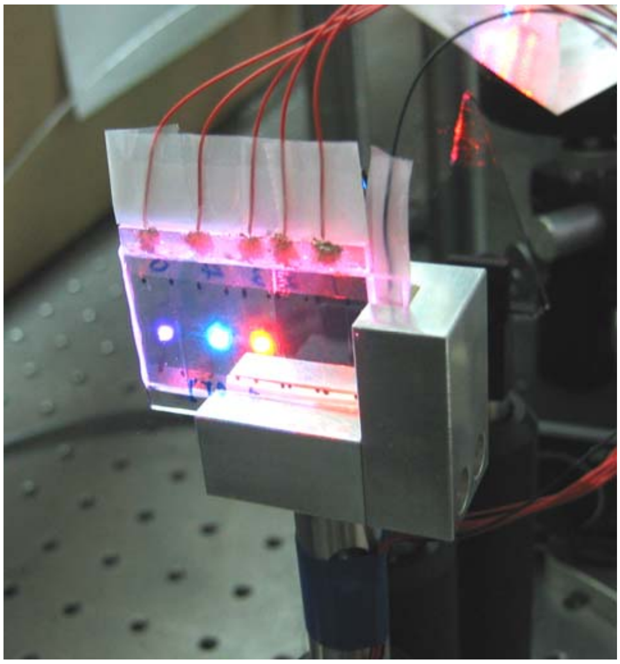

Transmittance of the LC-SLM

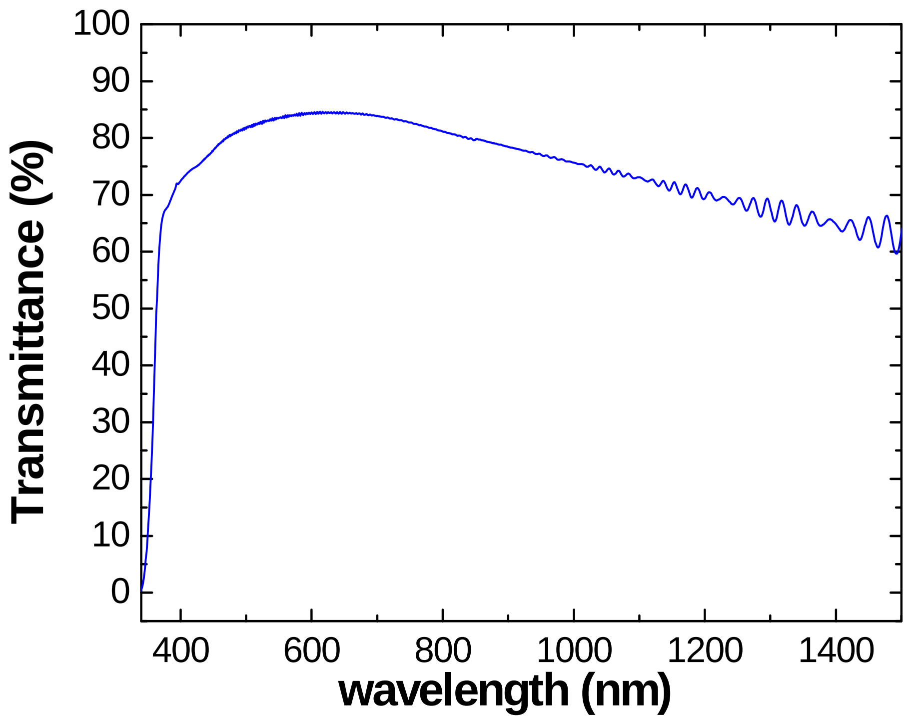

Phase modulation characteristics: Commercial vs Home-made

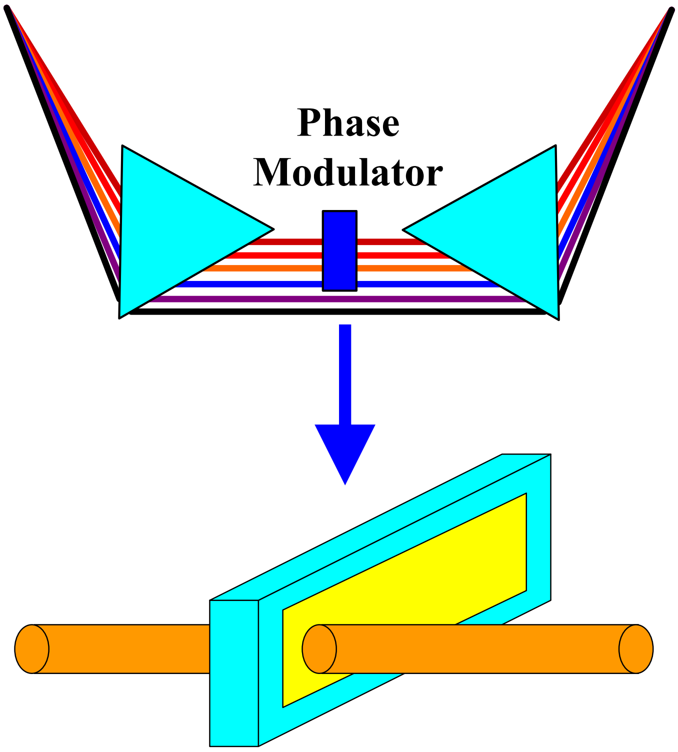

Spatial Light Modulator

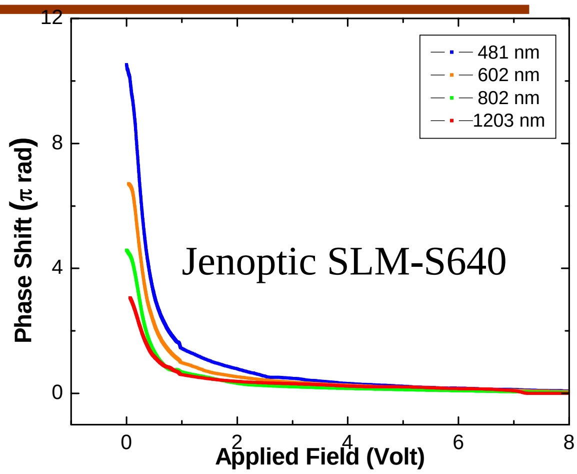

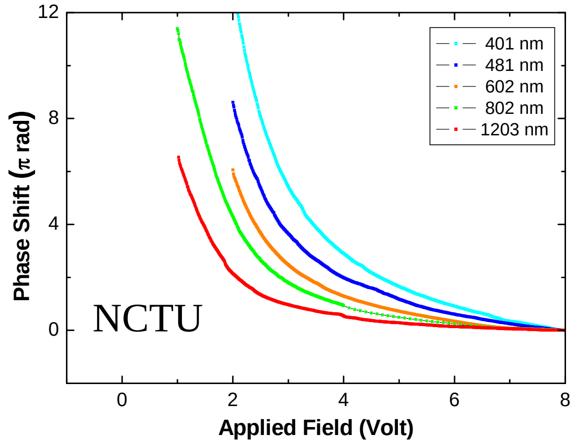

Phase Optimization

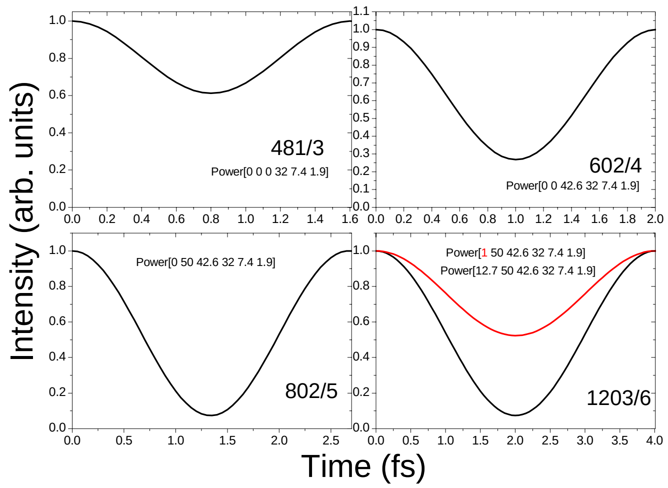

7=6+6-5
=6+5-4
=5+5-3
=6+4-3
=5+4-2
=6+3-2
=5+3-1
=6+2-1
=4+4-1

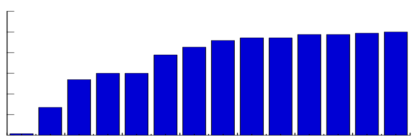

Raman sidebands order & 4 wave-mixing order

Raman Order	nm	cm^{-1}	4 wave-mixing order
	∞	0	
-3	2407	4155	
-2	1203	8310	1
-1	802	12465	2
0	602	16620	3
1	481	20775	4
2	401	24930	5
3	344	29085	6
4	301	33240	7
5	267	37395	8
6	241	41550	9
7	219	45705	10
8	201	49860	11
9	185	54015	

How to measure the pulse width?

Autocorrelation is standard way to measure ultrafast pulsewidth. However it could not be done here because of the wide bandwidth.

Solution: Correlation using pulses formed by the sidebands themselves.

Synthesize two pulses from the subsets of sidebands and electronically delay one pulse with respect to the other. Measure the resulting four-wave signal with a photomultiplier.

simulation

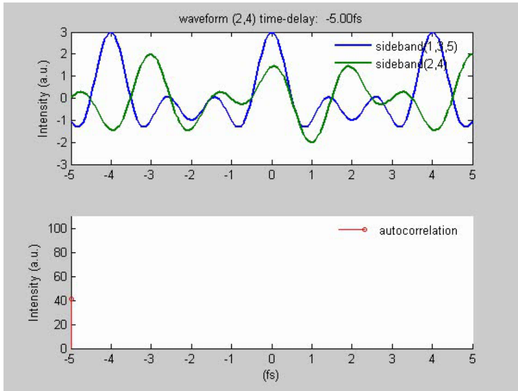

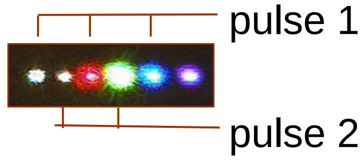

Cross correlation Results

6 sidebands commensurate condition

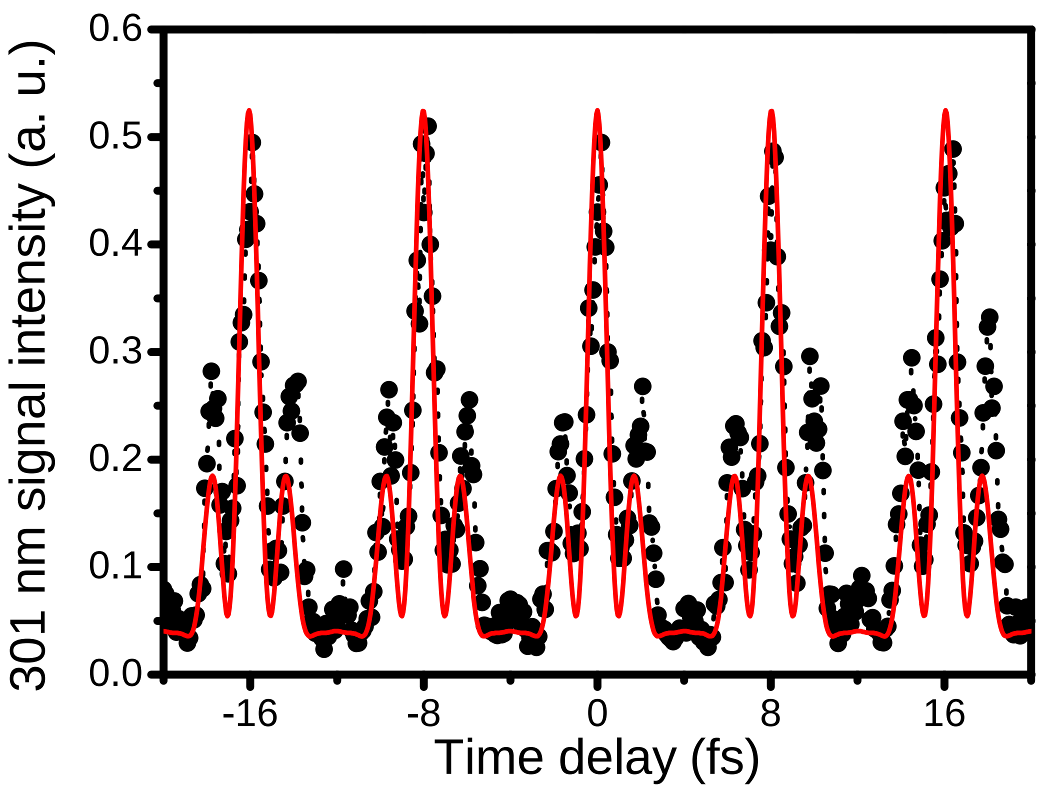

Cross correlation Results

7 sidebands commensurate condition

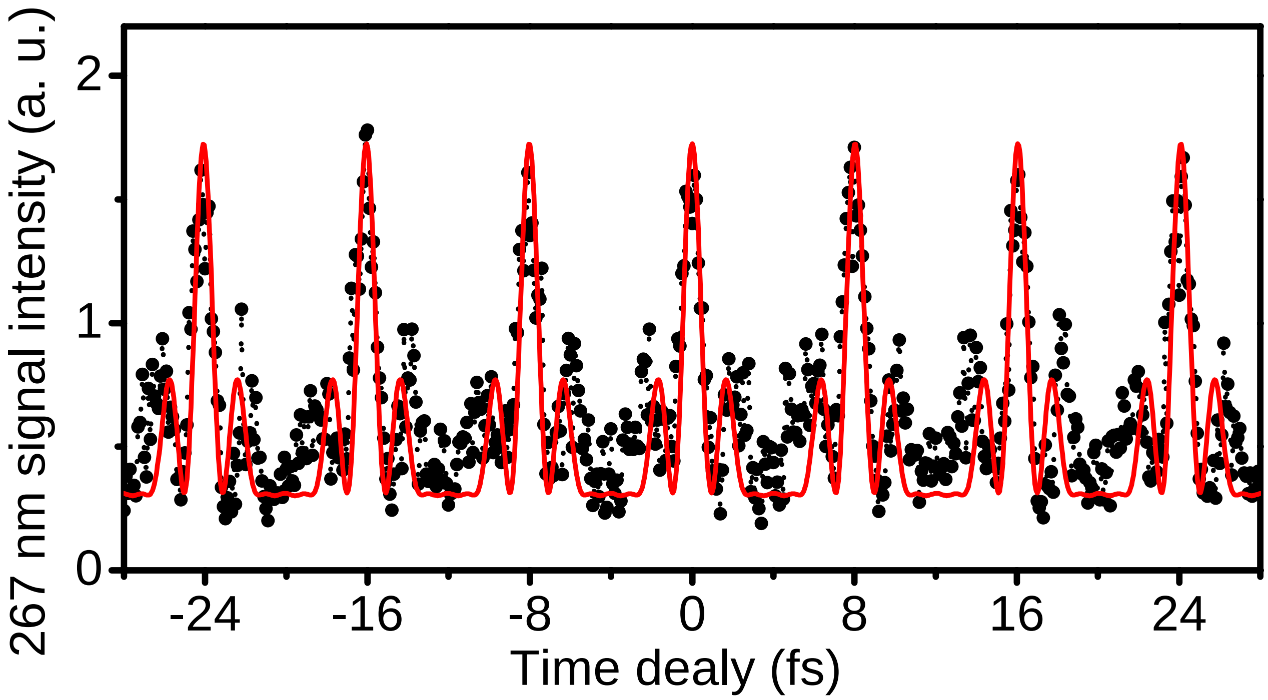

Commensurate pulse train

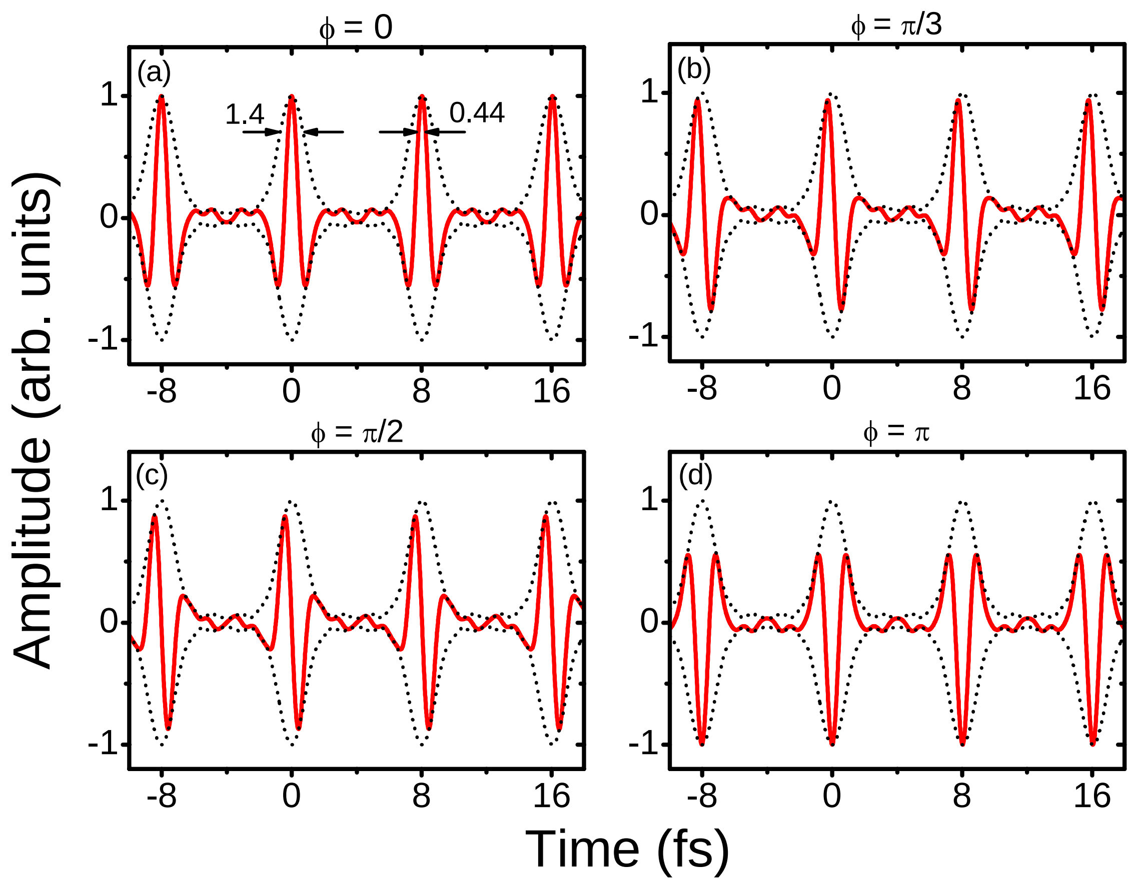

Summary

- **0.833 cycle** per pulse
- **1.4 fs** envelope
- **440 as** cycle width
- constant carrier envelope phase
- 2 ns pulse train duration
- 8.0 fs pulse spacing
- **~1 MW** peak power

Possibilities

Technology

- Generate subfemtosecond single-cycle pulses: add more sidebands and improve sideband power
- Perform autocorrelation of sub-femtosecond pulses
- Increase pulse-to-pulse spacing
- Develop control of carrier envelope phase
- Extract single pulse from pulse train
- Modulate in photonic crystal fiber
- Develop pulse control in vacuum

Science

- Optical-deep uv, xuv attosecond pump-probe
- Ultrafast tomography: tracing molecular vibrational wavefunction
- Low energy electron dynamics in atoms, semiconductors, etc.
- Attosecond nonlinear optics
- Test new theories…….
- …….
- …….

Proposed attosecond Setup at NTHU

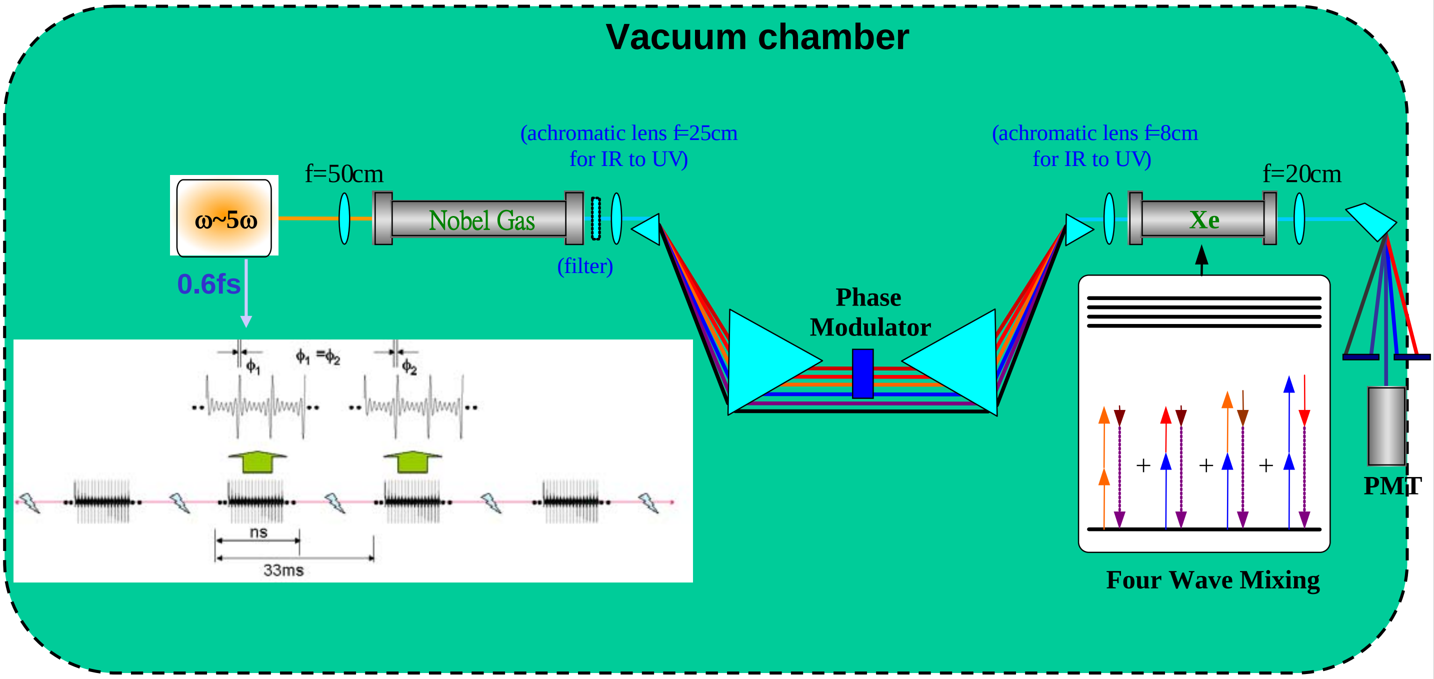

Space within one optical table

Acknowledgements

• Profs. Ru-Pin Pan (Ru-Pin Chao), Jung Y. Huang, H. Y. Ahn (NCTU), Dr. Chuck C. K. Lee, Dr. Chao-Yuan Chen, Cho-Fan Hsieh, Chia-Jen Lin , Yu-Tai Li, Dr. T. A. Liu, Dr. T. R. Tsai, Dr. Yi-Chao Wang, Dr. Jin-Wei Chen, Dr. Chia-Rong Sheu

• Prof. Andy H. Kung (Academia Sinica)

• Dr. Jamin Shieh (NDL)

• Profs. M. Hangyo, M. Tani (Osaka U.)

• Prof. X. –C. Zhang (RPI)

• Support of the National Science Council and Academic Top University Program of Ministry of Education

Thank you
for your attention!